University of Alberta

Molecular basis for regulation of Protein Phosphatase-1c by TIMAP

by

Micheal James Shopik

A thesis submitted to the Faculty of Graduate Studies and Research
in partial fulfillment of the requirements for the degree of

Master of Science

Department of Biochemistry

Edmonton, Alberta
Fall 2008

Your file Votre référence
ISBN: 978-0-494-47410-5
Our file Notre référence
ISBN: 978-0-494-47410-5

Abstract

TGFβ-inhibited membrane associated protein (TIMAP) is a Protein Phosphatase-1 (PP-1c) regulatory protein which targets the phosphatase to the plasma membrane. TIMAP can be phosphorylated and this activates associated PP-1c activity.

There are few crystal structures of PP-1c regulatory subunits and there is no three-dimensional information on TIMAP. A structural model was generated predicting that TIMAP binds PP-1c and wraps around the C-terminal tail of the phosphatase, with the active site of PP-1c accessible to solvent.

TIMAP bound both PP-1cβ and PP-1cγ isoforms and was characterized as an inhibitor of PP-1c activity toward phosphorylase *a* and *p*-nitrophenol phosphate. Truncated $TIMAP^{46-292}$ was less potent inhibiting PP-1c, suggesting a C-terminal TIMAP-PP-1c interaction site which enhances phosphatase inhibition. Substitution of Asp or Glu for Ser333 and Ser337 to mimic phosphorylation of TIMAP relieved inhibition of PP-1cγ. This suggested the C-terminal PP-1c interaction site on TIMAP may involve a region encompassing Ser333/Ser337. TIMAP reduced cdk2/CyclinA phosphorylation of PP-1cγ at Thr311, suggesting the PP-1c C-terminal tail is inaccessible when TIMAP is bound.

Acknowledgements

The first person I wish to extend my deepest gratitude and thanks is Dr Charles Holmes. Charles, thank you for all you have done for me. You took me in and provided me with an opportunity to further my education and open my eyes to the world of research and science. Over the years you have been nothing but positive and supportive. Your enthusiasm about research was contagious. I can't thank you enough for your efforts and your help in putting together this thesis.

I wish to extend sincere thanks to Dr Ballermann. Your support and encouragement has been influential and a very optimistic presence for me during my studies.

Dr James, I wish to thank you for your help. Your positive attitude has been a great help to me throughout my degree.

I could not have achieved what I have without the help of the members of the Holmes Lab. It has been a great environment to work in. I wish to thank Mikolaj Raszek, Andrea Fong, and Hue Anh Luu for their helpful suggestions and for watching all my practice talks along the way. Kathleen Perrault, Marcia Craig, Cindy Lee, and Tamara Skene, thank you, you have always been helpful as well.

Other members of the Department of Biochemistry have provided support for me throughout my degree, especially John Paul Glaves. Thank you, your help with my defence seminar was crucial and thanks for all the insightful discussions about the hockey pool. For helping me out with the GST vector, I would like to thank Dr Young.

Laiji Li, thank you for your insight and for always taking an interest in my work. I appreciated your point of view and suggestions.

I would not be where I am without my family. I will forever be in debt to my parents. Words fail me when trying to think of how to really thank my family for all they have done for me. Mom, Dad, and Nicole, thank you. I can't tell you how much I appreciate everything you have done for me.

I think that I should give an honorable mention to all of the trees that went down in order to make this thesis.

And to my one and only Kimberly, how can I ever thank you? You have inspired me like nothing else. I truly feel that without you and all of the love and support you have given me, I could not have achieved what I have. Kimberly, you have been my rock and I have leaned on you more than you know. You have had a role in every stage of the creation of this thesis! Thank you for being the light at the end of my tunnel.

Table of contents

Chapter 1: Introduction..... 1

1.1 Reversible phosphorylation.....1

1.1.1 Ser/Thr Phosphatases.....3

1.2 Protein Phosphatase-1.....5

1.2.1 Isoforms and tissue expression of Protein Phosphatase-1 catalytic subunit.....5

1.2.2 Structure of the PP-1c Catalytic Subunit (PP-1c).....7

1.2.3 Inhibition of PP-1c by microcystin, an environmental toxin.....9

1.2.4 Microcystin sepharose: an important tool for purification and identification of PP-1c complexes.....11

1.3 Regulation of PP-1c.....12

1.3.1 Controlling the activity of a promiscuous enzyme.....12

1.3.2 The RVXF motif mediates regulatory subunit binding to PP-1c.....12

1.3.3 Regulating catalytic activity of PP-1c by endogenous inhibitors.....15

1.3.4 Regulation of PP-1c by phosphorylation.....16

1.4 Regulation of PP-1c activity in smooth muscle relaxation.....18

1.4.1 Myosin Phosphatase: A complex of PP-1cβ and regulatory subunits.....19

1.4.2 MYPT1 targets PP-1cβ to myosin.....20

1.4.3 Ankyrin Repeats: a structural motif facilitating protein-protein interactions..23

1.4.4 The MYPT family of proteins.....24

1.4.5 TGF-β1-Inhibited Membrane Associated Protein: the coolest member of the MYPT family.....26

1.5 Goals of the thesis.....29

Chapter 2: Methods and Materials..... 32

2.1 Materials.....32

2.2 Cloning and mutagenesis of bovine TIMAP..... 32

2.3 Expression and purification of TIMAP.....33

2.4 Cloning of human Protein Phosphatase-1cγ and rat Protein Phosphatase-1cβ.... 35

2.5 Expression and Purification of rat PP-1cβ and human PP-1cγ.....35

2.6 Microcystin sepharose binding assays.....36

2.7 Generation of a Structural Model of TIMAP bound to PP-1c.....37

2.8 Phosphorylation of glycogen phosphorylase for phosphorylase a assays..... 38

2.9 Protein Phosphatase-1 inhibition assays.....39

2.9.1 Protein Phosphatase-1 inhibition assays using phosphorylase *a* substrate.....39

2.9.2 Evaluation of Protein Phosphatase-1 phosphorylase *a* assay results.....40

2.9.3 PP-1c inhibition assays using *p*-nitrophenol phosphate substrate.....41

2.9.4 Evaluation of PP-1c *p*-nitrophenol phosphate assay results..... 42

2.10 Phosphorylation of Protein Phosphatase-1 by cdk2/CyclinA.....43

Chapter 3: Results.....45

3.1 Modeling studies of TIMAP bound to PP-1c..... 45

3.2 Expression of GST-TIMAP.....50

3.3 GST-TIMAP binds to PP-1c on microcystin sepharose.....54

3.4 GST-TIMAP inhibits PP-1c activity toward phosphorylase *a*.....57

3.5 GST-TIMAP inhibition of PP-1c toward PNPP substrate.....62

3.6 Investigating the mechanism of PP-1c regulation by phosphorylated TIMAP.....67

3.6.1 Phospho-mimic mutants of TIMAP bind PP-1c on microcystin sepharose....67

3.6.2 Inhibition of PP-1c toward phosphorylase *a* by TIMAP phospho-mimic mutants....69

3.6.3 Phospho-mimic mutants of TIMAP exhibit reduced inhibition of PP-1c toward PNPP....72

3.7 GST-TIMAP blocks cdk2/CyclinA phosphorylation of the PP-1c C-terminal tail....74

3.8 GST-TIMAP$^{46-453}$ can be phosphorylated by cdk2/CyclinA....81

Chapter 4: Discussion, Conclusions, and Future Directions....83

4.1 Discussion....83

4.1.1 Predicted mechanism of interaction between TIMAP and PP-1....83

4.1.2 Expression and purification of GST-TIMAP....84

4.1.3 GST-TIMAP binds PP-1cβ and PP-1cγ attached to microcystin sepharose...85

4.1.4 GST-TIMAP inhibits PP-1c phosphorylase *a* activity....87

4.1.5 Phospho-mimic mutants of GST-TIMAP$^{46-453}$ inhibit PP-1cβ and PP-1cγ phosphorylase *a* activity with differing potency....89

4.1.6 TIMAP binding to PP-1c decreases cdk2/CyclinA phosphorylation of PP-1c....91

4.2 Summary and Conclusions....93

4.3 Future Directions....96

Bibliography....98

List of Tables

Table 3-1 Summary of the IC_{50} values for GST-TIMAP inhibition of PP-1cβ and PP-1cγ using ^{32}P-radiolabelled phosphorylase *a* as PP-1c substrate 61

Table 3-2 Summary of IC_{50} values for GST-TIMAP inhibition of PP-1cβ and PP-1cγ using *p*-nitrophenol phosphate as substrate.....66

List of Figures

Figure 1-1 The opposing action of Ser/Thr Kinases and Protein Phosphatase-1.....3

Figure 1-2 The PPP family of phosphatases share a similar catalytic site.....5

Figure 1-3 Amino acid sequences of three isoforms of the catalytic subunit of human PP-1c.....6

Figure 1-4 The Structure of the catalytic subunit of human PP-1..... 8

Figure 1-5 The catalytic site of PP-1c and mechanism of phosphate removal..... 9

Figure 1-6 The chemical structure of the cyclic heptapeptide toxin microcystin-LR...10

Figure 1-7 Catalytic Subunit of PP-1 with microcystin bound in the active site.....11

Figure 1-8 The RVXF binding groove of PP-1c is located in a region distinct from the phosphatase active site 14

Figure 1-9 Regulation of PP-1c by cdk2/CyclinA phosphorylation of a Thr residue the C-terminal tail..... 17

Figure 1-10 The phosphorylation state of myosin light chain is governed by the opposing activities of myosin phosphatase and myosin light chain kinase.....19

Figure 1-11 Myosin Phosphatase is a trimeric complex of PP-1cβ, MYPT1 and M20.....20

Figure 1-12 The Structure of MYPT1 bound to PP-1cβ.....22

Figure 1-13 The structural features of ankyrin repeats.....23

Figure 1-14 The MYPT family of proteins.....25

Figure 1-15 Amino acid sequence and domain structure of TIMAP.....27

Figure 3-1 A predicted structural model illustrating the potential mode of TIMAP binding to PP-1cβ.....48

Figure 3-2 A Close-up view of residues predicted to interact with the LAMR1.....49

Figure 3-3 Primary structure and features of GST-TIMAP utilized for the characterization of TIMAP regulation of PP-1c.....52

Figure 3-4 Preparations of GST-TIMAP and PP-1c visualized by SDS-PAGE 53

Figure 3-5 GST-TIMAP binds PP-1cβ and PP-1cγ immobilized on microcystin-sepharose.....55

Figure 3-6 GST does not interact with PP-1c and GST-TIMAP does not bind microcystin sepharose in the absence of PP-1c 56

Figure 3-7 GST-TIMAP is a potent inhibitor of human PP-1cβ phosphatase activity toward phosphorylase *a* substrate.....59

Figure 3-8 GST-TIMAP potently inhibits human PP-1cγ phosphatase activity toward phosphorylase *a* substrate.....60

Figure 3-9 Inhibition of PP-1cβ activity by GST-TIMAP using PNPP substrate.....64

Figure 3-10 GST-TIMAP inhibits PP-1cγ activity toward PNPP substrate.....65

Figure 3-11 Phospho-mimic double mutants of GST-TIMAP bind to PP-1cβ and PP-1cγ immobilized on microcystin sepharose.....68

Figure 3-12 TIMAP phospho-mimic mutants S333D/S337D and S333E/S337E do not differ from GST-TIMAP$^{46-453}$ in their inhibition of PP-1cβ activity toward phosphorylase *a* substrate.....70

Figure 3-13 Phospho-mimic mutants of TIMAP S333D/S337D and S333E/S337E demonstrate a reduced ability to inhibit PP-1cγ activity toward phosphorylase *a* substrate.....71

Figure 3-14 S333D/S337D and S333E/S337E are not potent inhibitors of PP-1c activity toward PNPP substrate: a comparison of PP-1c inhibition using 100nM GST-TIMAP in inhibition assays.....73

Figure 3-15 GST-TIMAP$^{46-292}$ reduces cdk2/CyclinA phosphorylation of PP-1cγ.....76

Figure 3-16 GST-TIMAP$^{46-453}$ reduces cdk2/CyclinA phosphorylation of PP-1cγ.....77

Figure 3-17 GST-TIMAP^{WT} reduces cdk2/CyclinA phosphorylation of PP-1cγ..... 78

Figure 3-18 Surface representation of the predicted model of TIMAP bound to PP-1c and the proximity of the cdk2/CyclinA phosphorylation site.....80

Figure 3-19 GST-TIMAP$^{46-453}$ can be phosphorylated by cdk2/CyclinA.....82

Figure 4-1 The basis of PP-1c regulation by TIMAP..... 95

List of Abbreviations

A_{405}	Absorbance, measured at 405nm
aa	amino acid
Adda	3-amino-9-methoxy-2,6,8-trimethyl-10-phenyl-deca-4,6-dienoic acid
ATP	Adenosine triphosphate
BSA	bovine serum albumin
CAAX	(Cys)-(aliphatic aa)-(aliphatic aa)-(Xaa)
cdk	cyclin dependent kinase
cpm	counts per minute
CTRL	control
D-Masp	D-erythro-β-methyl aspartic acid
DNA	deoxyribonucleic acid
DTT	dithiolthreitol
E.coli	*Escherichia coli*
EDTA	ethylene diamine tetraacetic acid
EGTA	ethylene glycol tetraacetic acid
FCP	transcription factor IIF-associated C-terminal domain phoshatase
FPLC	fast-performance liquid chromatography
G_M	glycogen-binding subunit of PP-1c from skeletal muscle
GSK-3	glycogen synthase kinase-3
GST	glutathione S-transferase
HEPES	4-(2-hydroxyl)-1-piperazineethanesulfonic acid
I-1	inhibitor-1
I-2	inhibitor-2
IC_{50}	concentration of inhibitor causing 50% inhibition of enzyme activity
IPTG	isopropyl-β-D-thiogalactoside
kDa	kilo Dalton
LAMR1	37kDa/67kDa non-integrin laminin receptor
MBS85	myosin binding subunit of mass 85kDa
MC	microcystin (microcystin-LR specifically)
MDCK	Madin-Darby canine kidney cells

Mdha	*N*-methyldehydroalanine
mRNA	messenger ribonucleic acid
MLC	myosin regulatory light chain
MLCK	myosin regulatory light chain kinase
MP	myosin phosphatase
MYPT	myosin phosphatase targeting subunit
NLS	nuclear localization signal
PP-1c	protein phosphatse-1 catalytic subunit
PP-2B	protein phosphatase-2B, or calcineurin
PP-*X*c	protein phosphatase-(4-7) catalytic subunit (PPP family members)
PCR	polymerase chain reaction
PKA	protein kinase A
PMSF	phenylmethylsulfonyl fluoride
PNPP	*p*-nitrophenol phosphate
PPP	phosphoprotein phosphatase family
PPM	Mg^{2+}-dependent phosphoprotein phosphates family
SDS-PAGE	sodium dodecyl sulfate-polyacrylamide gel electrophoresis
SMART	simple modular architecture research tool
TCA	trichloroacetic acid
TIMAP	TGFβ-inhibited membrane associated protein
TGFβ	transforming growth factor β
Tris-HCl	trishydroxymethylaminomethane hyrdochloride
WT	wildtype
Xaa	any amino acid

Standard Amino Acids

Glycine	Gly	G
Alanine	Ala	A
Valine	Val	V
Leucine	Leu	L
Isoleucine	Ile	I
Methionine	Met	M
Proline	Pro	P
Phenylalanine	Phe	F
Tryptophan	Trp	W
Serine	Ser	S
Threonine	Thr	T
Tyrosine	Tyr	Y
Asparagine	Asn	N
Glutamine	Gln	Q
Cysteine	Cys	C
Lysine	Lys	K
Arginine	Arg	R
Histidine	His	H
Aspartic Acid	Asp	D
Glutamic Acid	Glu	E

Chapter 1: Introduction

1.1 Reversible phosphorylation

Reversible phosphorylation of proteins is an exquisite means of control that regulates almost every aspect of cell life. The importance of this process is embodied in the fact that at least 30% of proteins encoded in the human genome can be phosphorylated on serine (Ser), threonine (Thr) or tyrosine (Tyr) residues [1,2]. The focus of this thesis will be on the reversible phosphorylation of serine and threonine residues. Protein phosphorylation is reversible due to the action of two separate enzymes: protein kinases and protein phosphatases. Protein kinases catalyze the addition of phosphate to proteins, and it is thought that the human genome encodes for ~400 serine/threonine kinases [3]. Protein phosphatases are the opposite - they catalyze the removal of phosphate groups from proteins, and are outnumbered by their kinase counterparts, as there are approximately 25 serine/threonine phosphatase catalytic subunits [3]. Reversible phosphorylation plays a role in many processes in life, from cell cycle progression, muscle contraction, glycogen metabolism, and even learning and memory. Phosphorylation modulates these processes in a myriad of ways: by increasing or decreasing biological function of proteins, marking proteins for life or destruction, disrupting or facilitating protein-protein interactions or even changing the cellular location of proteins [1].

Underlining the importance of reversible phosphorylation of proteins is that aberrant regulation of this process can cause disease. This is exemplified in the quest to utilize both protein kinase and phosphatase inhibitors as drug targets [4-6]. Protein kinases are very specific in the phosphorylation of their substrates, and as a result, make

good targets for drugs [4]. In contrast, Ser/Thr protein phosphatases tend to be very broad in their substrate specificity, making it more difficult to target their activity with inhibitors. However, one of the more specific Ser/Thr phosphatases, Protein Phosphatase 2-B (PP-2B or calcineurin) is a major drug target, and the most widely used immunosuppressant drug cyclosporine is a potent inhibitor of this phosphatase [7].

The Ser/Thr Protein phosphatases do not directly oppose the action of a specific Ser/Thr protein kinase. Protein phosphatases achieve specificity in the form of regulatory proteins [8,9]. The classical example of this is embodied in Protein Phosphatase-1 (PP-1c). PP-1c dephosphorylates serine and threonine residues of a huge number of different substrates. PP-1c gains its specificity in the form of a vast array of regulatory subunits which modulate its phosphatase activity both spatially and temporally, and this results in tight control over the broad range of activity of the catalytic subunit. Figure 1-1 illustrates this concept.

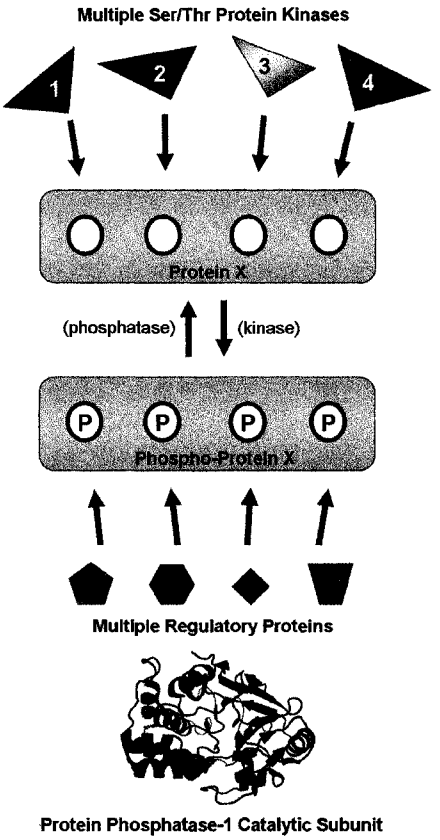

Figure 1-1. The opposing action of Ser/Thr Kinases and Protein Phosphatase-1. The activity of Ser/Thr protein kinases is very specific as opposed to the activity of the Ser/Thr phosphatase Protein Phosphatase-1 (PP-1c). Ser/Thr kinases greatly outnumber their phosphatase counterparts. While each kinase may phosphorylate a specific site on a target protein, PP-1c can dephosphorylate many sites of a vast number of different proteins. Specificity is conferred upon PP-1c by regulatory proteins which target PP-1c to specific cellular locations and substrates.

1.1.1 Ser/Thr Phosphatases

The Ser/Thr phosphatases have historically been categorized on their preference dephosphorylating the β or α subunit of phosphorylase kinase, and their sensitivity to inhibitors [10]. Type 1 phosphatase, or Protein Phosphatase-1 (PP-1c) dephosphorylates the β subunit of phosphorylase kinase and is inhibited by I-1 and I-2. Type 2 phosphatases are insensitive to inhibition by I-1 and I-2 and dephosphorylate the α subunit of phosphorylase kinase. The type 2 phosphatases are subdivided further on the

basis of their requirement for divalent cations. Protein Phosphatase-2A (PP-2Ac) is active in the absence of divalent cations, while Protein Phosphatase-2B (PP-2B, also known as calcineurin) and Protein Phosphatase-2C (PP-2C) require divalent cations for activity [10].

With advances in molecular cloning, several more Ser/Thr phosphatases have been identified, leading to re-classification of the Ser/Thr phosphatases into separate families. The phosphoprotein phosphatase (PPP) family consists of PP-1c, PP-2Ac, PP-2B (calcineurin), PP-5, and novel members PP-4, PP-6 and PP-7. PP-2C is the sole member of the PPM family, classified on the basis of its dependency on Mg^{2+} ions for activity [2,5,10,11]. There is also another Mg^{2+} dependent family recently characterized, the FCP family, which has one member [3,11].

PP-1c, PP-2Ac and PP-2B of the PPP family all share a highly homologous 280 amino acid catalytic domain, and are most divergent in their non-catalytic N- and C-terminal regions. Figure 1-2 illustrates the similarity of the active sites of these phosphatases. Of the three enzymes, calcineurin has the most substrate specificity, while PP-1c and PP-2Ac have broad substrate specificity. Due to their wide and often overlapping range of substrates, it is necessary to have tight control over these enzymes, both of spatial location and catalytic activity. This control comes in the form of regulatory proteins which direct and modulate PP-1c and PP-2Ac phosphatase activity. The regulation of PP-1c will be the focus of this thesis.

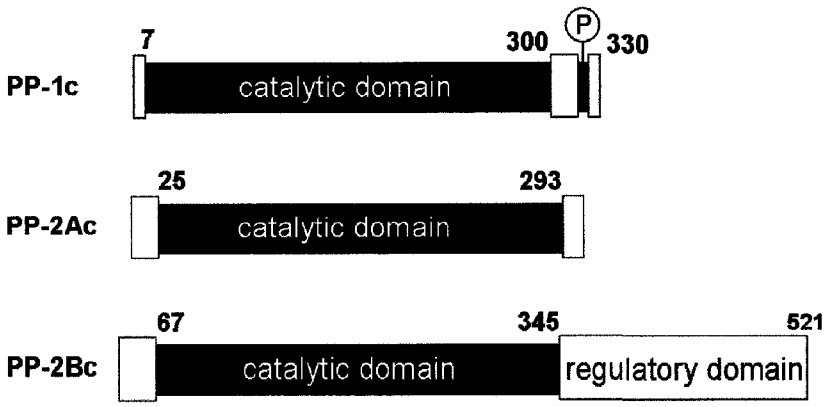

Figure 1-2. The PPP family of phosphatases share a similar catalytic site.
Diagrams of the catalytic subunits of PP-1c, PP-2Ac and PP-2Bc (calcineurin catalytic subunit) are shown highlighting the similarity of the active sites of the three phosphatases. The catalytic site of each phosphatase is composed of a core 280 amino acid domain which is highly homologus between the PPP phosphatases. The phosphatases differ in their N- and C-terminal regions. PP-1c has a regulatory phosphorylation site in its C-terminal domain, and PP-2Bc has a regulatory domain which regulatory proteins bind to modulate activity of the phosphatase.

1.2. Protein Phosphatase-1

1.2.1 Isoforms and tissue expression of Protein Phosphatase-1 catalytic subunit

PP-1c is a 37 kDa protein widely conserved amongst eukaryotes. Mammals express 4 isoforms of PP-1c, generated from 3 distinct genes. The 4 isoforms are PP-1cα, PP-1cβ (also known as PP-1cδ), PP-1cγ1 and PP-1cγ2. PP-1cγ1 and PP-1cγ2 are encoded by the same gene and are splice variants. (PP-1cγ1 will be referred to as PP-1cγ in the rest of this thesis.) A comparison of the sequences of PP-1cα, PP-1cβ and PP-1cγ is depicted in figure 1-3.

```
                10         20         30         40         50         60
PP1α  MSDSEKLNLD SIIGRLLEVQ GSRPGKNVQL TENEIRGLCL KSREIFLSQP ILLELEAPLK
PP1β  MADGE-LNVD SLITRLLEVR GCRCGKIVQM TEAEVRGLCI KSREIFLSQP ILLELEAPLK
PP1γ  MADLDKLNID SIIQRLLEVR GSKPGKNVQL QENEIRGLCL KSREIFLSQP ILLELEAPLK

                70         80         90        100        110        120
PP1α  ICGDIHGQYY DLLRLFEYGG FPPESNYLFL GDYVDRGKQS LETICLLLAY KIKYPENFFL
PP1β  ICGDIHGQYY DLLRLFEYGG FPPESNYLFL GDYVDRGKQS LETICLLLAY KIKYPENFFL
PP1γ  ICGDIHGQYY DLLRLFEYGG FPPESNYLFL GDYVDRGKQS LETICLLLAY KIKYPENFFL

               130        140        150        160        170        180
PP1α  LRGNHECASI NRIYGFYDEC KRRYNIKLWK TFTDCFNCLP IAAIVDEKIF CCHGGLSPDL
PP1β  LRGNHECASI NRIYGFYDEC KRRFNIKLWK TFTDCFNCLP IAAIVDEKIF CCHGGLSPDL
PP1γ  LRGNHECASI NRIYGFYDEC KRRYNIKLWK TFTDCFNCLP IAAIVDEKIF CCHGGLSPDL

               190        200        210        220        230        240
PP1α  QSMEQIRRIM RPTDVPDQGL LCDLLWSDPD KDVQGWGEND RGVSFTFGAE VVAKFLHKHD
PP1β  QSMEQIRRIM RPTDVPDTGL LCDLLWSDPD KDVQGWGEND RGVSFTFGAD VVSKFLNRHD
PP1γ  QSMEQIRRIM RPTDVPDQGL LCDLLWSDPD KDVLGWGEND RGVSFTFGAE VVAKFLHKHD

               250        260        270        280        290        300
PP1α  LDLICRAHQV VEDGYEFFAK RQLVTLFSAP NYCGEFDNAG AMMSVDETLM CSFQILKPAD
PP1β  LDLICRAHQV VEDGYEFFAK RQLVTLFSAP NYCGEFDNAG GMMSVDETLM CSFQILKPSE
PP1γ  LDLICRAHQV VEDGYEFFAK RQLVTLFSAP NYCGEFDNAG AMMSVDETLM CSFQILKPAE

               310        320
PP1α  KNKGKYGQFS GLNPGGRPIT PPRNSA--K-AKK
PP1β  K-KAKY-QYG GLN-SGRPVT PPRTANPPK--KR
PP1γ  K-K-K----- -PNAT-RPVT PPR-GMITKQAKK
```

Figure 1-3. Amino acid sequences of three isoforms of the catalytic subunit of human PP-1c.
The figure depicts sequence alignments of three isoforms of human PP-1c. The isoforms differ mainly in the N- and C-terminal regions. The numbers across the top of the sequences indicate amino acid position. In addition to the sequences shown here, PP-1cγ is alternatively spliced to produce the testis specific PP-1cγ2.

The different isoforms of PP-1c are ubiquitously expressed, with the exception of PP-1cγ2, which is expressed in the testis. PP-1cβ is the major isoform expressed in skeletal muscle [3,12]. All PP-1c isoforms are expressed in the same cells, however separate sub-cellular locations of each isoform have been identified [13]. It has been difficult determining roles of each isoform using knock-out mice as expression of other isoforms increases to compensate for the loss of the missing PP-1c [14].

It is thought that the differences in the N- and C-terminal sequences of PP-1c isoforms allow for regulatory proteins to distinguish and interact with specific PP-1c isoforms and modulate their activity to specific cellular functions and locations [15,16].

1.2.2 Structure of the PP-1 Catalytic Subunit (PP-1c)

The 3-dimensional structure of PP-1c has now been solved by several groups [16-24]. The structure of PP-1c is ellipsoidal in shape, and the active site is at the centre of a β-sandwich in the core of the enzyme. The active site is located at the junction of three grooves in the surface of the phosphatase. These grooves are known as the C-terminal groove, acidic groove and hydrophobic groove, based on the physical properties of each (i.e. the acidic groove contains many acidic residues) and they are highlighted in figure 1-4. In the active site are two divalent metal ions, the identities of which are presumed to be Fe^{2+} and Mn^{2+}, but this is not known for certain. This is due to the fact that all of the crystal structures of PP-1c have been solved using recombinant phosphatase (which requires Mn^{2+} for activity), and as such the three-dimensional structures of PP-1c contain two Mn^{2+} ions in the active site. The active site metal ions are coordinated by residues that are conserved among the PPP phosphatases. These metals are crucial for catalysis, as they coordinate a nucleophilic water molecule in the active site and enhance the electrophilicity of the phosphorus of the phosphate being removed [17,19]. The catalytic mechanism by which PP-1c removes phosphate groups from proteins is illustrated in figure 1-5.

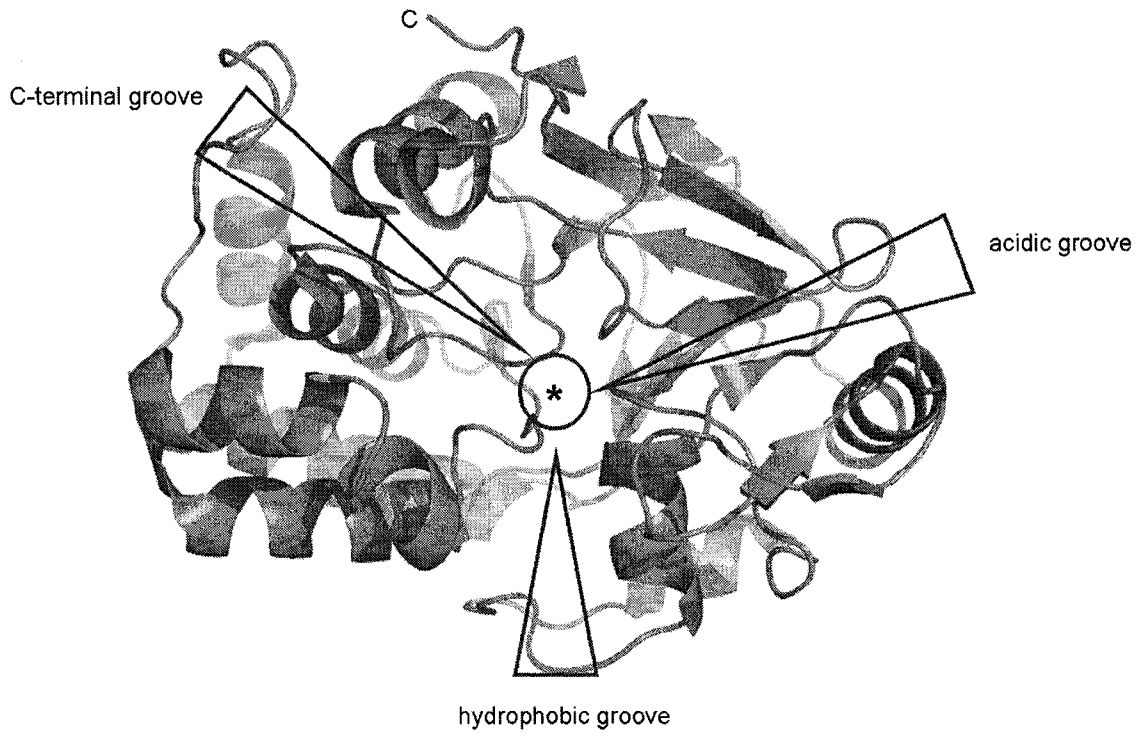

Figure 1-4. The Structure of the catalytic subunit of human PP-1.
There are three grooves in the surface of PP-1c. The C-terminal groove is composed of residues near the C-terminus. The acidic groove contains acidic residues and the hydrophobic groove contains hydrophobic residues. The three grooves converge at the active site (denoted by an asterisk).

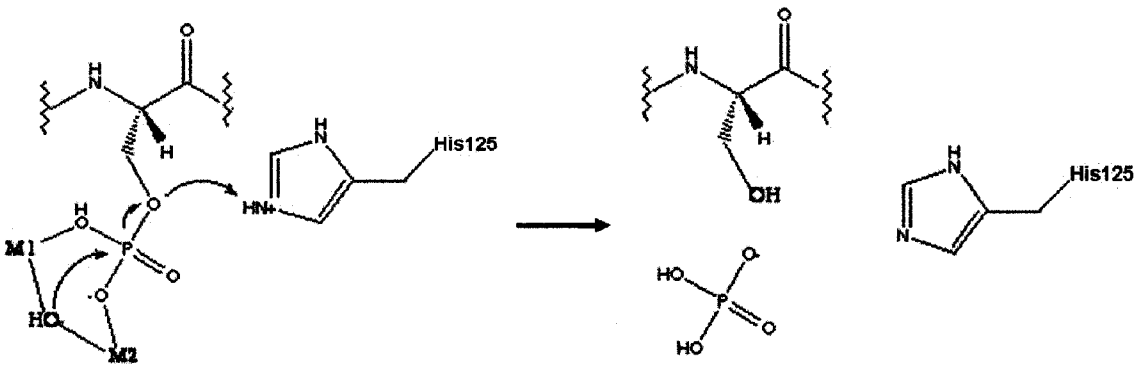

Figure 1-5. The mechanism of phosphate hydrolysis by PP-1c.
Two metal atoms (M1 and M2) are coordinated in the phosphatase catalytic site by several residues that are conserved among PPP phosphatases (residues not shown). In the proposed catalytic mechanism the OH^- molecule acts as a nucleophile that attacks the phosphorus atom, shown in the left panel. The arrows denote movement of electrons. The two metal ions are thought to coordinate and enhance the nucleophilicity of the OH^-. His125 of PP-1c donates a proton to the leaving group, which is a Serine residue in this figure. The proposed mechanism is a single step catalytic reaction [2,17,19].

1.2.3 Inhibition of PP-1c by microcystin, an environmental toxin

To date several environmental toxins that inhibit the activity of PP-1c have been identified and these are reviewed in [5,25,26]. One such toxin is microcystin, a cyclic peptide consisting of seven amino acids. Microcystin is named after the cyanobacteria it was first isolated from, *Microcystis aeruginosa*. To date there have been over 50 forms of microcystin identified. This is due to the fact that there are two variable amino acid positions in the cyclic peptide. The different microcystins are identified by suffix letters indicating the identity of the amino acids at the variable positions. For instance, Microcystin-LR (the most abundant form of the toxin) contains Leu and Arg at the two variable amino acid positions. The structure of microcystin is depicted in figure 1-6. In this thesis, "microcystin" will refer to microcystin-LR, unless noted otherwise. Microcystin is a potent inhibitor of PP-1c, with an IC_{50} of 0.3nM for PP-1cγ and 5nM for

PP-1cβ. Microcystin inhibits the phosphatase activity of all members of the PPP Ser/Thr phosphatase family in the nanomolar range with the exception of calcineurin, which is inhibited in the micromolar range.

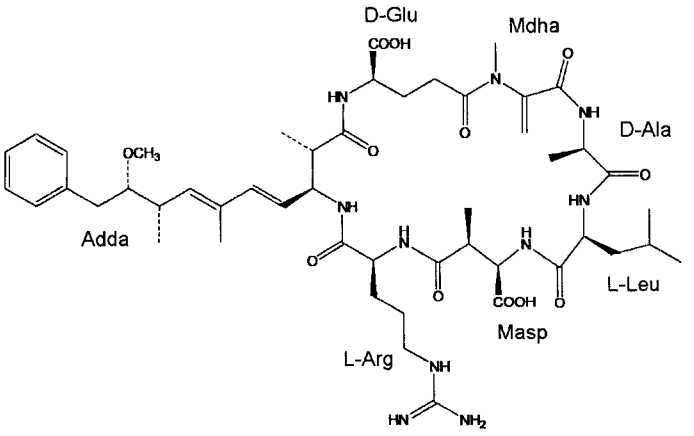

Figure 1-6. The chemical structure of the cyclic heptapeptide toxin microcystin-LR. Microcystin consists of seven amino acids, each of which is labeled in the figure. The L-Arg and L-Leu positions are variable. The non-standard amino acids in microcystin are: the unique β-amino acid Adda (3-amino-9-methoxy-2,6,8-trimethyl-10-phenyl-deca-4,6-dienoic acid), Mdha (*N*-methyldehydroalanine), and D-Masp (D-erythro-β-methyl aspartic acid).

The crystal structure of PP-1c in complex with microcystin-LR (shown in figure 1-7) reveals that microcystin binds to PP-1c by interacting at three sites on the phosphatase including the hydrophobic groove, the metal binding site of the catalytic centre, and the edge of the C-terminal groove (the β12-13 loop) [19]. The hydrophobic Adda side of microcystin chain packs into the hydrophobic groove of PP-1c, forming the first of the three interactions. A Leu side chain of microcystin packs closely to Tyr272 of PP-1c, an amino acid situated on the β12-β13 loop of the phosphatase. The β12-13 loop is known to be important for inhibitor binding to PP-1c [24,27]. A carbon atom of the Mdha side chain of microcystin can also form a covalent bond to Cys273 of the β12-13 loop, however this covalent bond is not necessary for inhibition of PP-1c phosphatase activity

[28]. Microcystin also interacts with a catalytic water molecule in the active site of PP-1c. It is thought that the sum of these interactions give rise to the potent inhibition of PP-1c phosphatase activity by microcystin.

Figure 1-7. Catalytic Subunit of PP-1 with microcystin bound in the active site. Microcystin (shown in yellow in stick representation) binds in the active site of PP-1c and inhibits phosphatase activity by blocking substrate access to the metal ions and water molecules involved in catalysis. In the figure the Adda side chain of microcystin is seen bound in the hydrophobic groove.

1.2.4 Microcystin sepharose: an important tool for purification and identification of PP-1c complexes

The ability of microcystin to bind at the active site of PP-1c has been exploited as a form of affinity chromatography that has been useful in purifying PP-1c and several regulatory proteins that bind to PP-1c [29,30]. This chromatography media has been generated by covalently attaching microcystin to sepharose. This attachment is carried out by linking the methyl dehydroxy alanine group of microcystin to aminoethanethiol. The aminoethanethiol-microcystin is attached to *N*-hydroxysuccinimide-activated thiol-sepharose. The result is a very specific form of affinity chromatography which binds to the PP-1c active site. This provides an effective method of immobilizing PP-1c, allowing

for the study of regulatory proteins which bind to PP-1c at locations other than the active site.

1.3. Regulation of PP-1c

1.3.1 Controlling the activity of a promiscuous enzyme

As mentioned earlier, PP-1c is considered a promiscuous enzyme due to its wide tissue expression, high level of activity and broad range of substrates and functions. A consequence of this is that there must be tight regulation of PP-1c activity in order to maintain a balance with the kinases it opposes, and coordinate dephosphorylation for normal cellular function. Because of its vast substrate specificity, PP-1c must be regulated in several ways, notably subcellular location, substrate specificity, and catalytic activity. This is achieved with protein partners called regulatory subunits [8]. Other methods of regulation of PP-1c include phosphorylation of a Thr residue of the C-terminal tail (i.e. Thr311 for PP-1cγ) by cyclin-dependent kinase2/CyclinA which serves to inhibit phosphatase activity.

1.3.2 The RVXF motif mediates regulatory subunit binding to PP-1c

To date there are over 200 regulatory proteins identified which bind to PP-1c (Mathieu Bollen, personal communication) and while some of these proteins may be similar, the bulk of this population is structurally unrelated [8]. There is one common structural motif these unrelated regulatory proteins all contain which targets them to PP-1c. This structural motif is known as the RVXF motif, named for the short conserved stretch of amino acids based on the consensus (R/K)(V/I)(Xaa)(F) amino acid sequence (where Xaa

is any amino acid but Proline) [18,31]. There is an amount of degeneracy allowed in the RVXF motif that still allows binding to PP-1c, and it is thought that the more variation there is in the RVXF sequence, the more transient the interaction is between PP-1c and the regulatory protein. Structural studies have shown that the RVXF motif binds to a hydrophobic pocket on PP-1c at a location remote from the active site as shown in figure 1-8 [18]. The interaction is primarily made between hydrophobic residues of PP-1c in the RVXF binding groove and the (V) and (F) residues of the RVXF motif. These hydrophobic residues of PP-1c involved in mediating the RVXF-PP-1c interaction are conserved among all human isoforms of PP-1c and through many vertebrate species [18].

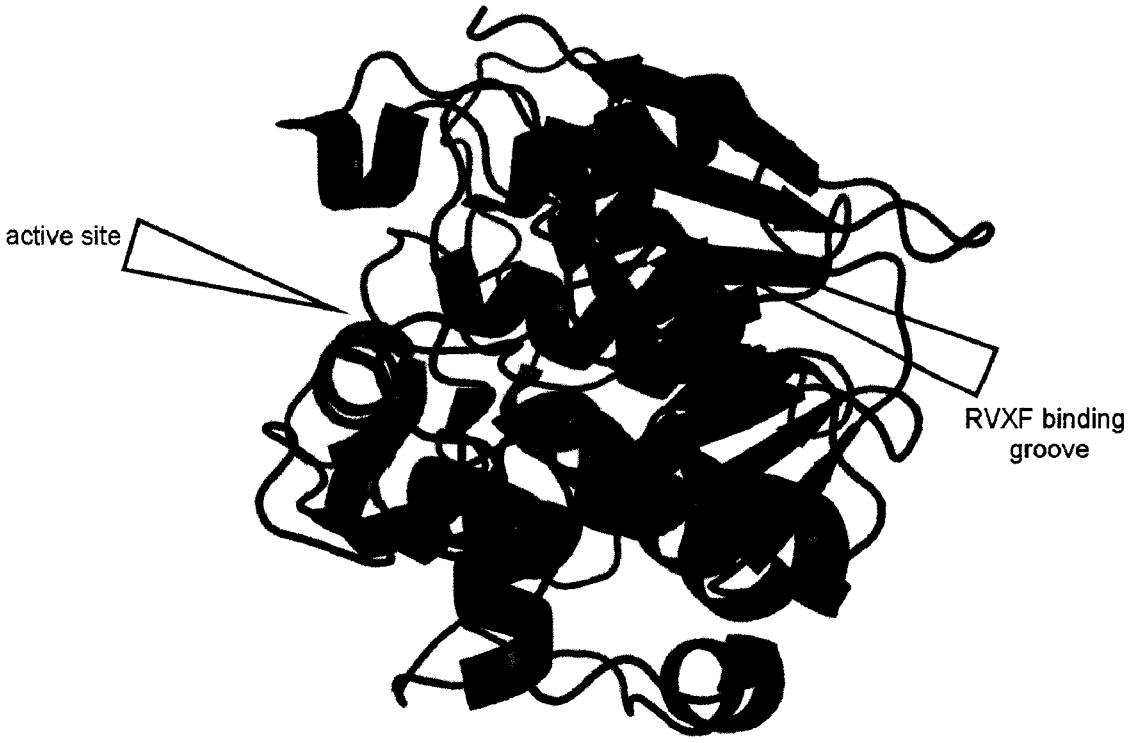

Figure 1-8. The RVXF binding groove of PP-1c is located in a region distinct from the phosphatase active site.
The three dimensional structure of the catalytic subunit of PP-1c is pictured in green, and the purple arrows point out the active site of the phosphatase and the location of the RVXF binding groove. This representation of PP-1c is a 90° rotation (to the left) of the structure illustrated in figure 1-4. Highlighted by a purple arrow, the RVXF binding groove is the site where the RVXF motif of PP-1c regulatory subunits bind to the phosphatase.

Binding of regulatory proteins to PP-1c is mutually exclusive. This is supported by the observations that short peptides containing an RVXF motif can bind competitively and disrupt binding of regulatory proteins to PP-1c [18,32]. In addition, mutation of the hydrophobic (V) or (F) residue can weaken or abolish binding of the regulatory protein [31]. It is important to note that binding to the RVXF groove of PP-1c has little effect on the conformation of the enzyme or catalytic activity. This is evident in the solved structure of PP-1c with an RVXF motif peptide bound [18], as there is little difference in

the conformation and architecture of PP-1c compared to other solved structures of PP-1c. Since the RVXF motif of regulatory proteins has little effect on conformation and activity, it is thought that this motif serves as an anchor that makes initial contact with PP-1c and then enables weaker secondary interactions to be made between the phosphatase and the regulatory protein, which can modulate phosphatase activity or substrate specificity [31,33].

1.3.3 Regulating catalytic activity of PP-1c by endogenous inhibitors

One mode by which PP-1c regulatory proteins modulate phosphatase catalytic activity is by inhibiting it. Two examples of PP-1c regulatory proteins that achieve this effect are Inhibitor-1 (I-1) and Inhibitor-2 (I-2). Both I-1 and I-2 are small, unstructured, heat stable cellular proteins that inhibit the activity very potently in the nanomolar range [34]. Both I-1 and I-2 contain an RVXF motif that facilitates their binding to PP-1c.

I-1 is an 18 kDa protein that is phosphorylated in order to inhibit PP-1c. I-1 is best known for its role in adrenalin signaling, where it is phosphorylated by Protein Kinase A (PKA) and inhibits the activity of PP-1 catalytic subunits [35]. In this context, there is a drive for increased protein kinase activity and decreased phosphatase activity. This is reflected by the fact that as PKA activity increases, levels of phosphorylated I-1 increase, inhibiting a pool of PP-1c, maintaining low phosphatase activity.

Inhibitor-2 is a 23 kDa protein which does not need to be phosphorylated to inhibit PP-1c. I-2 inhibits PP-1c in a two step process; the first being rapid inhibition, and the second being the formation of latent complex resulting in long term inhibition of the PP-1c. This latent complex eventually dissociates after phosphorylation of I-2 by

Glycogen Synthase Kinase-3 (GSK-3). The exact roles of I-2 are still unclear, however it has been suggested that I-2 inhibition of PP-1c regulates cardiac contractility [36], and cell division [37]. It has been proposed that the I-2 complex with PP-1c may serve as a chaperone promoting the correct fold of the phosphatase [38]. It is also thought that the latent inactive complex of I-2-PP-1c maintains a pool of PP-1c in an inactive state, ready to interact with regulatory proteins and targeting subunits upon reactivation and dissociation from I-2 [38].

1.3.4 Regulation of PP-1c by phosphorylation

The phosphorylation of substrates by cyclin dependent kinases (cdk's) results in the ordered progression through the cell cycle [39,40]. Cyclin dependent kinases form complexes with different Cyclin proteins for maximal kinase activity, and different Cyclins specify cdk activity through different stages of the cell cycle.

Substrates for cdk2 possess a consensus phosphorylation site consisting of Ser/Thr-Pro-Xaa-Lys/Arg (where Xaa can be any amino acid) [41]. PP-1c is known to be a substrate for cdk2/CyclinA, and cdk2/CyclinA phosphorylates PP-1c at a Thr residue in the C-terminal tail of the phosphatase [42-44]. This Thr corresponds to T320 in PP-1cα, T317 in PP-1cβ and T311 in PP-1cγ. The phosphorylation site is found in the sequence **T**PPR (the phosphorylation site is highlighted in bold), which is conserved for all isoforms of PP-1c.

The phosphorylation of PP-1c by cdk2/CyclinA has an inhibitory effect on phosphatase activity. This PP-1c inhibition is thought to be auto-inhibitory, and the phosphorylated C-terminal tail is thought to fold back on the phosphatase catalytic

subunit and block access to the active site. It has been suggested that the phosphorylated C-terminal tail folds along the C-terminal groove (figure 1-4) and places the phospho-Thr residue in the active site where it serves as a pseudo-substrate blocking the active site and decreasing PP-1c activity [17]. This effect is illustrated in figure 1-9. This phosphorylation dependent inhibition of PP-1c can slowly be relieved by auto-dephosphorylation of the C-terminal tail, returning PP-1c to an active state.

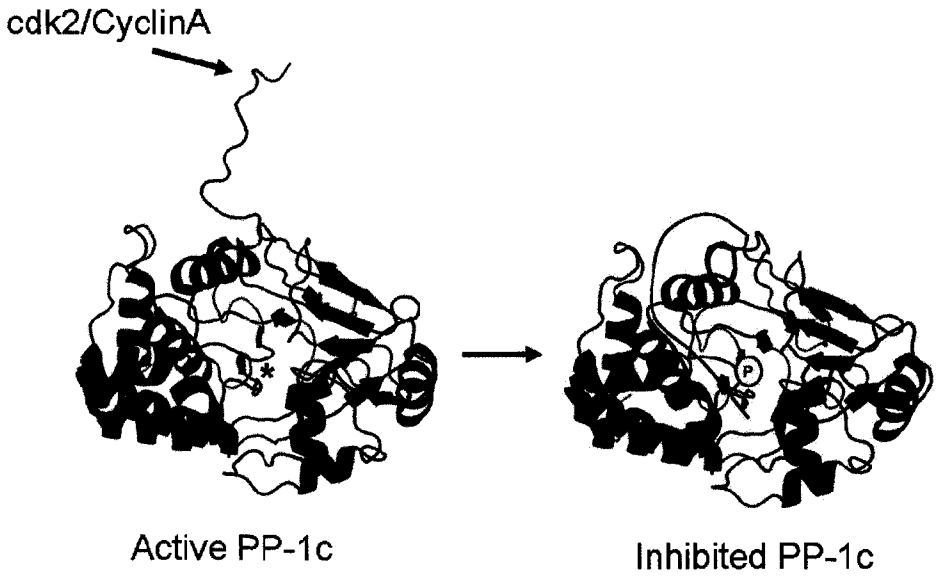

Figure 1-9. Regulation of PP-1c by cdk2/CyclinA phosphorylation of a Thr residue the C-terminal tail.
Depicted in blue is a diagram of PP-1c in an active state. The active site of the phosphatase is denoted by an asterisk. Upon phosphorylation by cdk2/CyclinA, the C-terminal tail is proposed to fold back on the active site along the C-terminal groove, placing the phospho-Thr residue in the active site. The phospho-Thr residue acts as a pseudo-substrate and blocks the active site from other substrates, inhibiting PP-1c activity.

The cellular significance of cdk2/CyclinA inhibitory phosphorylation of PP-1c is that it plays a role in signaling the exit from the G_1-phase of the cell cycle to S-phase.

When PP-1cα is mutated such that it cannot be phosphorylated and is kept constitutively active, the cell cycle halts in G_1-phase [44,45].

1.4 Regulation of PP-1c activity in smooth muscle relaxation

As mentioned earlier, regulatory subunits of PP-1c modulate the activity of PP-1c in different ways, such as deceasing catalytic activity, changing the subcellular location of PP-1c, or modifying the substrate specificity of PP-1c. A classical from of regulatory subunit regulation of PP-1c is exemplified in the modulation of PP-1c activity in smooth muscle relaxation. PP-1c is targeted to myosin by a regulatory protein termed the myosin phosphatase targeting subunit 1 (MYPT1). MYPT1 regulates both the substrate specificity and cellular location of PP-1c and will be discussed here.

Type II myosin is a motor complex that is associated with actin fibers in cells, and plays a role in the contraction and relaxation of smooth muscle [46]. Type II myosin consists of 2 myosin II heavy chains, and 2 myosin light chains (MLC). Phosphorylation of MLC by myosin light chain kinase (MLCK) at Ser19 facilitates contraction of smooth muscle. Dephosphorylation of MLC inhibits smooth muscle contraction and promotes relaxation, and this is performed by myosin phosphatase (MP), a holoenzyme complex containing PP-1cβ. Other processes mediated by the phosphorylation of MLC include formation of stress fibers and cell migration [46]. Thus it is the coordinated control of phosphorylation levels of MLC resulting from the balance between the activity of MP and MLCK that governs the process of smooth muscle contraction and other myosin functions. This is illustrated in figure 1-10.

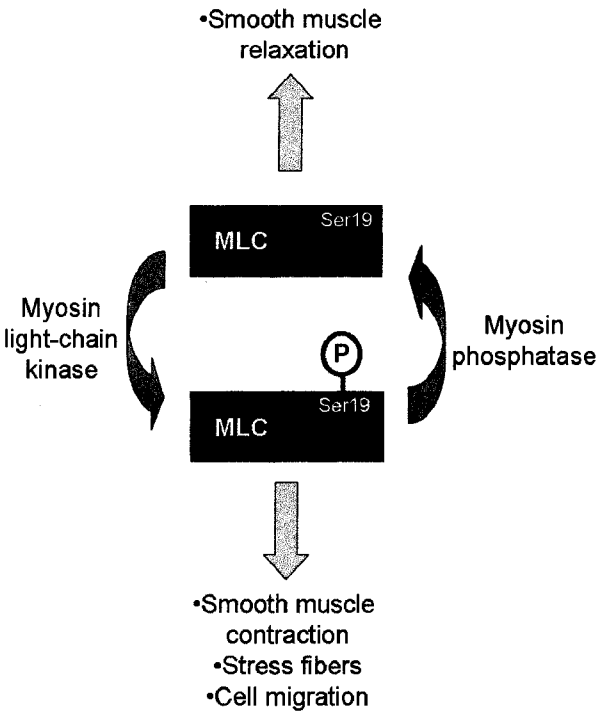

Figure 1-10. The phosphorylation state of myosin light chain is governed by the opposing activities of myosin phosphatase and myosin light chain kinase.
The phosphorylation of myosin light chain (MLC) on Ser19 by myosin light chain kinase results in contraction of smooth muscle and other cellular activities of the myosin complex. MLC is dephosphorylated by myosin phosphatase (a PP-1cβ holoenzyme) and this results in smooth muscle relaxation. The phosphorylation state of MLC is dependent on the relative activities of myosin light chain kinase or myosin phosphatase.

1.4.1 Myosin Phosphatase: A complex of PP-1cβ and regulatory subunits

Myosin phosphatase (MP) is a holoenzyme complex consisting of PP-1cβ, myosin phosphatase targeting subunit 1 (MYPT1), and a small 20 kDa protein M20 [47-49]. The composition of MP is depicted in figure 1-11. PP-1cβ is the PP-1c isoform present in myosin phosphatase [47]. The exact function of the M20 subunit is not known. MYPT1 is a PP-1c regulatory protein that binds PP-1cβ and targets it to myosin light chains, and specifically modulates PP-1cβ activity for this substrate. A description of PP-1c regulation by MYPT1 will follow.

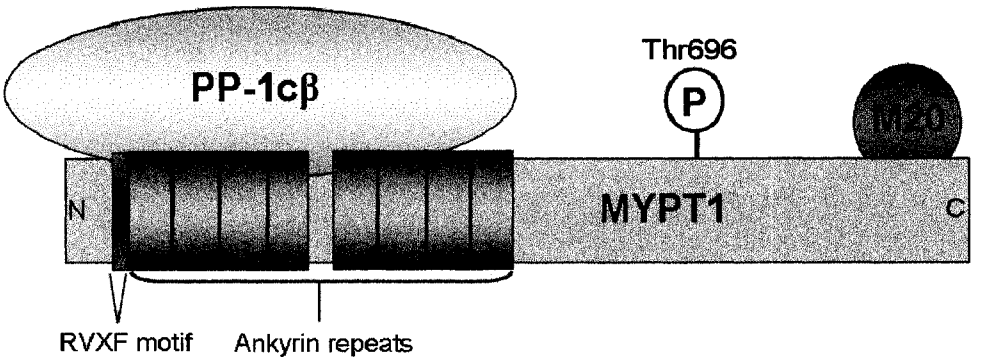

Figure 1-11. Myosin Phosphatase is a trimeric complex of PP-1cβ, MYPT1 and M20. The figure illustrates that myosin phosphatase is a trimeric holoenzyme composed of PP-1cβ, MYPT1, and M20. Other features of myosin phosphatase are depicted and are discussed in the text.

1.4.2 MYPT1 targets PP-1cβ to myosin

MYPT1 is a 110 kDa PP-1c regulatory protein that targets PP-1cβ to MLC. MYPT1 possesses a PP-1c binding RVXF motif in residues ^{35}KVKF^{38} (depicted in figure 1-11). As a component of myosin phosphatase and regulatory subunit of PP-1cβ, MYPT1 regulates the subcellular location of PP-1cβ, but also modulates the catalytic activity of the phosphatase. When in complex with MYPT1, PP-1cβ activity is increased toward its targeted substrate MLC, while at the same time phosphatase activity is inhibited toward other cellular substrates such as phosphorylase *a*. Monomeric PP-1cβ does not dephosphorylate MLC in the absence of MYPT1 [47,50]. MYPT1 is known to be phosphorylated at Thr696 by Rho-kinase, and this phosphorylation inhibits myosin phosphatase activity [51]. It is thought that the phosphorylated Thr residues folds into the active site of PP-1cβ and inhibits the phosphatase as a pseudo-substrate.

The crystal structure of MYPT1 (residues 1-299) in complex with PP-1cβ has been solved [16]. This is a significant crystal structure as it marked the first structure of a regulatory protein bound to PP-1c.

As can be seen in figure 1-12, MYPT1 binds to PP-1cβ via its RVXF motif and makes extensive contacts with the phosphatase via ankyrin repeats and an N-terminal arm. The structure illustrates that MYPT1 has 8 ankyrin repeats which bind and surround the C-terminal tail of PP-1cβ. Ankyrin repeats are a structural motif in proteins that are known to facilitate protein-protein interactions (more on ankyrin repeats will follow). These repeats make specific interactions with two Tyr residues in the C-terminal tail of the phosphatase. These Tyr residues are not present in the other PP-1c isoforms (refer to figure 1-3), and the structure suggests that specific interactions between the PP-1cβ C-terminal tail and MYPT1 are responsible for the preferential binding of PP-1cβ in myosin phosphatase. There is also an important interaction between a long arm formed by amino acids 1-34 of MYPT1 and the bottom portion of the PP-1cβ catalytic subunit. It is thought that the sum of the PP-1cβ interactions between the N-terminal 34 amino acids and the binding of the ankyrin repeats re-model the active site of PP-1cβ, making it more suited to dephosphorylate MLC, and unable to dephosphorylate other substrates such as phosphorylase *a*. This is supported by biochemical data indicating that the ankyrin repeat region is required for inhibition of PP-1cβ toward substrates other than MLC, and other studies which indicate that the N-terminal region of MYPT1 confers activity toward MLC [32,47,50].

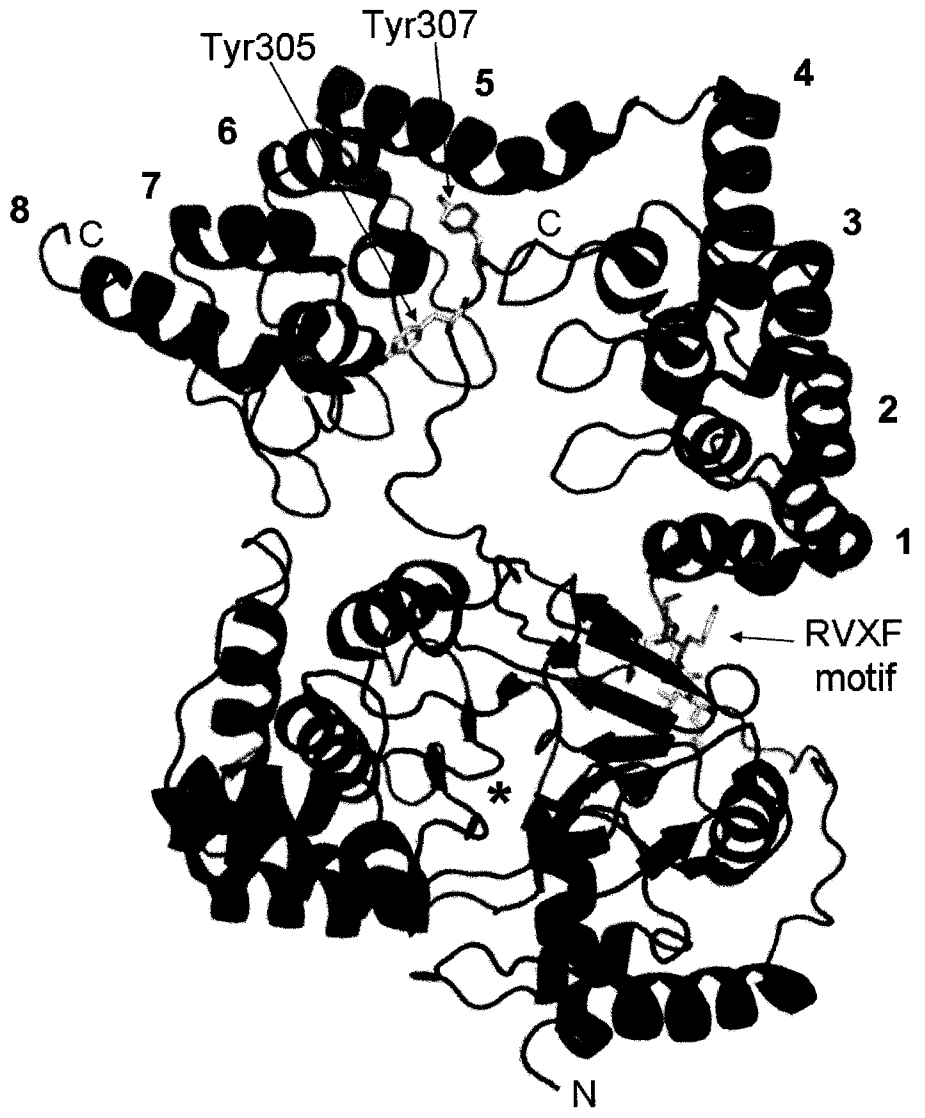

Figure 1-12. The Structure of MYPT1 bound to PP-1cβ.
MYPT1 (1-299) makes extensive contacts with PP-1cβ which remodel the active site of PP-1cβ, increasing activity toward myosin light chains while inhibiting phosphatase activity toward other substrates such as phosphorylase *a*. MYPT1 is on top, pictured in red, and PP-1cβ (pictured in blue) is in the centre surrounded by MYPT1. The RVXF motif of MYPT1 (shown in yellow in stick representation) binds to PP-1c in the RVXF binding groove (see figure 1-8). The ankyrin repeats of MYPT1 hug the C-terminal tail of PP-1cβ, and make specific interactions with Tyr305 and Tyr307 of the phosphatase (shown in stick representation in yellow). The N-terminal domain of MYPT1, which is known to activate PP-1cβ toward phosphorylated myosin light chain substrate wraps around the phosphatase contributing to the re-shaping of the catalytic site of PP-1cβ (denoted with an asterisk). The ankyrin repeats of MYPT1 are numbered 1-8.

1.4.3 Ankyrin Repeats: a structural motif facilitating protein-protein interactions

Ankyrin repeats are structural motifs in proteins that consist of a consensus 33 amino acid repeat [52-54]. The repeats are a structural feature of the three-dimensional fold of a protein, do not possess enzymatic activity, and are thought to function primarily in mediating protein-protein interactions.

Ankyrin repeats consist of a canonical (α-helix)-(loop)-(α-helix)-(β-hairpin loop) fold. This motif folds to a three-dimensional structure characterized by two anti-parallel α-helices stacked side by side, followed by a β-hairpin loop that extends out from the helix bundle at an angle of 90°. The structure of ankyrin repeats is illustrated in figure 1-13. As multiple repeats pack together, the helices stack against each other, and the β-hairpin loops pack together, forming a platform having interfaces suitable for other proteins to interact with.

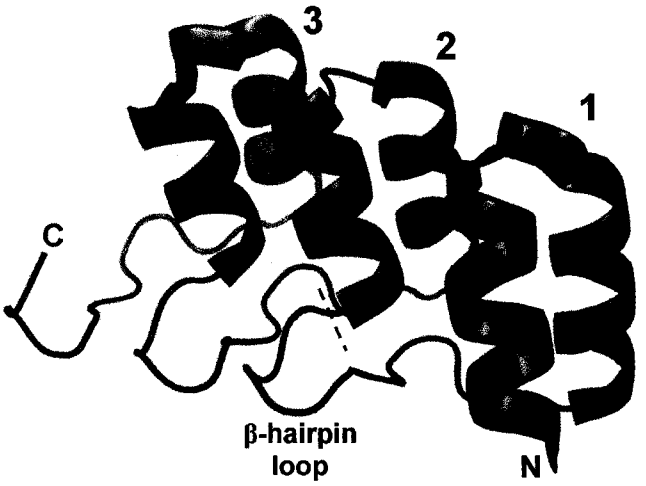

Figure 1-13. The structural features of ankyrin repeats.
Shown are three ankyrin repeats (numbered) and their structural features. The dashed line denotes the boundary between repeats 1 and 2. In an individual repeat two α-helices pack together in an anti-parallel manner and are followed by a β-hairpin loop. The α-helices of repeats 1 and 2 are numbered. The loops extend outward from the helices at an angle of 90°. The ends of the loop are often involved in protein-protein interactions. Interactions can also occur on the outside face of the helices (along the surface of α-helix2 in this figure).

1.4.4 The MYPT family of proteins

The MYPT family of proteins contains four more members in addition to the original and best characterized member MYPT1. These other members vary in their degree of sequence similarity to MYPT1, however the most divergent member of the family still possesses 31% sequence identity to MYPT1. The family includes MYPT1, MYPT2, Myosin Binding Subunit of mass 85 kDa (MBS85), MYPT3, and TGFβ-Inhibited Membrane Associated Protein (TIMAP) [48,49] which are illustrated in figure 1-14.

MYPT2 is a 982 residue protein with a mass of 110 kDa, and is highly homologous to MYPT1, sharing a sequence identity of 61% [55]. MYPT2 is expressed preferentially in heart, skeletal muscle, and brain, and was found to be the major myosin targeting subunit for myosin phosphatase in striated muscle [12]. MBS85 is another closely related protein to MYPT1 and shares 39% sequence identity with MYPT1. MBS85 is an 85 kDa protein which shares many of the same structural features as MYPT1 [56]. However little is known about substrates and roles of MBS85. A common trait among MYPT1, MYPT2 and MBS85 is that they all share the common ability to target PP-1cβ and facilitate dephosphorylation of MLC, and inhibit PP-1cβ activity toward phosphorylase *a* [48,49].

A 58 kDa protein, MYPT3 is the smallest member of the MYPT family [57]. MYPT3 shares similar features with other family members such as ankyrin repeats and a PP-1c targeting RVXF motif, but differs in the C-terminal region, where MYPT3 contains a CAAX box motif. A CAAX box motif is a Cys residue followed by any two aliphatic amino acids AA, and then any amino acid, X. This motif is a prenylation site that localizes the protein to the cell membrane. The feature of MYPT3 that sets it apart

from other MYPT family members is its ability to inhibit PP-1c activity toward MLC and phosphorylase *a* [57]. Like other members of the MYPT family, MYPT3 is thought to associate preferentially with PP-1cβ [58]. MYPT3 is known to be phosphorylated by PKA at Ser 351 and this phosphorylation increases associated PP-1c activity toward substrates [58]. MYPT3 has recently been shown to mediate the translocation of a transcription factor to the nucleus in a manner that is dependent on its ability to inhibit PP-1c activity [59].

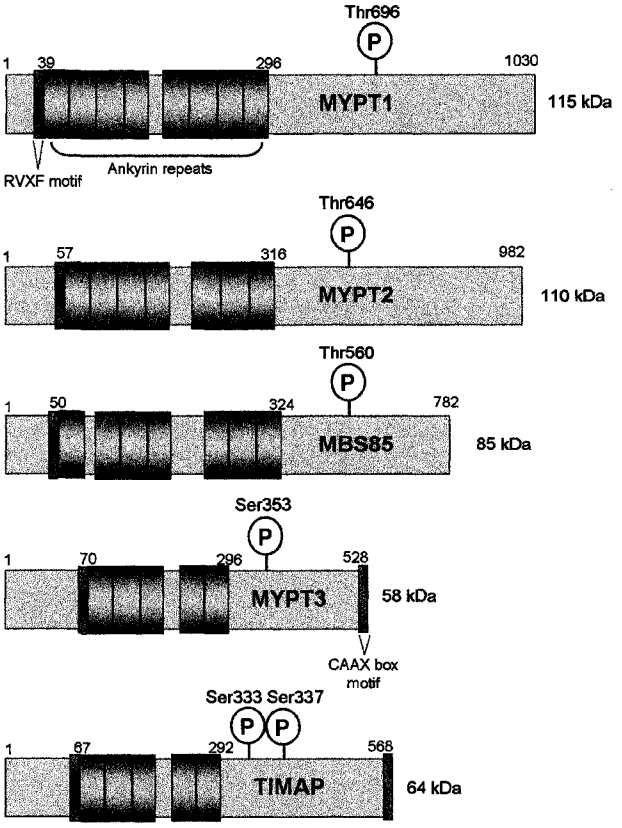

Figure 1-14. The MYPT family of proteins.
Shown is the domain structure of the current known members of the MYPT family of proteins. Amino acid numbers are indicated in the figure. Each member possesses an RVXF motif which facilitates interaction with PP-1c, located immediately N-terminal a region of ankyrin repeats. Each MYPT family member has a regulatory phosphorylation site which inhibits PP-1c activity (in the case of MYPT1, MYPT2 and MBS85) or activates PP-1c activity (in the case of MYPT3 and TIMAP). The masses of each protein are indicated. MYPT3 and TIMAP both contain a CAAX box motif localizing each to the cell membrane.

1.4.5 TGF-β-Inhibited Membrane Associated Protein: the coolest member of the MYPT family

TGF-β-Inhibited Membrane Associated Protein (TIMAP) is the newest characterized member of the MYPT family. TIMAP shares 31% sequence identity with MYPT1, but is most closely related to MYPT3, with which it shares 44.7% sequence identity. TIMAP is a 64 kDa protein highly expressed in endothelial and hematopoietic cells, and has also been found in the CNS, lung, spleen, kidney and testis [60]. TIMAP mRNA levels are downregulated by transforming growth factorβ (TGFβ) signaling [60].

The amino acid sequence and domain structure of TIMAP is presented in figure 1-15. TIMAP contains a PP-1c targeting RVXF motif in amino acids ^{64}KVSF^{66}. TIMAP also contains a predicted coiled-coil region, a nuclear localization sequence (NLS), five predicted ankyrin repeats, two phosphorylation sites, and a C-terminal CAAX box motif. The CAAX box motif signals for prenylation of TIMAP, and this prenylation facilitates TIMAP association with the plasma membrane. When the C-terminal CAAX box is disrupted, TIMAP is found in the nucleus [60]. TIMAP has also been found in high local concentration in filopodia [61].

a.

```
MASHVDLLTE LQLLEKVPTL ERLRAAQKRR AQQLKKWAQY EQDLQHRKRK[50]
HERKRSTGGR RKKVSFEASV ALLEASLRND AEEVRYFLKN KVSPDLCNED[100]
GLTALHQCCI DNFEEIVKLL LSHGANVNAK DNELWTPLHA AATCGHINLV[150]
KILVQYGADL LAVNSDGNMP YDLCEDEPTL DVIETCMAYQ GITQEKINEM[200]
RAAPEQQMIS DIHCMIAAGQ DLDWVDAQGA TLLHIAGANG YLRAAELLLD[250]
HGVRVDVKDW DGWEPLHAAA FWGQMQMAEL LVSHGASLSA RTSMDEMPID[300]
LCEEEEFKVL LLELKHKHDV IMKSQLRHKS SLSRRTSSAG SRGKVVRRAS[350]
LSDRTNLYRK EYEGEAILWQ QRSASEDQRN STYNGDIRET RTDQENKDPN[400]
PRLEKPVLLS EFPTKIPHSD MDMPVENGLR APVSTYQYAL CNGDVWKVHE[450]
VPDYSMAYGN PGVADATPSW SGYKEQSPQT LLELKRQRAA AKLLSHPFLS[500]
THLGSGVSRT GEGSSEGKAP LIGGRTSPYS SNGTSVYYTV TSGDPPLLKF[550]
KAPIEEMEEK VHGCCRIS[568]
```

b.

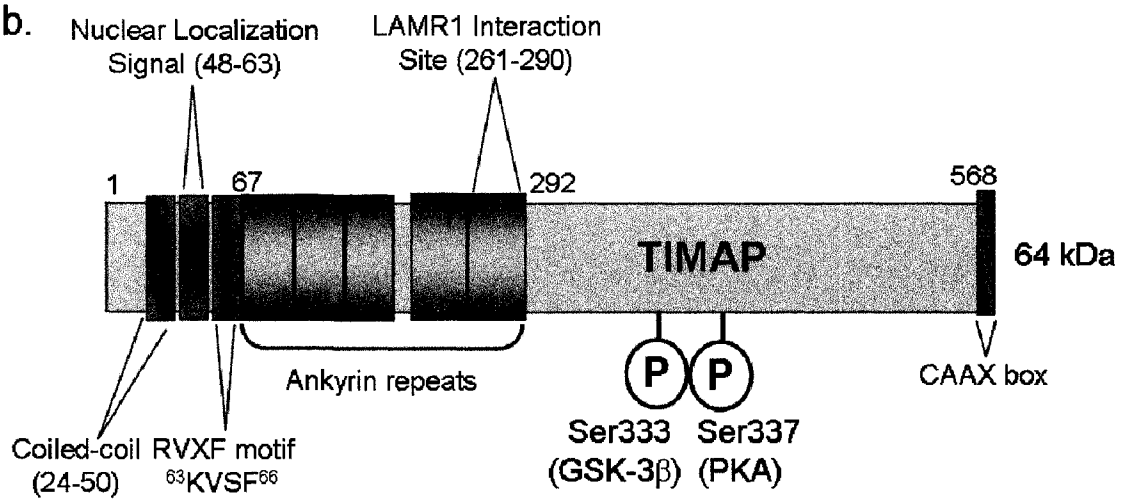

Figure 1-15. Amino acid sequence and domain structure of TIMAP.
Panel a depicts the amino acid sequence of human TIMAP. The numbers are references for amino acid number. Panel b illustrates the domain structure and predicted features of TIMAP. 64 kDa refers to the mass of TIMAP and the numbers refer to amino acid number. There are five predicted ankyrin repeats in TIMAP. Residues 261-292 interact with the LAMR1. TIMAP also possesses a predicted coiled coil domain from residues 24-50, a nuclear localization signal in amino acids 48-63, and RVXF motif in ^{63}KVSF^{66}. TIMAP is phosphorylated on Ser333 by GSK-3β and Ser337 by PKA. The C-terminal residues represent a CAAX box which localizes TIMAP to the plasma membrane.

TIMAP has recently been shown to interact with PP-1cβ in endothelial cells [62]. Direct interaction of TIMAP with other isoforms of PP-1c has not been shown. TIMAP association with PP-1c targets the phosphatase to the plasma membrane, where PP-1c

dephosphorylates its substrates. To date there are two known PP-1c substrates that TIMAP targets the phosphatase to, and these are described below.

It has been established that TIMAP binds to the 37kDa/67kDa non-integrin laminin receptor (LAMR1) [63]. The LAMR1 is a trans-membrane cell surface receptor which binds to laminin-1 (recently reviewed in [64]). The LAMR1 is best known for its involvement in tumor progression and metastasis [65] and as the cell surface receptor of the Prion Protein [66]. TIMAP binds to the LAMR1 via amino acids 261-290, residues which correspond to one of the predicted ankyrin repeats of TIMAP (refer to figure 1-15b). TIMAP binding to the LAMR1 recruits PP-1c, which results in dephosphorylation of the LAMR1 [63]. This TIMAP dependent dephosphorylation of the LAMR1 is thought to regulate the formation of filopodia [61].

It has been suggested that TIMAP associates with moesin [62], a protein that acts as a membrane-cytoskeleton linker and regulates cell adhesion and morphogenesis [67]. TIMAP targets PP-1c to moesin, resulting in dephosphorylation of moesin by the phosphatase [62]. It is notable that MYPT1 is also able to facilitate dephosphorylation of moesin by PP-1c, and that these family members both target PP-1c to a common substrate [68].

TIMAP is known to be phosphorylated at two Ser residues C-terminal to its ankyrin repeats (figure 1-15b). This is a common theme among MYPT family proteins to have a regulatory phosphorylation site(s) downstream from the ankyrin repeats (refer to figure 1-14). TIMAP is phosphorylated on Ser333 by Glycogen Synthase Kinase-3β (GSK-3β) and on Ser 337 by Protein Kinase A (PKA) [61]. The phosphorylation of Ser337 serves as a priming phosphorylation for GSK-3β, as GSK-3β preferentially

phosphorylates Ser residues that have a "priming" phosphorylation 4 amino acids downstream [69].

Phosphorylation of TIMAP on Ser333 and Ser337 was observed to decrease binding between PP-1c and TIMAP. This decrease in association is accompanied with a concomitant increase in PP-1c phosphatase activity [61]. The molecular basis for this effect is not well understood. It has been proposed that phosphorylation of TIMAP results in increased dephosphorylation of the LAMR1. This effect was observed using mutants of TIMAP in which Ser333 and Ser337 were changed to acidic amino acids to mimic phosphorylation [61]. PP-1c is able to dephosphorylate TIMAP, and this presumably allows for re-association of PP-1c and TIMAP, and reduction of phosphatase activity. In this scenario TIMAP may act as an inhibitor of bound PP-1c in a manner reminiscent of MYPT3 [58].

1.5 Goals of the thesis

TIMAP has many of the hallmark characteristics of a PP-1c regulatory protein. Indeed, TIMAP shares several traits with the well characterized classical PP-1c targeting subunit MYPT1. TIMAP targets PP-1c to a specific cellular location, and in doing so, TIMAP targets PP-1c to specific substrates. But what is the effect of TIMAP on other PP-1c substrates? Does TIMAP binding to PP-1c alter the substrate specificity of the phosphatase? How does TIMAP bind to PP-1c? Does it bind in a manner similar to MYPT1 or MYPT3? Does TIMAP associate with and modulate the activity of other isoforms of PP-1c? What is the molecular basis for the decreased association between phosphorylated TIMAP and PP-1c?

The body of knowledge about the regulation of PP-1c by TIMAP is miniscule compared to that of MYPT1. Advances in recent years have done much to enhance knowledge about the relationship between the TIMAP and PP-1c, but there is still much to learn. It is the regulation of PP-1c by TIMAP that will be the focus of this thesis.

The objectives of this thesis include:

1. Of the massive number of proteins thought to bind to PP-1c, there exists only a handful of three-dimensional structures. At the beginning of this study, there was only one structure of a protein bound to PP-1c, so our first objective was to produce a structural model predicting the basis of interaction between TIMAP and PP-1c.
2. We predict that TIMAP binds to PP-1c in a 1:1 complex. Another objective was to investigate the ability of TIMAP to bind to PP-1c directly, and determine if TIMAP can directly interact with other isoforms of PP-1c.
3. TIMAP targets PP-1c to two known proteins and facilitates their dephosphorylation. We aimed to investigate the effect of TIMAP on PP-1c activity toward other substrates.
4. The molecular basis for the decreased association between phosphorylated TIMAP and PP-1c is not well understood. Our next objective was to investigate the molecular basis for this effect using site-directed mutagenesis and phospho-mimic amino acids. The effect of the phospho-mimic mutant TIMAP on PP-1c activity was to be explored as well.

5. Based on structural data, it is known that MYPT1 associates with the C-terminal tail of PP-1cβ. We planned to determine if TIMAP associates with the C-terminal tail of PP-1c in the same manner. If TIMAP binds to PP-1c in the same mode as MYPT1, the C-terminal tail of PP-1c should be inaccessible to phosphorylation by cdk2/CyclinA in the presence of TIMAP.

Chapter 2: Methods and Materials

2.1 Materials

All chemical reagents used were purchased from Sigma or Fisher unless noted. All restriction enzymes were purchased from Invitrogen. Polymerase chain reaction (PCR) was carried out with polymerase from Stratagene. DNA primers were purchased from Integrated DNA Technologies. Glutathione Sepharose 4B was purchased from GE Healthcare. *p*-Nitrophenol phosphate was purchased from Sigma. All chromatography columns and media were purchased from GE Healthcare unless noted. cdk2/CyclinA was purchased from New England Biolabs. Phosphorylase b and phosphorylase kinase were purchased from Sigma.

2.2 Cloning and mutagenesis of bovine TIMAP

The cDNA encoding bovine TGFβ-Inhibited Membrane Associated Protein (TIMAP) (amino acids 1-568) (provided by Dr Barbara Ballermann, University of Alberta) was subcloned into the His-Tag vector pET28a (Novagen) by Hue Anh Luu. Efforts at expressing full length His6-TIMAP did not produce soluble protein. We switched to the glutathione S-transferase (GST) affinity tag system for expression and purification of TIMAP. TIMAP was truncated to residues 46-292, as this construct contains all predicted ankyrin repeats of the protein, and removed a predicted coiled-coil domain in the N-terminal region of TIMAP, potentially increasing protein solubility. TIMAP was cloned into the GST-tag vector pGEX-4T3 (donated by Dr Howard Young, University of Alberta, also commercially available from GE Healthcare). pGEX-4T3 contains a thrombin cleavage site for removal of the GST tag, is IPTG inducible and encodes for

ampicillin resistance. We were successful purifying GST-TIMAP$^{46-292}$, and followed this by producing a longer construct of amino acids 46-453 of TIMAP. We substituted Ser333 and Ser337 of TIMAP with Asp or Glu to mimic phosphorylated amino acids, and this was carried out with the GST-TIMAP$^{46-453}$ construct. The phospho-mimic double mutants were termed GST-TIMAP$^{46-453S333D/S337D}$ and GST-TIMAP$^{46-453S333E/S337E}$. Additionally, full length wildtype TIMAP was inserted into pGEX-4T3. All PCR was performed with primers from Integrated DNA Technologies and cloned *pfu* Turbo polymerase (Stratagene). All mutagenesis of TIMAP was carried out with primers from Integrated DNA Technologies, cloned *pfu* Turbo polymerase (Stratagene) and *dpnI* restriction enzyme (Invitrogen) following the guidelines of the Stratagene Quickchange Mutagenesis kit.

2.3 Expression and purification of TIMAP

E. coli BL-21 Rosetta cells (Novagen) were transformed and used for expression of all constructs of GST-TIMAP. BL-21 Rosetta cells were utilized as they exhibited the highest expression of GST-TIMAP. Transformed BL-21 Rosetta cells were cultured in an overnight 100ml culture of superbroth media (containing 200mg/L ampicillin and 34mg/L chloramphenicol) at 37°C with shaking. 2 x 10ml of this overnight culture was used to inoculate 2 x 1L of superbroth media (containing 200mg/L ampicillin and 34mg/L chloramphenicol) the next day. Cells were grown at 37°C until an optical density (at 600nm) of 0.7 was reached. Protein expression was induced by addition of 0.1mM IPTG at 18°C for 7 hours. Cells were harvested by centrifugation at 4000xg for 25 minutes at 4°C. Harvested cells were resuspended in 50mM HEPES (pH 7.5) (containing

5mM EDTA, 5mM EGTA, 2.0mM Benzamidine, 1.0mM PMSF, 1mM DTT, 10μg/ml leupeptin, 10μg/ml pepstatin, 10μg/ml aprotinin, 10μg/ml chymostatin, and 10μg/ml DNaseA) at a ratio of 5ml buffer/g cells. Resuspended cells were then lysed using an Aventis Emulsiflex cell disrupter, with three passes at 20000psi. Lysed cells were centrifuged at 13700xg in a Beckman F0630 rotor for 45 min at 4°C. The clarified lysate was combined with 4-5ml glutathione sepharose 4B (GE Healthcare) and allowed to incubate on an end-over-end rotator for 90 minutes at 4°C. The glutathione sepharose and bound GST-TIMAP was collected by centrifugation in a Beckman J6B rotor at 2500xg for 5 minutes. The GST-TIMAP bound to glutathione sepharose was washed four times with 50ml of 50mM HEPES buffer (pH7.5) containing 5mM EDTA, 5mM EGTA and 1mM DTT. GST-TIMAP was eluted with 3 x 10ml of 30mM reduced glutathione in 50mM Tris-HCl (pH 8.0). Purified protein at this stage was analyzed by sodiumdodecyl sulfate-polyacrylamide gel electrophoresis (SDS-PAGE) in the method of Laemmli [70], before elutions were pooled and concentrated in Millipore concentration tubes. The "elution pool" was dialyzed overnight in buffer containing 50mM Tris (pH 7.5), 100mM NaCl, 1mM DTT to remove the 30mM glutathione. The purified GST-TIMAP was then concentrated further in Millpore concentrator tubes. Glycerol was added to 50% (to prevent freezing during storage) and GST-TIMAP was stored at -20°C. Protein concentration was determined by Bradford assay (Bio-Rad). Determined protein concentrations of GST-TIMAP were double checked by SDS-PAGE, comparing band densities with samples of known concentration using the densitometry software ImageQuant (Molecular Dynamics).

2.4 Cloning of human Protein Phosphatase-1cγ and rat Protein Phosphatase-1cβ

Human Protein Phosphatase-1cγ (PP-1cγ) was cloned by Hue Anh Luu from a human teratocarcinoma NT2 cDNA library (Stratagene) and subcloned into the cloning vector pBluescriptSK (Stratagene). Human PP-1cγ was subsequently cloned into the pCW vector for expression. Rat PP-1cβ was cloned into the pCW vector for expression as well. The pCW vector is IPTG inducible and encodes for ampicillin resistance for selection.

2.5 Expression and Purification of rat PP-1cβ and human PP-1cγ

Expression and purification of PP-1cβ and PP-1cγ was essentially identical with the exception that 8L of culture was used to grow PP-1cβ. Transformed *E.coli* DH5α cells were cultured in a 100ml culture of LB media containing 200μg/ml ampicillin, 1mM $MnCl_2$, and 0.01% vitamin B_1 overnight at 37°C with shaking. The next day this culture was used to inoculate 4L of LB media, at a ratio of 10ml of overnight culture per 1L. The large culture of LB media also contained 1mM $MnCl_2$ and 0.1% vitamin B_1. The large cultures were allowed to grow at 37°C with shaking until an OD_{600} of 0.7 was reached. Protein expression was induced by addition of 1mM IPTG and allowed to induce at 37°C with shaking overnight. Cells were harvested by centrifugation in a Beckman J6B rotor at 4000xg for 25 minutes at 4°C. Harvested cells were resuspended in Buffer A containing 50mM imidazole (pH 7.5), 0.5mM EDTA, 0.5mM EGTA, 100mM NaCl, 2.0mM $MnCl_2$, 3.0mM DTT, 2.0mM benzamidine, 0.5mM PMSF, 10% glycerol, 2μg/ml pepstatin, 2μg/ml leupeptin, 2μg/ml aprotinin, and 2μg/ml DNaseA at a ratio of 5ml per gram of cells. Cells were lysed with three passes through an Aventis Emulsiflex cell disrupter at 20000psi. The lysed cells were centrifuged in a Beckman F0630 rotor at 13700xg for 45

minutes at 4°C. The lysate was collected and loaded on to a heparin-sepharose CL-6B column (GE Healthcare) using an AKTA FPLC system (GE Healthcare). Protein was eluted using a linear 400ml gradient from 100mM to 500mM NaCl. 5ml fractions were collected and assayed using a 60µl *p*-Nitrophenol phosphate (PNPP) activity assay. The most active fractions were pooled and diluted with Buffer B containing 50mM imidazole, 5mM EDTA, 2.0mM $MnCl_2$, 2.0mM DTT, and 20% glycerol (pH 7.5). The pooled fractions were diluted until the NaCl content was below 70mM. The sample was then loaded on a 30ml inhibitor-2-sepharose column using the AKTA FPLC system. It has previously been shown that affinity chromatography with inhibitor-2-sepharose is an effective form of purification of PP-1c [71]. This column was generated by Hue Anh Luu in our laboratory by combining purified recombinant human inhibitor-2 protein with activated CH-sepharose 4B (GE Healthcare). The column was washed with 3 column volumes of Buffer B before elution of PP-1c with Buffer + 1M NaCl. 3 column volumes of Buffer B + 1M NaCl were used to elute all bound PP-1c. Fractions were assayed using a PNPP assay and most active fractions were pooled and concentrated using Millipore concentrator tubes to 1-2mg/ml. Glycerol was added to a concentration of 50% and protein stored at -20°C.

2.6 Microcystin sepharose binding assays

Microcystin sepharose was prepared by Cindy Lee in the Holmes laboratory. This was prepared by linking the methyl dehydroxy alanine group of microcystin to aminoethanethiol. The aminoethanethiol-microcystin was attached to *N*-hydroxysuccinimide-activated thiol-sepharose (GE Healthcare) [29]. The microcystin

sepharose was equilibrated in buffer A containing 50mM Tris-HCl, 0.1mM EDTA, 0.5mM $MnCl_2$ and 0.2% β-mercaptoethanol (pH 7.5). PP-1c (1.4nmol) and an equimolar amount of GST-TIMAP were combined with 50µl of resin and buffer A was added to a final volume of 500µl (excluding the volume of resin). The mixture was allowed to incubate on an end-over-end rotator for 90 minutes at 4°C. The microcystin sepharose resin was collected by centrifugation for 1 minute in a bench-top centrifuge (Ependorf) at 14000rpm. The resin was then washed four times with 1ml Buffer A + 100mM NaCl. After washes were completed, 50µl of SDS-PAGE loading buffer (62.5mM Tris-HCl pH 6.8, 25% glycerol, 2% sodium dodecylsulfate, 1% bromophenol blue, 5% β-mercaptoethanol) was added to the resin for analysis by SDS-PAGE.

2.7 Generation of a Structural Model of TIMAP bound to PP-1c

A three-dimensional structural model of TIMAP bound to PP-1cβ was generated using a program called Swiss-Model, a modeling program that generates structural predictions on the basis of sequence homology [72-74]. A model of the three-dimensional structure of a given protein can be generated if the given protein shares a minimum 30% sequence similarity with another protein whose three-dimensional structure is known. This structure is used by Swiss-Model as a template to predict the three-dimensional structure of the protein of interest. To construct a predicted model, Swiss-Model requires the sequences of the two homologous proteins to be aligned with a sequence alignment program. The sequence alignment and template structure are submitted to an online automated server which generates the structural model.

TIMAP shares 31% sequence identity with myosin phosphatase targeting subunit-1 (MYPT1), regulatory protein which targets PP-1cβ to myosin. The structure of MYPT1 (residues 1-299) has been solved in complex with PP-1cβ [16]. This structure was used as the template for the model of TIMAP.

The sequences of TIMAP and MYPT1 were aligned using a program called T-COFFEE [75]. The sequence alignment, as well as the structure of MYPT1 (protein database accession code 1S70) were submitted to Swiss-Model. The result was a three-dimensional structural model of TIMAP amino acids 52-322. Using pre-determined structural information for PP-1cβ (from the template structure of MYPT1 bound to PP-1cβ), a structural model of $TIMAP^{52-322}$ bound to PP-1cβ was constructed. This was carried out using pymol, a software program used for producing high quality 3D images of small molecules and proteins (DeLano Scientific).

2.8 Phosphorylation of glycogen phosphorylase for phosphorylase a assays

^{32}P-radiolabelled phosphorylase *a* was prepared for PP-1c activity assays by phosphorylation of glycogen phosphorylase b (Sigma) by phosphorylase kinase (Sigma). 50mg of phosphorylase b was resuspended in 500µl of H_20 and dialyzed overnight in "phos a" buffer (50mM Tris pH 7.0 + 1mM EDTA, 0.1% β-mercaptoethanol), plus 25mM sodium fluoride (a phosphatase inhibitor) at 4°C. 500U of phosphorylase kinase was resuspended in 200µl of H_20 and dialyzed in the same conditions. The next day, the phosphorylase b was warmed to 37°C and added to a reaction containing 20mM magnesium acetate, 0.23mM $CaCl_2$, 0.25mM EDTA, 12.5mM sodium glycerolphosphate, 12.5mM Tris (pH 8.6), and 1 mCi ^{32}P-γ-ATP. The total reaction volume was 1.5 ml. The

phosphorylase kinase was added last. The reaction was allowed to proceed for a minimum of 30 minutes with ^{32}P-γ-ATP at 30°C before addition of 1mM cold ATP. After addition of the cold ATP the reaction was allowed to proceed for minimum 30 minutes more at 30°C. The reaction was quenched by addition of 1.5ml of saturated ammonium sulfate solution. The mixture was kept on ice for 1 hour and then centrifuged at 13700xg in a Beckman F0630 rotor (at 4°C) for 20 minutes. The pellet was resuspended in 1.5 ml "phos a" buffer (50mM Tris (pH 7.0, containing 1mM EDTA and 0.1% β-mercaptoethanol), before addition of 1.5ml more saturated ammonium sulfate solution. The mixture was allowed to sit on ice for 1 hour before a second spin, this time at 8000xg (for ease of resuspension) for 20 minutes (at 4°C). The pellet was resuspended in 1.5 ml of "phos a" buffer (50mM Tris (pH 7.0) containing 1mM EDTA, and 0.1% β-mercaptoethanol) before thorough dialysis in the same buffer to remove residual ^{32}P-γ-ATP and any ^{32}P-inorganic phosphate. The finished product phosphorylase *a* was stored as a crystalline suspension (at a concentration of about 12.5mg/ml) in 200µl aliquots at 4°C.

2.9 Protein Phosphatase-1c inhibition assays

2.9.1 PP-1c inhibition assays using phosphorylase *a* substrate

PP-1c assays were performed in 30µl reaction volumes as described in Holmes (1991) [76], using ^{32}P-labelled glycogen phosphorylase *a* as substrate for PP-1c. The assay buffer consisted of 50mM Tris-HCl (pH 7.0), 0.1mM EDTA, 1mg/ml BSA, 1mM $MnCl_2$, and 0.2% β-mercaptoethanol. All proteins in the assay were diluted in this buffer unless noted. 10µl of PP-1cβ or PP1-cγ (diluted to 0.96nM and 0.25nM final concentration

respectively, in the 30µl reaction) were incubated with 2µl of GST-TIMAP sample (at various dilutions), and 8µl of assay buffer. This was allowed to pre-incubate for 10 minutes at 30°C. The reaction was initiated with the addition of 10µl of ^{32}P-radiolabelled phosphorylase *a* (to a final concentration of 10µM) in assay buffer (as above, but without 1mM $MnCl_2$, and including 3.75mM caffeine). The reaction was allowed to proceed for 10 min at 30°C and was stopped by addition of 200µl of ice-cold 20% trichloroacetic acid (TCA). The samples were placed on ice for 2 min and then centrifuged in a bench-top centrifuge (Ependorf) at 14000rpm for 2 min. The supernatant containing TCA-soluble released ^{32}P-labelled phosphate (200µl) was added to 1ml of aqueous scintillation fluid and the radioactivity was measured (as counts per minute, cpm) in a Wallac 1209 RackBeta scintillation counter. All reactions were performed in duplicate, and assays were repeated 3-4 times.

2.9.2 Evaluation of PP-1c phosphorylase *a* assay results

Inhibition of PP-1c in the phosphorylase *a* assay has a sigmoidal behavior in plots of PP-1c activity (percent of control) vs. log inhibitor concentration [77]. The inhibition curve is linear in the 30-60% PP-1c activity range, and this area of the curve was utilized in calculating the IC_{50} of TIMAP of PP-1c toward phosphorylase *a*. The percent PP-1c activity (of control) can be calculated as follows:

$$\text{PP-1c Activity (\% of control)} = \frac{\text{(sample - blank)}}{\text{(control - blank)}} \times 100\%$$

Where sample is the amount of PP-1c activity (in cpm) resulting after inclusion of an inhibitor such as TIMAP, blank is the background cpm from free ^{32}P-phosphate (i.e. phosphorylase *a* alone and no added phosphatase), and control is the maximal amount of PP-1c phosphatase activity (in cpm) in the 10 minute reaction in absence of inhibitor or TIMAP.

The inhibition of PP-1c by TIMAP is affected by the amount of phosphatase included in the assay [77]. The amount of phosphatase added to the reaction is monitored by the proportion of ^{32}P-phosphate released (termed % release) from phosphorylase *a* (measured in cpm) in the assay compared to the total amount of counts (in cpm) of ^{32}P-phosphate present. This total is measured by counting 10µl of phosphorylase *a* substrate in 1ml of scintillation fluid.

$$\% \text{ Release} = \frac{(\text{control} - \text{blank})}{(\text{total} - \text{blank})} \times 1.15 \times 100\%$$

Again control refers to the maximal activity of PP-1c in the assay (minus the blank, as defined above) and total refers to the total cpm of ^{32}P-phosphate in 10µl of phosphorylase *a* as mentioned above. 1.15 is a dilution factor as 200µl of the reaction is counted from the total 230µl reaction volume. When determining the IC_{50} of TIMAP, the % release was standardized as close as possible to 15%.

2.9.3 PP-1c inhibition assays using *p*-nitrophenol phosphate substrate

All constituents of the *p*-nitrophenol phosphate (PNPP) inhibition assays were diluted in assay buffer consisting of 50mM Tris-HCl (pH 8.3), 0.1mM EDTA, 30mM $MgCl_2$,

1mg/ml BSA, 0.2% β-mercaptoethanol, and 0.5mM $MnCl_2$. The PNPP phosphatase assay reactions were carried out at 30°C in a total volume of 60µl in 96-well plates. PP-1cβ or PP-1cγ was added to a reaction mixture (final concentration of 59nM for PP-1cβ and 33nM for PP-1cγ) that contained assay buffer, and 2µl of TIMAP at various dilutions. The mixtures were pre-incubated for 15min at 30°C before the reaction was initiated with the addition of PNPP substrate to a final concentration of 5mM. The dephosphorylation reaction was allowed to proceed for 45min at 30°C before the measuring absorbance at 405nm (A_{405}) in a Perkin Elmer plate reader. Reactions were done in duplicate and assays were repeated at least 3 times.

2.9.4 Evaluation of PP-1c *p*-nitrophenol phosphate assay results

The PNPP assay is a colorimetric assay based on the principle that PP-1c dephosphorylates the chemical substrate *p*-nitrophenol phosphate, resulting in liberated phosphate, and *p*-nitrophenol. Since the assay is carried out at a basic pH of 8.3, *p*-nitrophenol is converted to the *p*-nitrophenolate anion, which is yellow and absorbs light strongly in the region of 405nm. As a result, increased PP-1c activity toward PNPP correlates with an increase in yellow color in the reaction. This increase in yellow color (and thus PP-1c activity) is quantitated by measuring the absorbance of the reaction at 405nm (A_{405}) [78].

PNPP assay results were analyzed in a similar manner to those of the phosphorylase *a* assays. The colorimetric PNPP assay behaves in a sigmoidal manner when % PP-1c activity (relative to control) is plotted against TIMAP concentration. There is a linear portion along the inhibition curve from which the IC_{50} of TIMAP toward

PP-1c activity (with PNPP substrate) was calculated. % PP-1c activity was calculated as follows:

$$\text{PP-1c Activity (\% of control)} = \frac{\text{(sample - blank)}}{\text{(control - blank)}} \times 100\%$$

Here sample refers to the A_{405} for a reaction with TIMAP included, and control is the A_{405} for a reaction containing only PP-1c and represents maximal PP-1c activity. Blank refers to the A_{405} for a reaction consisting of only buffer plus PNPP. To maintain consistency in comparing assay data in determining the IC_{50} of TIMAP vs. PP-1c the A_{405} for controls was kept constant in the range of 0.4-0.6.

2.10 Phosphorylation of Protein Phosphatase-1c by cdk2/CyclinA

cdk2/CyclinA phosphorylation reactions were carried out according to procedures described by Dohadwala (1994) [42], with some changes. PP-1cγ (0.03nmol, 4μM final concentration) was combined with reaction buffer (containing 40mM Tris-HCl pH 7.5, 10mM $MgCl_2$, 2mM DTT, 0.5mM $MnCl_2$, 0.38μM ^{32}P-γ-ATP), and a slight molar excess of GST-TIMAP (0.045nmol, final concentration 6μM) in a total volume of 7.5μl. Control reactions were also set up consisting of PP-1c (0.03nmol) alone in reaction buffer, and GST-TIMAP (0.045nmol) alone in reaction buffer. The phosphorylation reactions were pre-incubated for 15min at 30°C before the addition of cdk2/CyclinA (1μl of 50000units/ml enzyme stock) to start the reaction. The phosphorylation was allowed to proceed for 30min at 30°C and was stopped with the addition of an equal volume of SDS-PAGE loading buffer and boiling for 5min. Since PP-1c can auto-dephosphorylate its C-

terminal tail, parallel reactions were set up with the inclusion of the PP-1c inhibitor microcystin (36ng, 4.2μM final concentration) to inhibit phosphatase activity. This was carried out to produce a more robust signal for phosphorylation of PP-1c. Results of the phosphorylation were analyzed by SDS-PAGE and autoradiography. After staining the gel with coomassie blue dye, the radioactive bands were visualized by exposure to a Fuji autoradiography plate (Type BAS-IIIS) for a minimum of 24 hours. The autoradiograph was then scanned using a Molecular Dynamics Storm 840 scanner.

Chapter 3: Results

3.1 Modeling studies of TIMAP bound to PP-1c

While a wealth of three-dimensional structural information exists for the catalytic subunit of human PP-1, there is much less for regulatory proteins of PP-1c. There are over 200 proteins thought to bind to PP-1c, and thus far there is three-dimensional structural information about the binding and regulation of the phosphatase by only two PP-1c binding partners [16,20]. There is no three-dimensional structural information for TIMAP.

To aid and direct us in our characterization of the regulation of PP-1c by TIMAP, we developed a structural model for the interaction of these two proteins, as outlined in objective 1 of section 1.5 (p. 30). Using the online sequence homology-based modeling server Swiss-Model [72-74], a structural model of TIMAP was constructed comprising residues 51-322 bound to PP-1cβ. The model was constructed by exploiting the sequence homology between TIMAP and MYPT1 (which is 31% identity) and the previously determined crystal structure of MYPT1 (residues 1-299) bound to PP-1cβ [16]. Figure 3-1 displays the deduced model of $TIMAP^{51-322}$.

It can be seen that the proposed model possesses a similar overall architecture to the structure of $MYPT1^{1-299}$. Similar to the case of MYPT1, there are more ankyrin repeats in the structural model than predicted for the protein. Ankyrin repeats are a structural motif that consists of a repeat of two α-helices and a β-hairpin loop (refer to section 1.4.3 for ankyrin repeats). The model suggests there are 8 ankyrin repeats (numbered in figure 3-1) which wrap around the C-Terminal tail of PP-1cβ. The amino acid sequence of TIMAP predicts 5 predicted ankyrin repeats. MYPT1 also has 8 ankyrin

repeats in its structure while its amino acid sequence predicts 7. The active site of PP-1cβ is marked with an asterisk and is accessible to solvent in the predicted model. The arrow in figure 3-1 highlights amino acids ^{63}KVSF^{66} (the RVXF motif of TIMAP) binding in the RVXF binding groove of PP-1c. Binding at this site is crucial for TIMAP-PP-1c association, and ^{63}KVSF^{66} of TIMAP binds in this groove in a similar fashion to other PP-1c regulatory proteins in previously determined structures [16,18,20]. The crystal structure of PP-1cγ was solved in complex with a peptide consisting of the RVXF motif of the G_M regulatory protein (amino acids ^{63}RRVSFA^{69}), and in our structural model the RVXF motif of TIMAP binds PP-1c in the same pocket as this peptide [18].

TIMAP makes extensive protein-protein contacts with PP-1c in the model. One striking predicted interaction is how the ankyrin repeats of TIMAP wrap around the C-terminal tail of PP-1c. This would presumably allow TIMAP to discriminate between PP-1c isoforms in the same manner as MYPT1. Also, if TIMAP were to bind to PP-1c as predicted by the model, the active site of the phosphatase would be accessible to solvent, allowing access to small inhibitors and substrates. How this mode of TIMAP binding to PP-1c effects phosphatase activity remains to be seen, but in wrapping around the C-terminal tail in this manner, TIMAP may remodel the active site of PP-1c, modulating the phosphatase substrate specificity, i.e. increase PP-1c activity toward the LAMR1, and decrease activity to other PP-1c substrates. Based on this predicted model, TIMAP binds to PP-1c at a molar ratio of 1:1.

The model suggests several regions of TIMAP which may be involved in interactions with other binding partners along the surface of the ankyrin repeats. TIMAP is known to interact with the LAMR1 via TIMAP residues 261-290. This corresponds to

ankyrin repeat 7 in the model, highlighted in green in figure 3-1. The model suggests candidate residues which may be required for the interaction with the LAMR1 and these are presented in yellow in figure 3-2. There are four residues in particular, Gln274, Gln276, Glu279 and Ser 283 that could directly interact with the LAMR1. The side chains of these residues are predicted to project out into solution and may mediate the TIMAP-LAMR1 interaction.

Figure 3-1. A predicted structural model illustrating the potential mode of TIMAP binding to PP-1cβ.

TIMAP (residues 51-322) is shown bound to PP-1cβ. TIMAP (top, colored in cyan) wraps around the C-Terminal tail of PP-1cβ (bottom, colored in slate). This model was generated using Swiss-Model based on the structure solved by Terrak *et al.* (Nature 2004) [16] (pdb 1S70). Red asterisk indicates active site of PP-1cβ. The arrow indicates residues ^{63}KVSF^{66} (shown as sticks) of TIMAP predicted to interact with PP-1cβ in the RVXF binding groove of the phosphatase. The ankyrin repeats of TIMAP as predicted by the model are numbered 1-8. In the model ankyrin repeat 7 corresponds to amino acids 261-290 (shown in green). These residues are required for interaction with the LAMR1.

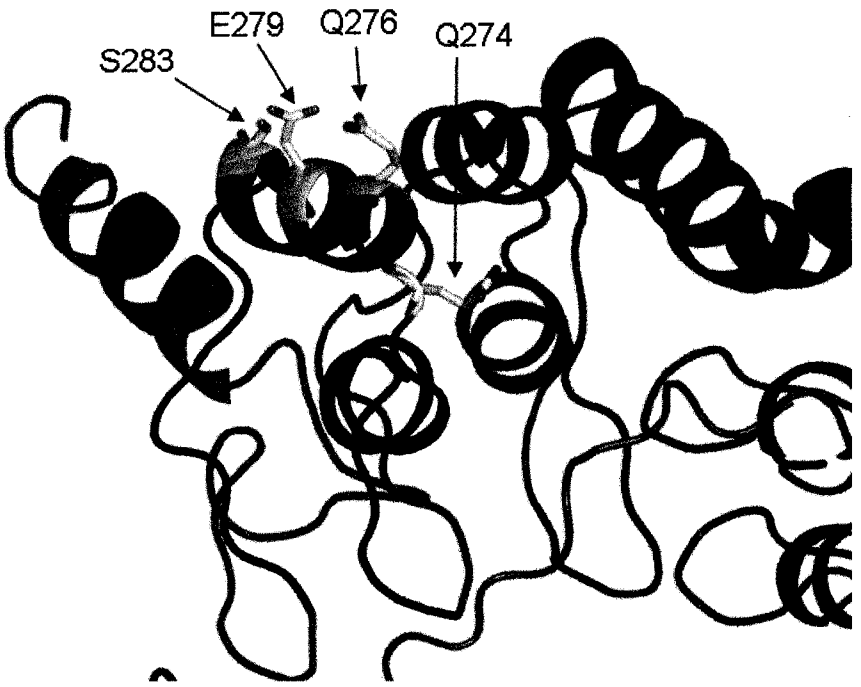

Figure 3-2. A close-up view of TIMAP residues predicted to interact with the LAMR1.

The figure displays a close-up view of ankyrn repeat 7 (colored green) of TIMAP (colored cyan) and amino acids of TIMAP predicted to be involved directly in interaction with the LAMR1. The C-terminal tail of PP-1cβ is visible in slate color. The model suggests four putative residues (Gln274, Gln276, Glu279 and Ser283, labeled by arrows) which project into solution and could directly bind to the LAMR1 (shown as sticks and colored according to element, yellow: carbon, red: oxygen, blue: nitrogen).

3.2 Expression of GST-TIMAP

Having identified a predicted structural model that suggested TIMAP interacts with PP-1c in a 1:1 complex, we set about testing this hypothesis experimentally. In order to begin our investigation of the regulation of PP-1c by TIMAP we attempted expressing bovine TIMAP with a hexa-His-tag vector pET28a in *E.coli*. However, this did not produce any soluble protein. We then decided to attempt a truncation of His6-TIMAP from both the N and C-Termini. Our rationale for truncation was as follows. There is a predicted coiled-coil domain in amino acids 24-50 of TIMAP, and since coiled-coil domains are known to facilitate oligomerization [79], we opted to truncate TIMAP at His46, in hopes this would improve solubility by decreasing aggregation. Amino acids 46-50 were retained, since they are polar amino acids that might aid in solubility. We truncated TIMAP at Thr292 at the C-terminus as this marks the end of the ankyrin repeats in TIMAP, and would be useful in identifying proteins which bind to TIMAP, since ankyrin repeats are known to mediate protein-protein interactions [53,54]. However, His6-TIMAP$^{46\text{-}292}$ did not yield soluble protein.

We switched to a glutathione S-transferase-tag (GST-tag) for expression of TIMAP$^{46\text{-}292}$, and used the GST vector pGEX-4T3. GST-tags are a used frequently for purifying proteins. A 26 kDa protein "tag" of GST is expressed on the N-terminus of TIMAP, and this aids in solubility of the expressed protein and provides a convenient method of purification using affinity chromatography [80]. We utilized a lower temperature for induction of protein expression, as was performed in purification of MYPT3 to obtain soluble protein [57]. Figure 3-3 contains a summary of the constructs of TIMAP created. Expression of GST-TIMAP$^{46\text{-}292}$ was followed by expression of GST-

TIMAP$^{46-453}$, a longer construct of TIMAP which contained two newly characterized phosphorylation sites at Ser333 and Ser337 [61] (see figure 3-3b). This longer construct of GST-TIMAP$^{46-453}$ was expressed using the same vector, and purified under the same conditions for GST-TIMAP$^{46-292}$. We eventually were able to express full length (amino acids 1-568) GST-TIMAP^{WT} in the same fashion. Figure 3-4 depicts the preparations of GST-TIMAP$^{46-292}$, GST-TIMAP$^{46-453}$, and GST-TIMAP^{WT} visualized by SDS-PAGE. Although pGEX-4T3 contains a thrombin cleavage site for removal of the GST-tag (thrombin is a protease commonly used for this purpose), efforts at cleavage and removal of the tag were unsuccessful as TIMAP was insoluble when the GST-tag was removed. It is known that GST does not interact with or have any effect on PP-1c catalytic activity [32], therefore our studies were carried out with the GST tag intact.

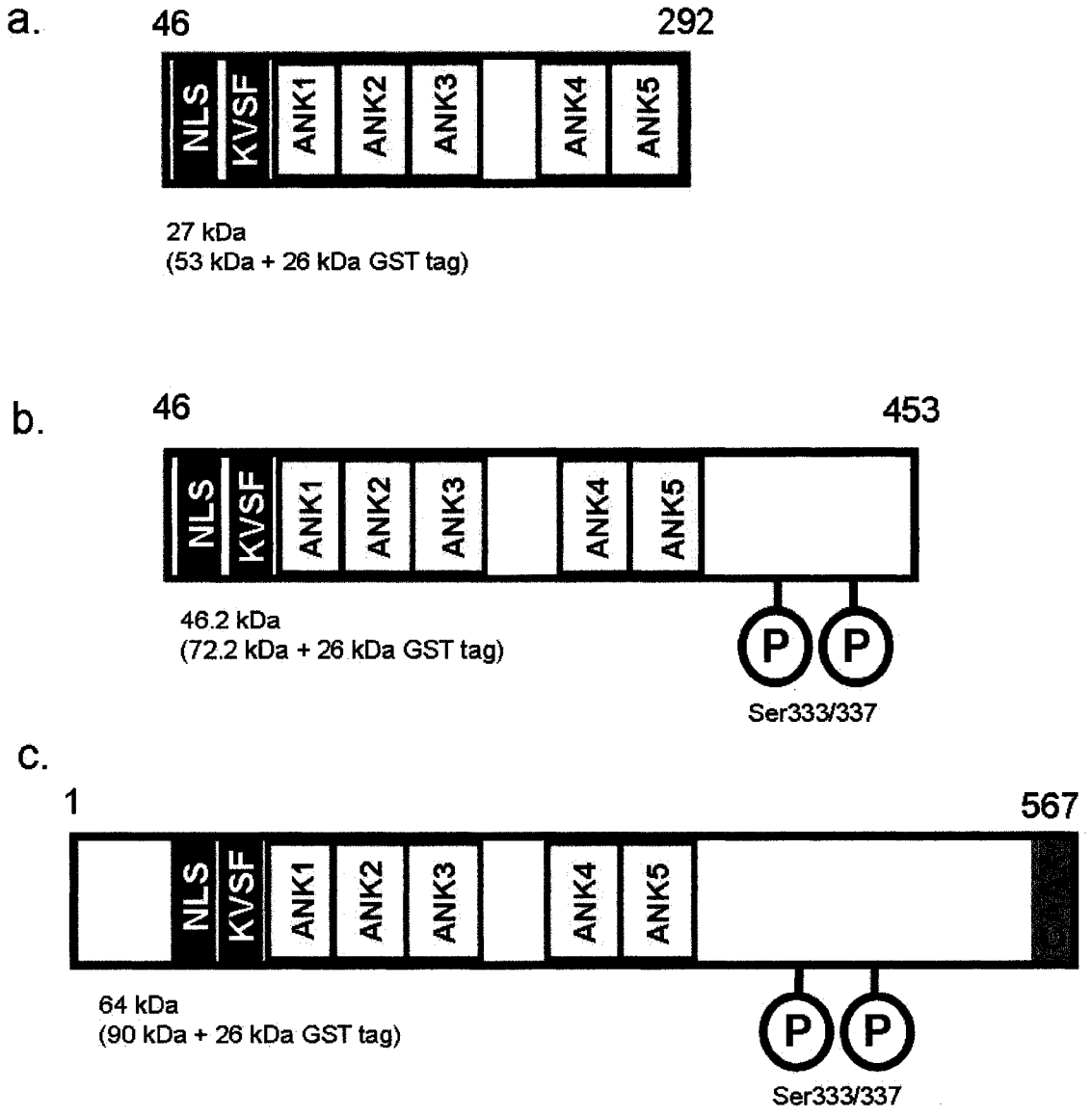

Figure 3-3. Primary structure and features of GST-TIMAP utilized for the characterization of TIMAP regulation of PP-1c.

Panels a-c represent the three different constructs of GST-TIMAP expressed in *E. coli*. a. depicts GST-TIMAP46-292, b. shows GST-TIMAP46-453 and c. illustrates wild-type GST-TIMAP. TIMAP contains a Nuclear Localization Sequence (NLS) for access to the nucleus, a PP-1c binding RVXF motif KVSF (Lys-Val-Ser-Phe) at amino acids 63-66. There are five predicted ankyrin repeats (ANK) in TIMAP to mediate protein-protein interactions. At residues 564-567 of the C-terminus is a CAAX box composed of amino acids CRIS (Cys-Arg-Ile-Ser) which localizes TIMAP to the plasma membrane. There are two phosphorylation sites on TIMAP, Ser333, a GSK-3β site and Ser337 a PKA phosphorylation site which primes the GSK-3β site. These features are illustrated on the diagrams of each construct, as well as molecular mass.

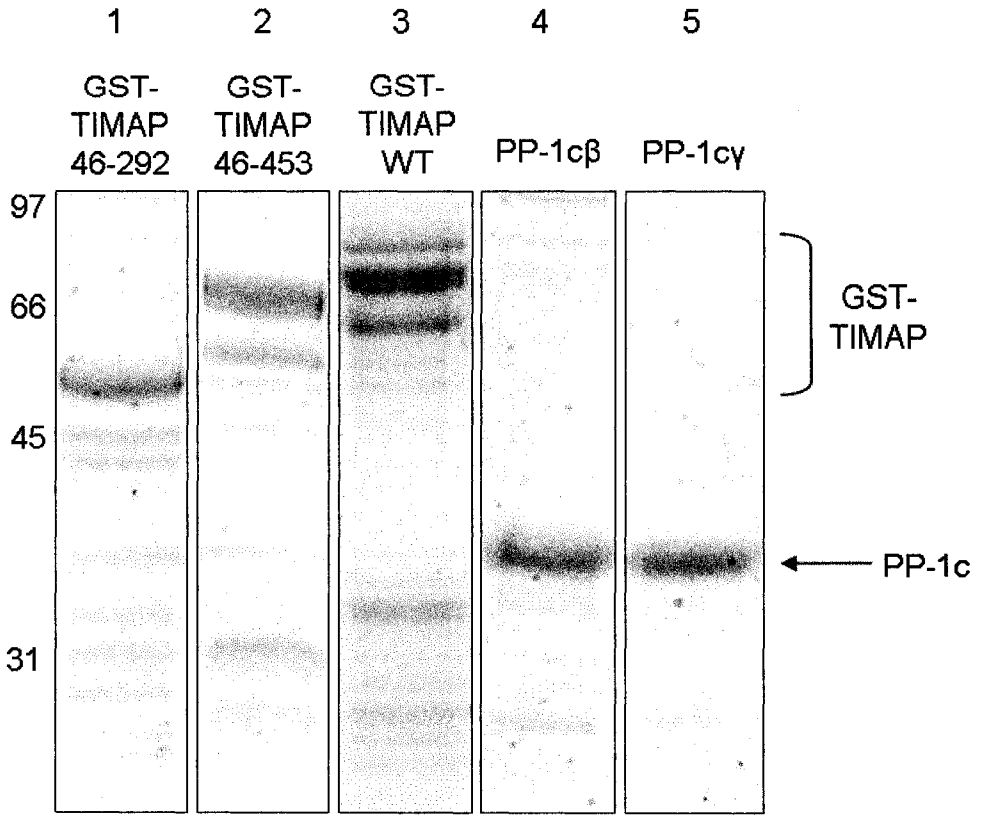

Figure 3-4. Preparations of GST-TIMAP and PP-1c visualized by SDS-PAGE. Depicted in figure 3-4 are five lanes from SDS-PAGE gels depicting typical preparations of GST-TIMAP and PP-1c. Lanes 1-3 contain GST-TIMAP$^{46\text{-}292}$, GST-TIMAP$^{46\text{-}453}$ and GST-TIMAP^{WT} respectively. Lanes 4-5 represent PP-1cβ and PP-1cγ preparations.

3.3 GST-TIMAP binds to PP-1c on microcystin sepharose

As stated in section 1.5 (p. 30), one of our objectives in this study was to investigate the ability of TIMAP to bind directly to PP-1c and explore whether TIMAP preferentially binds PP-1cβ over other isoforms. To tackle this objective, we utilized microcystin sepharose, a resin which binds and traps PP-1c via the active site of the phosphatase. This provides an effective method for immobilizing PP-1c that leaves the RVXF binding groove unoccupied. PP-1c regulatory proteins containing an RVXF motif (such as TIMAP) can bind to the phosphatase and be isolated in this manner. This technique has been used successfully in the past to detect proteins that bind to PP-1c [29,30,81]. We found that all three expressed constructs of GST-TIMAP (GST-TIMAP$^{46\text{-}292}$, GST-TIMAP$^{46\text{-}453}$ and wild type GST-TIMAP) bound to immobilized PP-1cβ, as demonstrated in figure 3-5a.

It has been shown that the MYPT family of proteins preferentially bind PP-1cβ [47,48,82], and that TIMAP associates with PP-1cβ in endothelial cells [62]. For this reason we expected GST-TIMAP to bind PP-1cβ, but not PP-1cγ. Surprisingly, the GST-TIMAP constructs all bound to PP-1cγ immobilized on microcystin sepharose as exhibited in figure 3-5b. Our findings illustrate that TIMAP has the ability to bind to both PP-1c isoforms PP-1cβ and PP-1cγ in a manner that does not require interaction with the active site of the phosphatase.

We also verified that the GST moiety is not responsible for the binding of GST-TIMAP to PP-1c on microcystin sepharose in figure 3-6a. GST-TIMAP does not interact with microcystin sepharose or sepharose alone in the absence of PP-1c as seen in figure 3-6b.

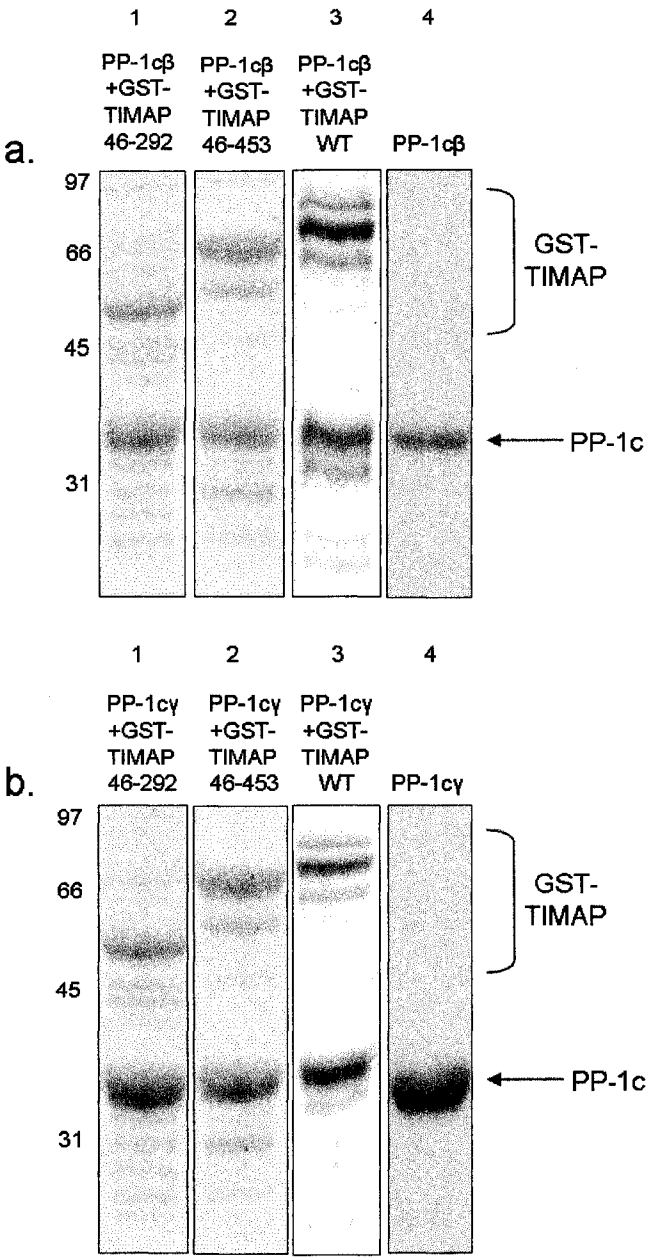

Figure 3-5. GST-TIMAP binds PP-1cβ and PP-1cγ immobilized on microcystin-sepharose.

Panel a illustrates binding of three different constructs of GST-TIMAP to PP-1cβ immobilized on microcystin sepharose. Lanes 1-3 are SDS-PAGE gels depicting that GST-TIMAP binds to PP-1cβ trapped on microcystin sepharose. Lane 4 is an SDS-PAGE gel depicting a control of PP-1cβ alone immobilized on microcystin sepharose. In panel b, lanes 1-3 are SDS-PAGE gels illusrtating the three constructs of GST-TIMAP bind to PP-1cγ immobilized on microcystin sepharose. Lane 4 is a gel showing the control of PP-1cγ alone on the resin. The GST-TIMAP and PP-1c bands are highlighted by indicators on the right.

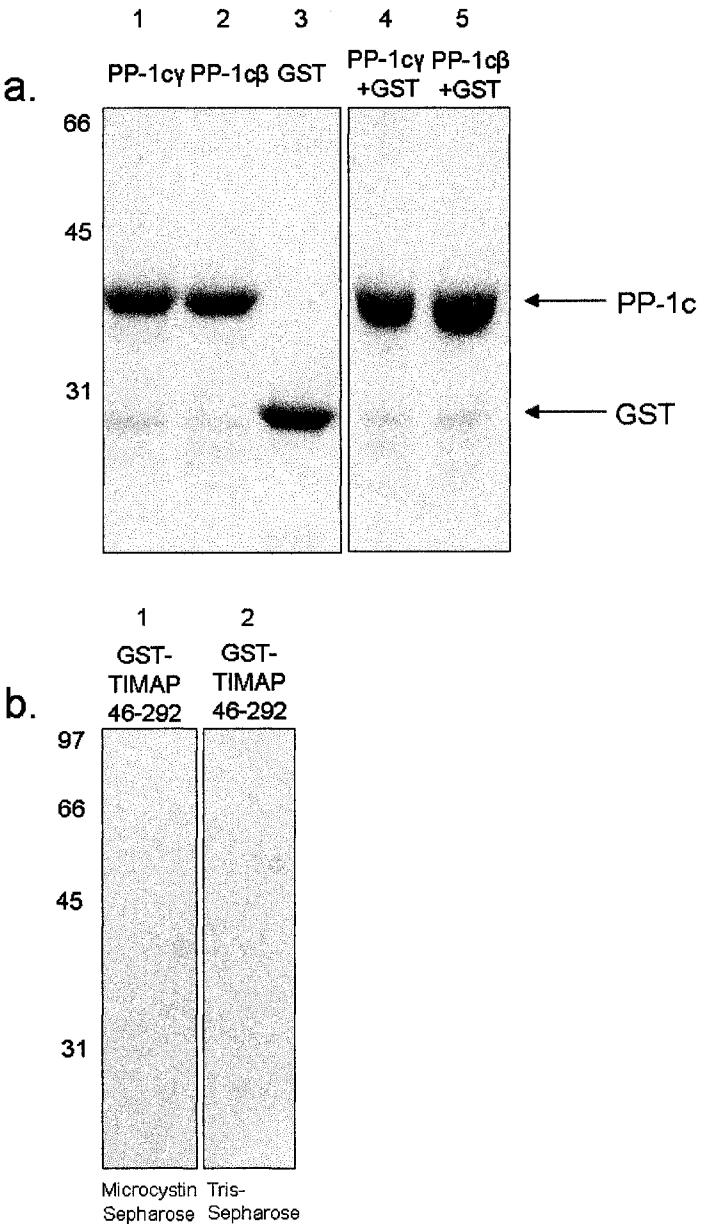

Figure 3-6. GST does not interact with PP-1c and GST-TIMAP does not bind microcystin sepharose in the absence of PP-1c.
Panel a illustrates that GST does not bind to PP-1c immobilized on microcystin sepharose. Lanes 1-3 are SDS-PAGE gels depicting PP-1cγ, PP-1cβ and GST *before* immobilization on microcystin sepharose. Lanes 4-5 illustrate that PP-1cγ and PP-1cβ bind are immobilized on microcystin sepharose, and that GST does not bind to either PP-1c isoform. This indicates that when GST-TIMAP binds to PP-1c immobilized on microcystin sepharose is not via the GST-tag. In panel b, lane 1 depicts SDS-PAGE gels which illustrate that GST-TIMAP does not interact with microcystin sepharose in the absence of PP-1c. Lane 2 indicates that GST-TIMAP does not interact with the sepharose moiety of microcystin sepharose.

3.4 GST-TIMAP inhibits PP-1c activity toward phosphorylase *a*

TIMAP is known to target PP-1c and facilitate dephosphorylation of two cellular substrates. However, it is not clear what effect TIMAP has on PP-1c activity toward other known substrates of the phosphatase, and this formed the basis of objective 3 of this study (p.30). It has been shown that MYPT3 potently inhibits the ability of PP-1c to dephosphorylate glycogen phosphorylase *a*, a physiological substrate of the phosphatase [57]. Since TIMAP shares 45% sequence identity to MYPT3, we predicted that TIMAP would inhibit PP-1c in a similar manner. We discovered that GST-TIMAP was a very potent inhibitor of PP-1c activity towards phosphorylase *a* as a substrate. We began by investigating the effect of all three forms of GST-TIMAP (GST-TIMAP$^{46\text{-}292}$, GST-TIMAP$^{46\text{-}453}$ and GST-TIMAP^{WT}) on PP-1cβ catalytic activity.

All constructs of GST-TIMAP inhibited PP-1cβ activity in the nanomolar range. Figure 3-7 displays dose-response curves that highlight this effect. GST-TIMAP$^{46\text{-}292}$ was the least potent inhibitor of PP-1cβ with an IC_{50} of 62nM. GST-TIMAP$^{46\text{-}453}$ and GST-TIMAP^{WT} inhibited PP-1cβ ten times more potently than GST-TIMAP$^{46\text{-}292}$. The IC_{50} for GST-TIMAP$^{46\text{-}453}$ was 0.6nM while the IC_{50} for GST-TIMAP^{WT} was 0.4nM. IC_{50} values for GST-TIMAP inhibition of PP-1c toward phosphorylase *a* are provided in table 3-1a.

We then investigated whether GST-TIMAP could inhibit the activity of PP-1cγ toward phosphorylase *a* substrate. We found all three GST-TIMAP constructs to be potent inhibitors of PP-1cγ activity. Dose-response curves presented in figure 3-8 illustrate this effect. GST-TIMAP$^{46\text{-}292}$ inhibited PP-1cγ with an IC_{50} of 72nM. Again GST-TIMAP$^{46\text{-}453}$ and GST-TIMAP^{WT} were more potent inhibitors of phosphatase activity (IC_{50} 0.8nM and 1.2nM respectively). The IC_{50} values for GST-TIMAP

inhibition of PP-1cγ toward phosphorylase *a* are summarized in Table 3-1b. GST was tested as a control for inhibition (to a concentration of 500nM) and had no effect on PP-1c activity in the phosphorylase *a* assay.

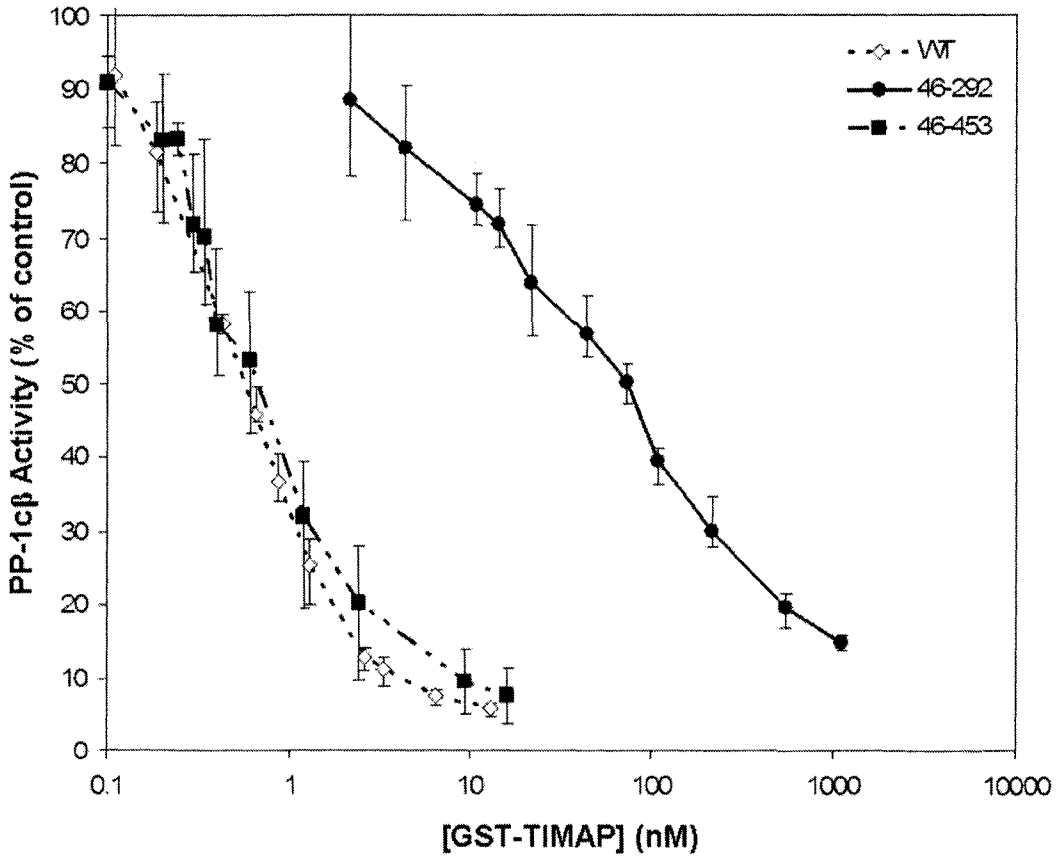

Figure 3-7. GST-TIMAP is a potent inhibitor of human PP-1cβ phosphatase activity toward phosphorylase *a* substrate.

Depicted in the figure are dose-response curves illustrating the effect of GST-TIMAP toward PP-1cβ activity with phosphorylase *a* as substrate. Shown are plots for GST-TIMAP^{WT} (◊ WT), GST-TIMAP$^{46\text{-}453}$ (■ 46-453), and GST-TIMAP$^{46\text{-}292}$ (● 46-292). IC_{50} values determined from the curves are summarized in table 3-1a.

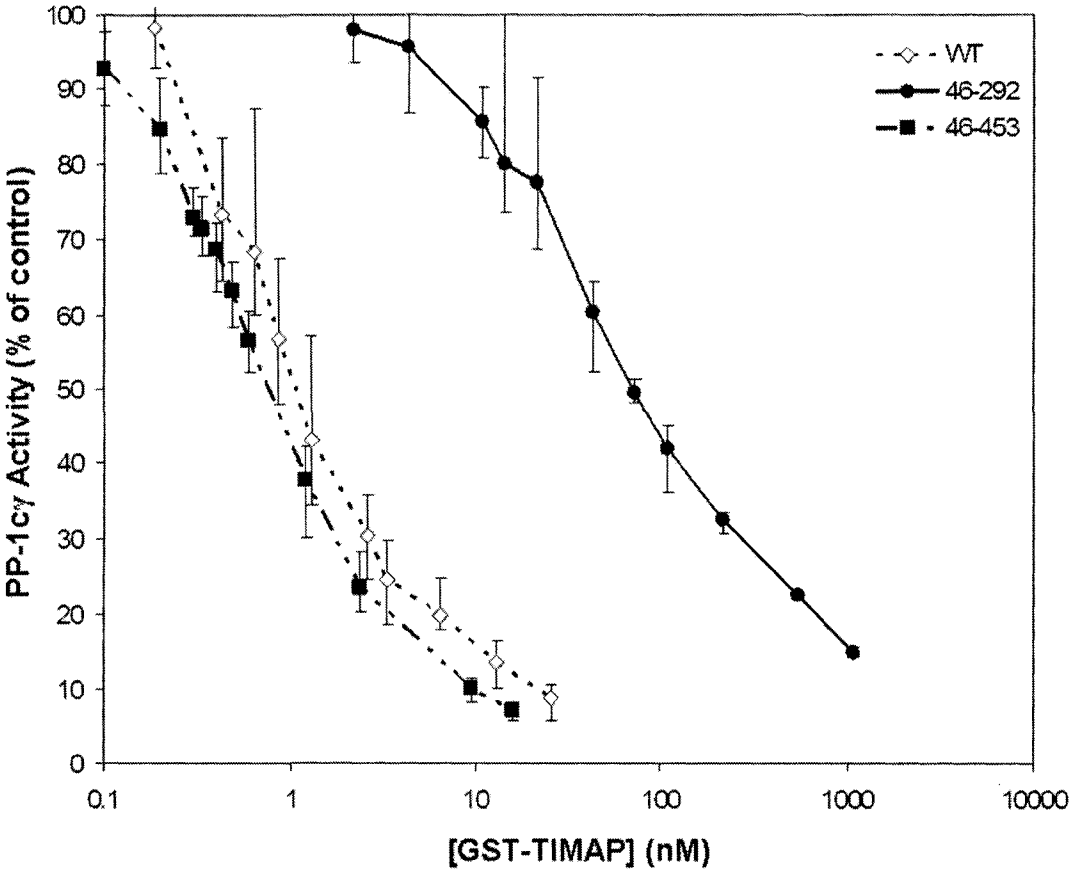

Figure 3-8. GST-TIMAP potently inhibits human PP-1cγ phosphatase activity toward phosphorylase *a* substrate.

The figure depicts dose-response curves which highlight the inhibitory effect of GST-TIMAP toward PP-1cγ activity with phosphorylase *a* as substrate. Plots are shown for GST-TIMAP^{WT} (◊ WT), GST-TIMAP$^{46\text{-}453}$ (■ 46-453), and GST-TIMAP$^{46\text{-}292}$ (● 46-292). IC_{50} values determined from the curves are summarized in table 3-1b.

a.

PP-1cβ	IC_{50} (nM)	(+/-)
46-292	62	13
46-453	0.6	0.4
46-453 DD	0.6	0.1
46-453 EE	0.4	0.1
WT	0.4	0.2

b.

PP-1cγ	IC_{50} (nM)	(+/-)
46-292	72	13
46-453	0.8	0.2
46-453 DD	8.5	5.4
46-453 EE	5.4	4.5
WT	1.2	0.7

Table 3-1. Summary of the IC_{50} values for GST-TIMAP inhibition of PP-1cβ and PP-1cγ using ^{32}P-radiolabelled phosphorylase *a* as PP-1c substrate.
Panel a contains IC_{50} values for inhibition of PP-1cβ phosphatase activity toward phosphorylase *a* activity by GST-TIMAP and Panel b displays IC_{50} values for inhibition of PP-1cγ by GST-TIMAP. The GST-TIMAP constructs listed in the table are as follows: GST-TIMAP$^{46\text{-}292}$ (46-292), GST-TIMAP$^{46\text{-}453}$ (46-453), GST-TIMAP$^{46\text{-}453\ S333D/S337D}$ (46-453 DD), GST-TIMAP$^{46\text{-}453\ S333E/S337E}$ (46-453 EE), and GST-TIMAP^{WT} (WT). (+/-) refers to the maximum value of outliers. IC_{50} values listed are average of at least three experiments.

3.5 GST-TIMAP inhibition of PP-1c toward PNPP substrate

We developed a model predicting how TIMAP interacts with PP-1c, and one feature of this model was an exposed active site of PP-1c when TIMAP is bound (refer to figure 3-1, p.48). We characterized TIMAP as a potent inhibitor of PP-1c activity toward phosphorylase *a* substrate, and to test our model further we investigated the effect of TIMAP on PP-1c activity with a small chemical substrate, *p*-nitrophenol phosphate (PNPP). Based on our predicted model, TIMAP should not inhibit PP-1c activity as potently toward a small substrate as PNPP.

We found that GST-TIMAP exhibits a drastically reduced ability to inhibit PP-1c activity versus the small chemical substrate *p*-nitrophenol phosphate (PNPP). Our most striking find in this regard was that GST-TIMAP$^{46\text{-}292}$ did not inhibit PP-1c (β or γ isoform) activity toward PNPP at all.

GST-TIMAP$^{46\text{-}453}$ inhibited PP-1cβ activity toward PNPP at an IC_{50} of 97nM. This is a 160-fold decrease in IC_{50} as compared to inhibition of PP-1c toward phosphorylase *a*. The IC_{50} of GST-TIMAP^{WT} was determined to be 103nM, a 258-fold decrease in potency as compared to inhibition of PP-1c activity toward phosphorylase *a*. These results are illustrated in dose-response curves in figure 3-9. The IC_{50} values are summarized in table 3-2a.

GST-TIMAP$^{46\text{-}453}$ and GST-TIMAP^{WT} were also inhibitors of PP-1cγ toward PNPP substrate. Figure 3-10 depicts dose-response curves for GST-TIMAP$^{46\text{-}453}$ and GST-TIMAP^{WT}. GST-TIMAP$^{46\text{-}453}$ inhibited PP-1c toward PNPP substrate at an IC_{50} of 180nM, while the IC_{50} of GST-TIMAP^{WT} was determined to be 266nM. This corresponds to a 220-fold decrease in potency of inhibition (for both forms of GST-TIMAP)

compared to their IC_{50} values determined inhibiting PP-1cγ toward phosphorylase *a*. The IC_{50} values of GST-TIMAP$^{46-453}$ and GST-TIMAP^{WT} are summarized in table 3-2b.

Taken together, the PNPP data support our model of TIMAP binding to PP-1c. GST-TIMAP is a potent inhibitor of PP-1c activity toward phosphorylase *a* substrate but at the same time, GST-TIMAP is not as potent at inhibiting PP-1c activity toward the small chemical substrate PNPP. The data suggest that PNPP may gain access to the active site of PP-1c. This is most strongly supported in the case of GST-TIMAP$^{46-292}$, which inhibits PP-1c in the nanomolar range toward phosphorylase *a*, and meanwhile does not inhibit PP-1c toward PNPP at all.

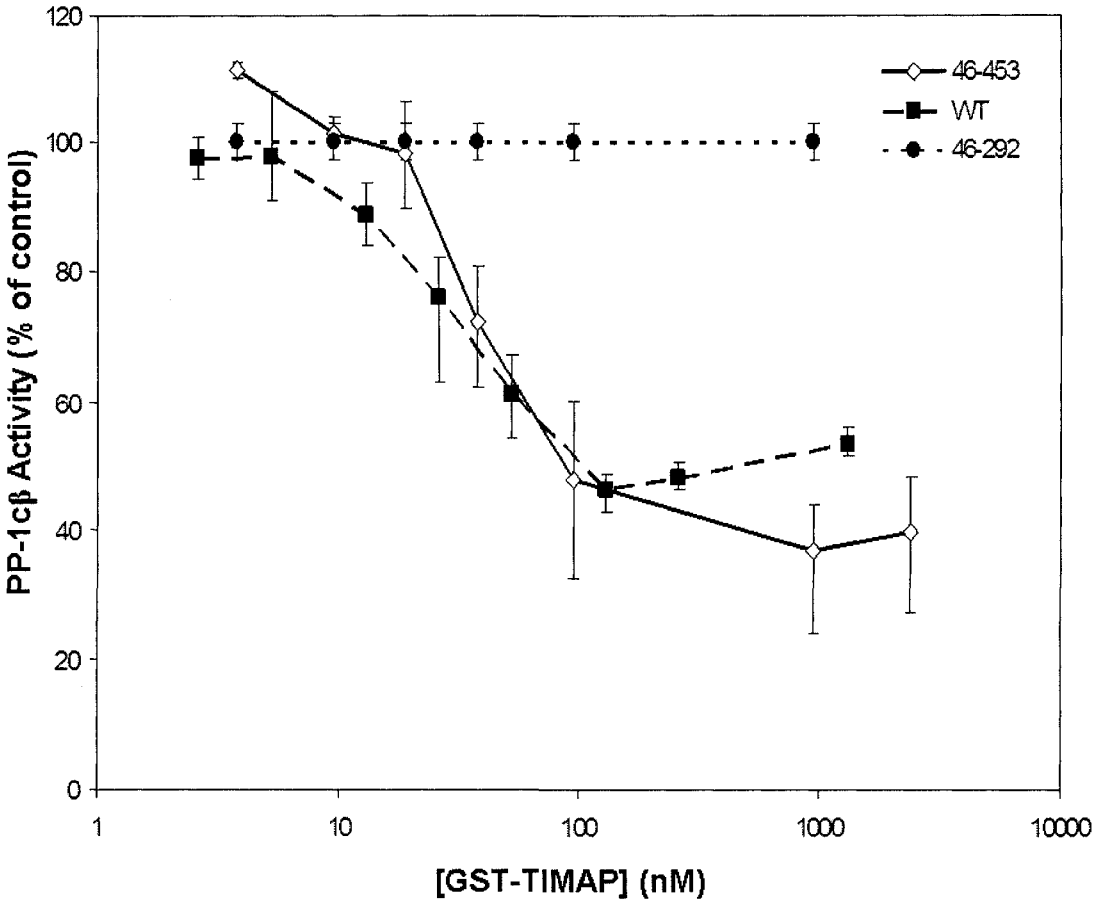

Figure 3-9. Inhibition of PP-1cβ activity by GST-TIMAP using PNPP substrate. Figure 3-9 displays dose-response curves illustrating the inhibition of PP-1cβ activity toward PNPP substrate by GST-TIMAP. Shown are curves for GST-TIMAP^{WT} (■ WT) and GST-TIMAP$^{46\text{-}453}$ (◊ 46-453). GST-TIMAP$^{46\text{-}292}$ (● 46-292) does not inhibit PP-1cβ activity toward PNPP substrate. The IC_{50} values for the inhibition of PP-1cβ by GST-TIMAP are summarized in Table 3-2a.

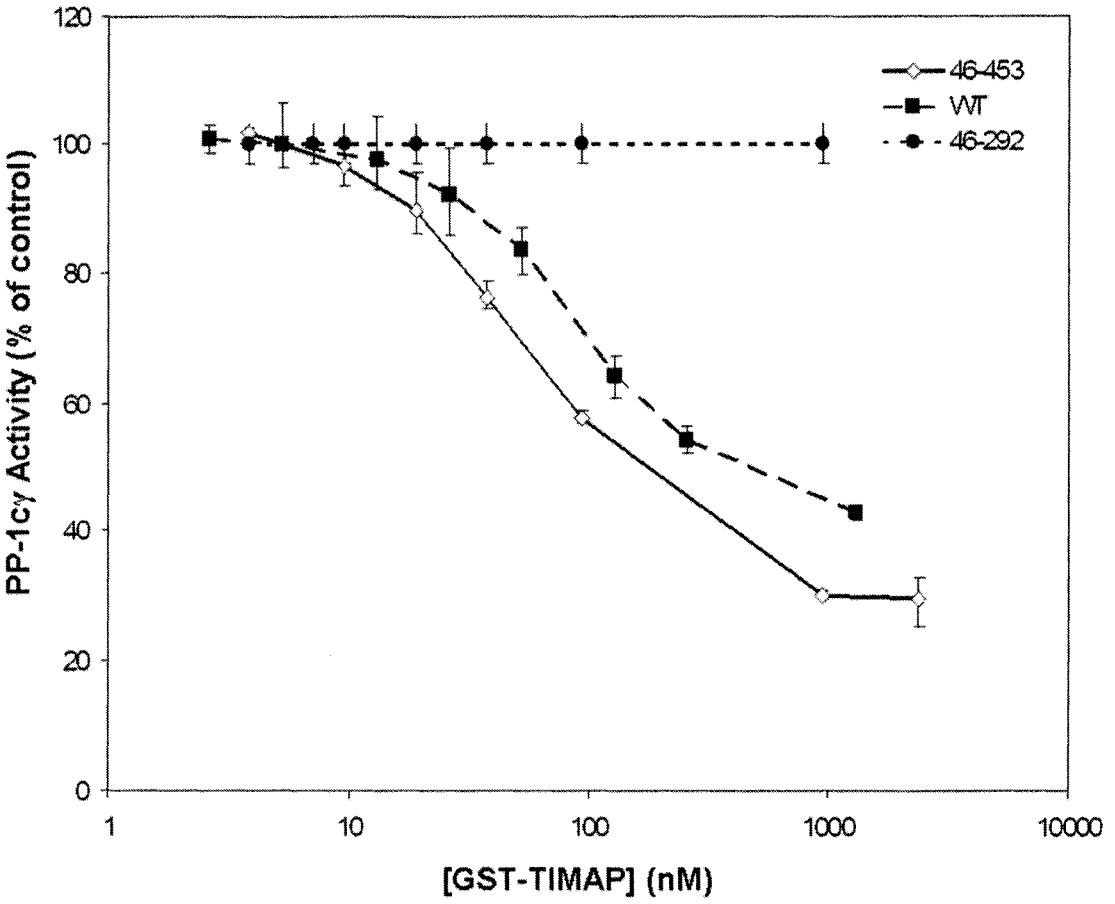

Figure 3-10. GST-TIMAP inhibits PP-1cγ activity toward PNPP substrate.
Dose-response curves illustrating the inhibition of PP-1cγ activity toward PNPP substrate by GST-TIMAP are displayed. GST-TIMAP^{WT} (■ WT) and GST-TIMAP$^{46\text{-}453}$ (◊ 46-453) curves are shown. GST-TIMAP$^{46\text{-}292}$ (● 46-292) does not inhibit PP-1cγ activity toward PNPP substrate. The IC_{50} values for the inhibition of PP-1cγ by GST-TIMAP are summarized in Table 3-2b.

a.

PP-1cβ	IC_{50} (nM)	(+/-)
46-453	97	10
WT	103	20

b.

PP-1cγ	IC_{50} (nM)	(+/-)
46-453	180	13
WT	266	10

Table 3-2. Summary of IC_{50} values for GST-TIMAP inhibition of PP-1cβ and PP-1cγ using *p*-nitrophenol phosphate as substrate.
Listed are IC_{50} values for GST-TIMAP^{WT} (WT) and GST-TIMAP$^{46\text{-}453}$ (46-453) for inhibition of PP-1cβ in panel a and PP-1cγ in panel b. The IC_{50} values shown are averages of at least 3 experiments. (+/-) refers to the maximum value of outliers.

3.6 Investigating the mechanism of PP-1c regulation by phosphorylated TIMAP

It has been previously shown that TIMAP is phosphorylated at Ser 333 and Ser 337 by Glycogen Synthase Kinase-3β (GSK-3β) and Protein Kinase A (PKA) respectively [61]. Li *et al.* (2007) demonstrated that the dual phosphorylation of TIMAP decreases the direct association of TIMAP and PP-1c, and as a result increases PP-1c activity [61]. However, the molecular mechanism of this effect is not completely understood, and exploring the molecular basis for this phenomenon was an objective of this thesis (p.30).

We set out to investigate the effect of the GSK-3β/PKA double phosphorylation using site-directed mutagenesis. We resorted to mutagenesis for these experiments as phosphorylated TIMAP can be de-phosphorylated by PP-1c, and this would mask any effects we would observe using phosphorylated TIMAP. To address this, we simultaneously changed Ser333 and Ser337 to Asp or Glu to mimic phosphorylation. Two double phospho-mimic mutants were made, GST-TIMAP$^{46\text{-}453S333D/S337D}$ (S333D/S337D) and GST-TIMAP$^{46\text{-}453S333E/S337}$ (S333E/S337E).

3.6.1 Phospho-mimic mutants of TIMAP bind PP-1c on microcystin sepharose

We examined whether the S333D/S337D and S333E/S337E phospho-mimic mutants would bind to PP-1c immobilized on microcystin sepharose. We predicted a decreased ability of the phospho-mimic mutants to bind to PP-1c based on the prior published results mentioned above. However, as seen in figure 3-11, the S333D/S337D and S333E/S337E mutants bound to both PP-1cβ and PP-1cγ isoforms immobilized on microcystin sepharose.

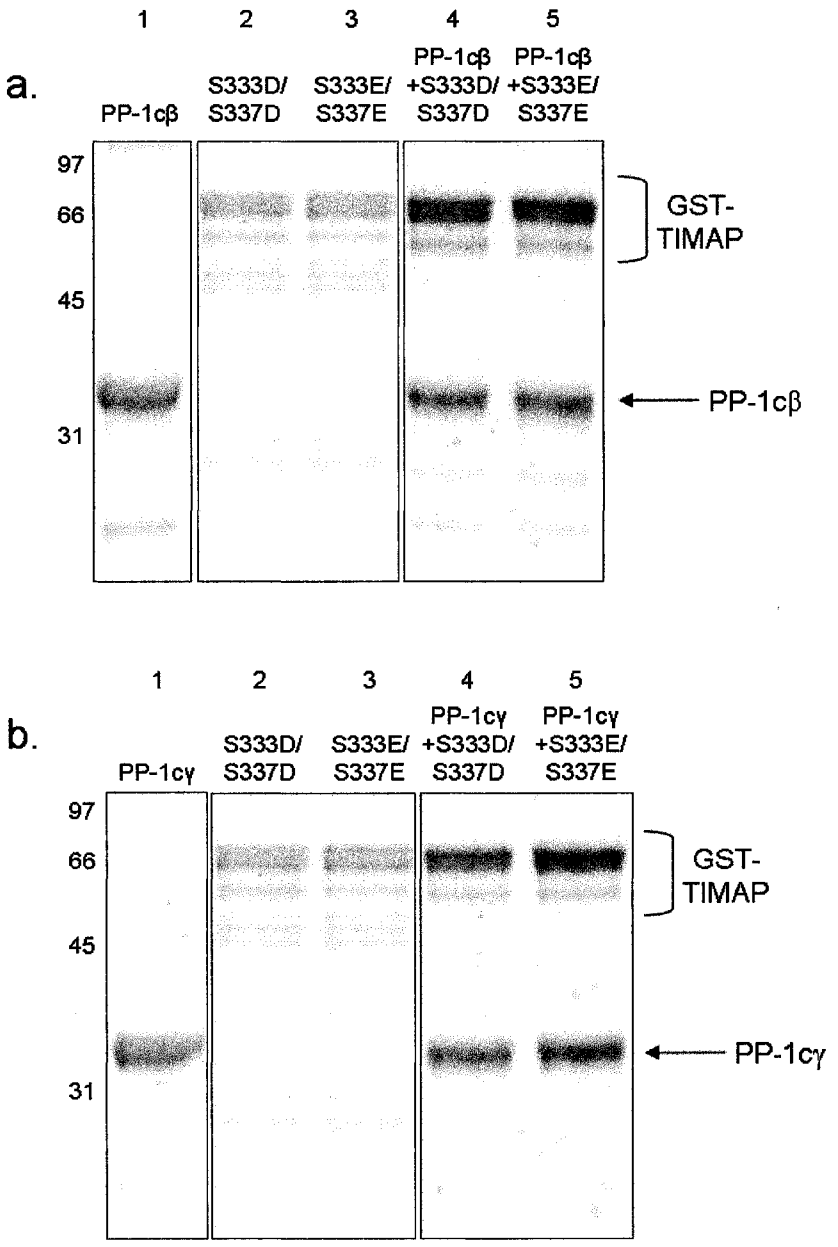

Figure 3-11. Phospho-mimic mutants of GST-TIMAP bind to PP-1cβ and PP-1cγ immobilized on microcystin sepharose.

The figure displays SDS-PAGE gels which illustrate binding of GST-TIMAP$^{46\text{-}453S333D/S337D}$ (S333D/S337D) and GST-TIMAP$^{46\text{-}453S333E/S337E}$ (S333E/S337E) to PP-1c immobilized on microcystin sepharose. Panel a exhibts results of phospho-mimic GST-TIMAP mutants binding to PP-1cβ. Panel b displays results of phospho-mimic GST-TIMAP mutants binding to PP-1cγ. In both panels lanes 1-3 represent PP-1c, S333D/S337D and S333E/S337E *before* immobilization on microcystin sepharose. Lanes 4 and 5 show S333D/S337D (lane 4) and S333E/S337E (lane 5) bind to immobilized PP-1c on microcystin sepharose.

3.6.2 Inhibition of PP-1c toward phosphorylase *a* by TIMAP phospho-mimic mutants

We explored the effect of the phospho-mimic mutants on PP-1c activity toward phosphorylase *a* substrate. We found that the S333D/S337D mutant inhibited PP-1cβ activity toward phosphorylase *a* with an IC_{50} of 0.6nM. The S333E/S337E mutant inhibited PP-1cβ as well, the IC_{50} being 0.4nM. Dose-response curves exhibiting this inhibition are in figure 3-12 and the IC_{50} values are listed in table 3-1a (p.61). Mutating Ser333 and Ser337 to phospho-mimic amino acids had no discernible effect on the inhibitory behavior TIMAP has on PP-1cβ activity toward phosphorylase *a*. The IC_{50} of GST-TIMAP$^{46-453}$ was 0.6nM, which is virtually the same as the determined IC_{50} values for the phospho-mimic mutants inhibition of PP-1cβ.

We determined the IC_{50} of S333D/S337D mutant to be 8.5nM for inhibition of PP-1cγ activity toward phosphorylase *a*. The S333E/S337E mutant inhibited PP-1cγ phosphorylase *a* activity with an IC_{50} of 5.4nM. Dose response curves illustrating these effects are in figure 3-13. Interestingly, both of the phospho-mimic mutants were much less potent inhibitors of PP-1cγ activity toward phosphorylase *a*. The S333D/S337D mutant was 11-fold less potent inhibiting PP-1cγ as compared to GST-TIMAP$^{46-453}$, while the S333E/S337E double mutant was 7-fold less potent inhibiting PP-1cγ as compared to GST-TIMAP$^{46-453}$. A summary of the IC_{50} values can be found in table 3-1b (p.61).

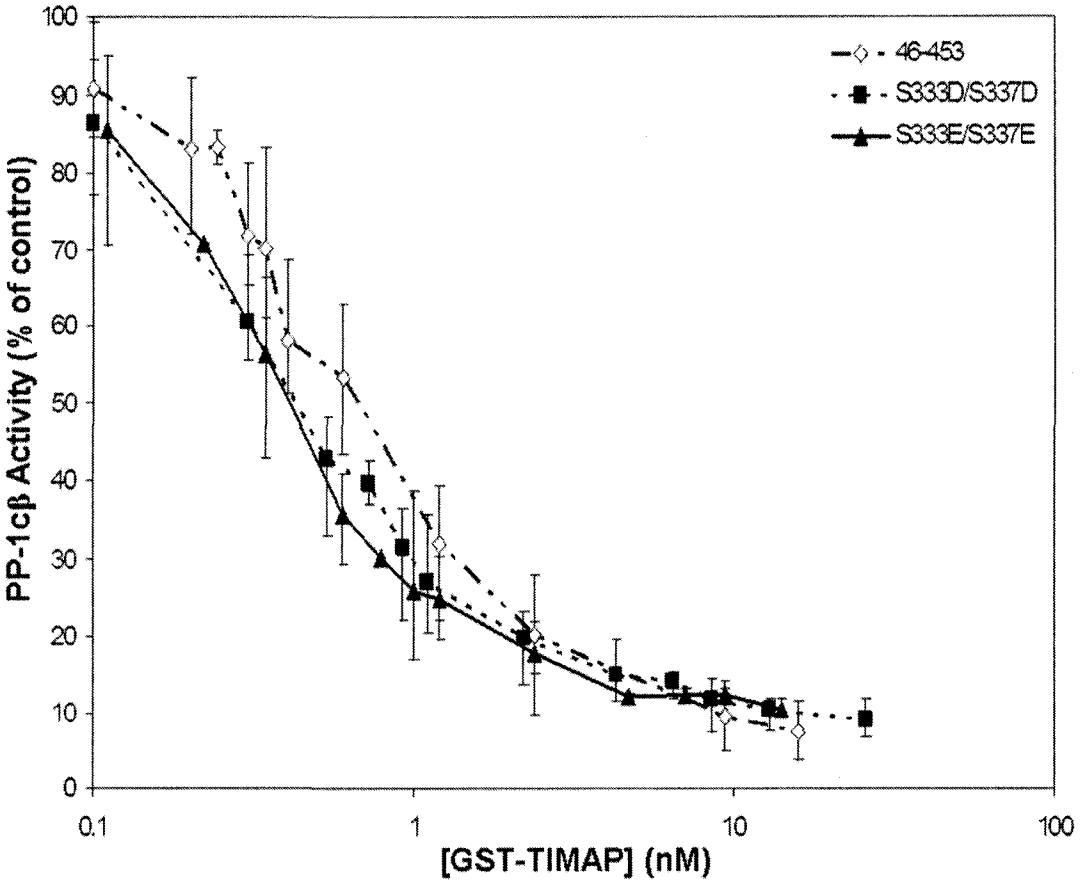

Figure 3-12. TIMAP phospho-mimic mutants S333D/S337D and S333E/S337E do not differ from GST-TIMAP$^{46-453}$ in their inhibition of PP-1cβ activity toward phosphorylase *a* substrate.

The figure displays dose-response curves of the effect of double mutations GST-TIMAP$^{46-453S333D/S337D}$ (■ S333D/S337D) and GST-TIMAP$^{46-453S333E/S337E}$ (▲ S333E/S337E) on PP-1cβ activity toward phosphorylase *a* substrate. In the figure dose-response curves of the phospho-mimic mutants are compared to the dose-response curve of GST-TIMAP$^{46-453}$ (◊ 453). The IC_{50} values determined from the graph are summarized in table 3-1a (p.61).

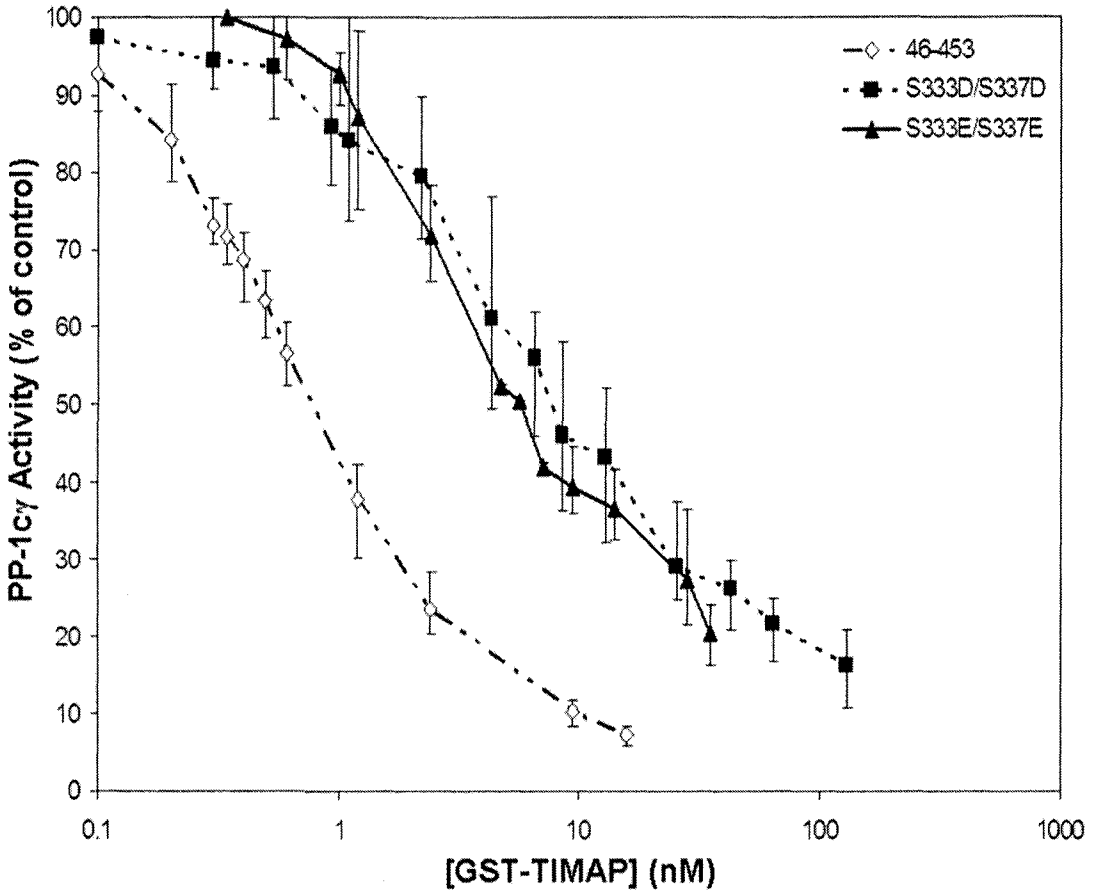

Figure 3-13. Phospho-mimic mutants of TIMAP S333D/S337D and S333E/S337E demonstrate a reduced ability to inhibit PP-1cγ activity toward phosphorylase *a* substrate.

Shown are dose-response curves of the effect of double mutations GST-TIMAP$^{46\text{-}453S333D/S337D}$ (■ S333D/S337D) and GST-TIMAP$^{46\text{-}453S333E/S337E}$ (▲ S333E/S337E) on PP-1cγ activity toward phosphorylase *a* substrate. Dose-response curves of the mutants are compared to the dose-response curve of GST-TIMAP$^{46\text{-}453}$ (◊ 453). The IC_{50} values determined from the curves are summarized in table 3-1b (p.61).

3.6.3 Phospho-mimic mutants of TIMAP exhibit a reduced ability to inhibit PP-1c toward PNPP substrate

Interestingly, both S333D/S337D and S333E/S337E phospho-mimic mutants are not potent inhibitors of PP-1c activity versus PNPP substrate. When tested at phospho-mimic mutant concentrations as high as 100nM, PP-1c activity remains as high as 60-70% for PP-1cβ and 80-90% for PP-1cγ. This effect is highlighted in figure 3-14. An IC_{50} of the S333D/S337D and S333E/S337E mutants could not be determined since concentrations as high as 300nM were unable to decrease PP-1c activity toward PNPP to less than 50%. These results further confirm that when TIMAP is bound to PP-1c the phosphatase active site may be accessible to solvent, which would allow access to a small chemical substrate such as PNPP. The weak inhibition of both PP-1cβ and PP-1cγ toward PNPP indicates that the presence of acidic side chains at the positions of Ser333 and Ser337 renders the phospho-mimic mutants unable to interact with PP-1c in the same manner as wildtype.

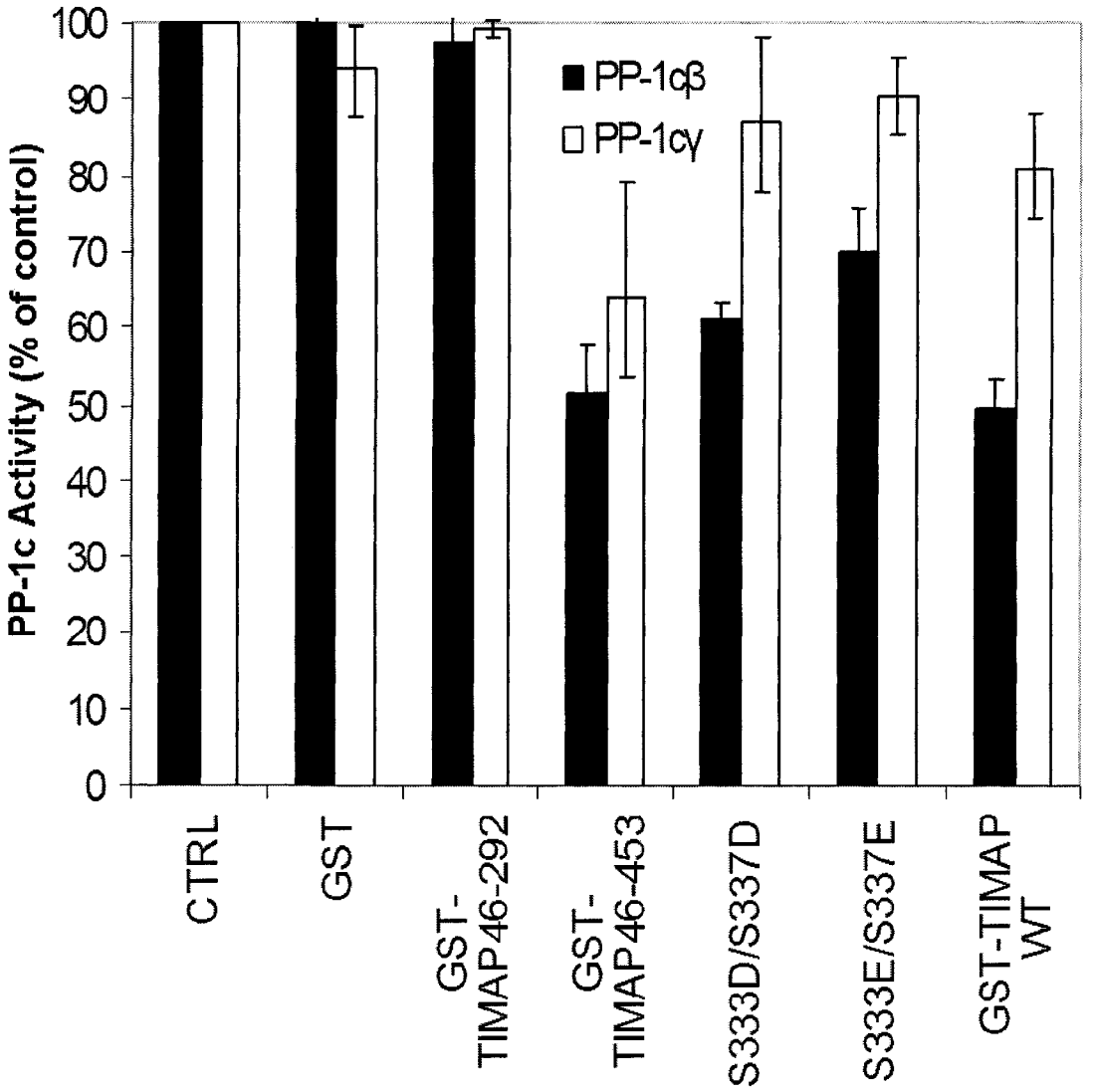

Figure 3-14. S333D/S337D and S333E/S337E are not potent inhibitors of PP-1c activity toward PNPP substrate: a comparison of PP-1c inhibition using 100nM GST-TIMAP in inhibition assays.

Shown is a graph summarizing inhibition of PP-1cβ and PP-1cγ activity toward PNPP substrate in the presence of 100nM of different GST-TIMAP proteins. The truncated form of GST-TIMAP$^{46\text{-}292}$ does not inhibit PP-1c activity versus PNPP substrate. However at 100nM concentration, GST-TIMAP$^{46\text{-}453}$, GST-TIMAP$^{46\text{-}453S333D/S337D}$ (S333D/S337D), GST-TIMAP$^{46\text{-}453S333E/S337E}$ (S333E/S337E) and GST-TIMAP^{WT} (GST-TIMAP WT) inhibit PP-1cβ and PP-1cγ activity toward PNPP substrate. The phospho-mimic mutants S333D/S337D and S333E/S337E are much less potent inhibiting PP-1c toward PNPP. Also shown is the control (CTRL) representing maximal PP-1c activity in the absence of GST-TIMAP. A control of GST was included as well and has no effect on the catalytic activity of PP-1c.

3.7 GST-TIMAP blocks cdk2/CyclinA phosphorylation of the PP-1c C-terminal tail

PP-1cγ is known to be phosphorylated by cdk2/CyclinA in the C-terminal tail of the phosphatase at Thr311 (Thr317 in PP-1cβ) [43,44]. An essential feature of our predicted model (figure 3-1, p.48) is that TIMAP binds and wraps around the C-terminal tail of PP-1c. An objective of this thesis was to determine whether the model is correct in this predicted mode of association between TIMAP and PP-1c (p.31), and we dealt with this objective by determining whether cdk2/CyclinA could phosphorylate PP-1c when TIMAP is bound. If the predicted model is correct, TIMAP would prevent the cdk2/CyclinA phosphorylation of the PP-1c C-terminal tail.

We found that GST-TIMAP$^{46\text{-}292}$, GST-TIMAP$^{46\text{-}453}$ and GST-TIMAP^{WT} all reduce the phosphorylation PP-1c by cdk2/CyclinA. This effect is illustrated in figures 3-15, 3-16, and 3-17. Lanes 1 and 2 of each figure are SDS-PAGE gels depicting the reaction contents. Lanes 3-6 represents the autoradiograph of the same gels. Two parallel sets of reactions were set up. In one set (results of which are pictured in lanes 3 and 4 of figures 3-15 through 3-17), microcystin was included in the phosphorylation reaction to suppress PP-1c activity. This was done to prevent the auto-dephosphorylation of the PP-1c C-terminal tail during the phosphorylation reaction. In the other set of reactions microcystin was not included, and these results are depicted in lanes 5 and 6 of figures 3-15 through 3-17. The inclusion of microcystin results in a stronger signal for phosphorylated PP-1c (compare lane 3 versus lane 5).

When the phosphorylation reaction is carried out with GST-TIMAP included in the reaction mixture, there is a marked decrease in the ability of cdk2/CyclinA to phosphorylate PP-1c. This effect is illustrated in lanes 4 and 6 of figures 3-15 through 3-

17. The band corresponding to phosphorylated PP-1c (visible in lanes 3 and 5) is drastically decreased when GST-TIMAP is included in the cdk2/CyclinA phosphorylation reaction (lanes 4 and 6). The results presented are experiments carried out using PP-1cγ, however identical results were observed using PP-1cβ (data not shown).

In lane 4 of figure 3-16, it can be seen that GST-TIMAP$^{46-453}$ does not prevent phosphorylation of PP-1c by cdk2/CyclinA to the same extent as GST-TIMAP$^{46-292}$ and GST-TIMAP^{WT} when microcystin is included in the reaction. Comparing lanes 4 and lane 6, there is still a band corresponding to phosphorylated PP-1c present in lane 4. With the inclusion of microcystin in the reaction and inhibition of PP-1c activity, it is evident that GST-TIMAP$^{46-453}$ can be phosphorylated by cdk2/CyclinA. More on the phosphorylation of GST-TIMAP$^{46-453}$ will follow. The results indicate that if GST-TIMAP$^{46-453}$ is phosphorylated, it is less effective in preventing phosphorylation of PP-1c by cdk2/CyclinA.

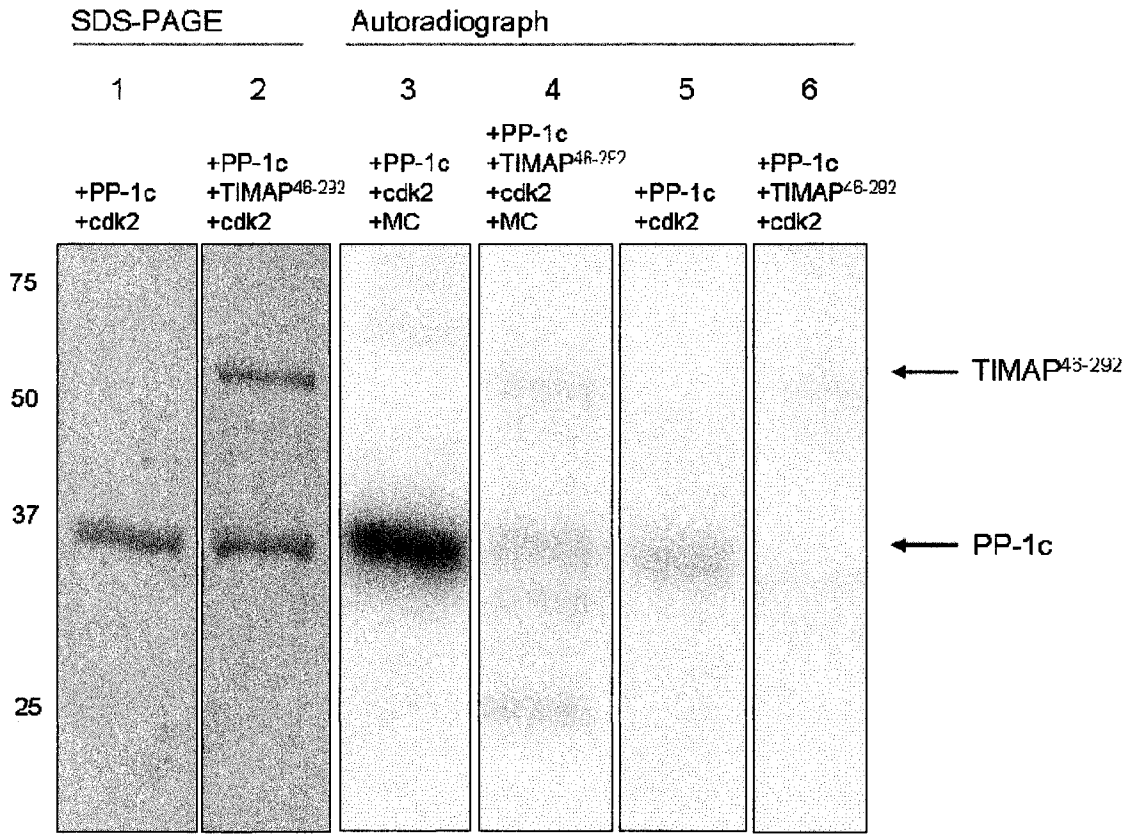

Figure 3-15. GST-TIMAP$^{46-292}$ reduces cdk2/CyclinA phosphorylation of PP-1cγ. Lanes 1 and 2 display SDS-PAGE gels illustrating reaction contents. Lanes 3-6 exhibit the autoradiograph of the reactions. Lanes 1 and 3 correspond to PP-1cγ plus cdk2/CyclinA, microcystin (MC), and ^{32}P-γ-ATP (lane 5 is the same except the reaction did not contain microcystin). There is a strong band corresponding to phosphorylated PP-1cγ in lane 3, and to a lesser extent in lane 5. Lanes 2 and 4 contain PP-1cγ plus GST-TIMAP (TIMAP$^{46-292}$), microcystin, cdk2/CyclinA and ^{32}P-γ-ATP (lane 6 is the same except the reaction did not contain microcystin). When GST-TIMAP$^{46-292}$ is present in the reaction, there is no phosphorylation of PP-1cγ, and the phospho-PP-1c band seen in lane 3 is vastly decreased in lanes 4 and 6.

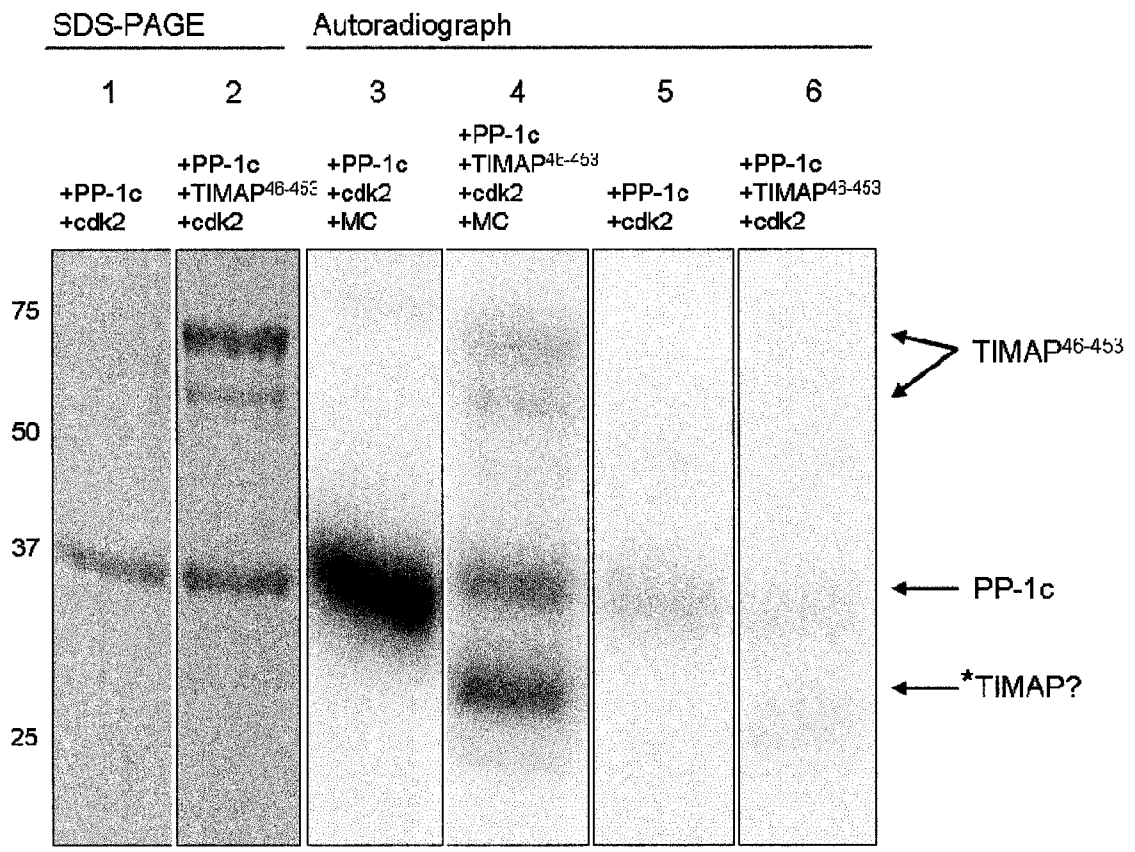

Figure 3-16. GST-TIMAP$^{46-453}$ reduces cdk2/CyclinA phosphorylation of PP-1cγ. Lanes 1 and 2 display SDS-PAGE gels illustrating reaction contents. Lanes 3-6 exhibit the autoradiograph of the reactions. Lanes 1 and 3 correspond to PP-1cγ plus cdk2/CyclinA, microcystin (MC), and ^{32}P-γ-ATP (lane 5 is the same except the reaction did not contain microcystin). There is a strong band corresponding to phosphorylated PP-1cγ in lane 3 and to a lesser extent in lane 5. Lanes 2 and 4 contain PP-1cγ plus GST-TIMAP (TIMAP$^{46-453}$), microcystin and cdk2/CyclinA with ^{32}P-γ-ATP (lane 6 is the same except the reaction did not contain microcystin). In the absence of microcystin and GST-TIMAP$^{46-453}$ is present in the reaction, there is no phosphorylation of PP-1cγ, and the phospho-PP-1c band seen in lane 3 and lane 5 is markedly decreased in lane 6. However, when microcystin is included in the reaction, phosphorylation of GST-TIMAP$^{46-453}$ is observed, and these bands are seen in lane 4. When GST-TIMAP$^{46-453}$ is phosphorylated (and a proteolytic fragment of GST-TIMAP$^{46-453}$, marked by an asterisk), there is a reduced ability to prevent phosphorylation of PP-1c (lane 4).

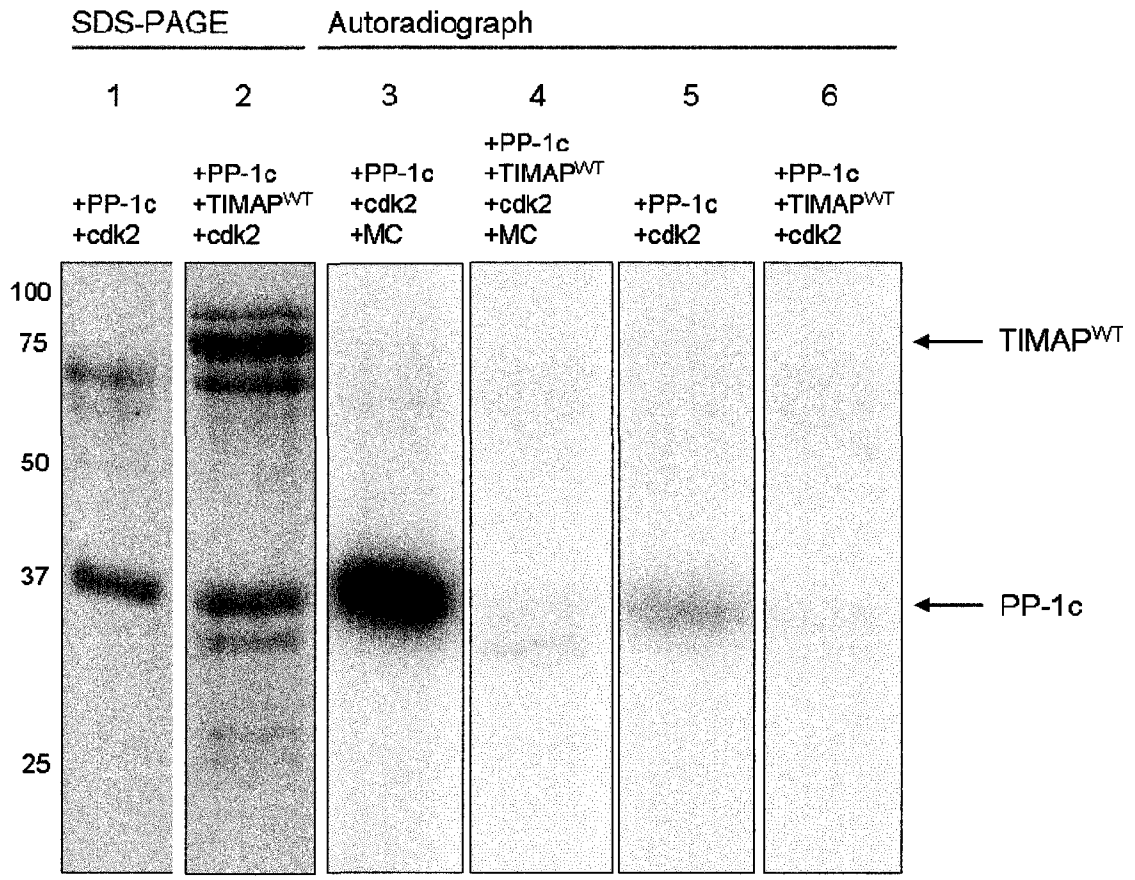

Figure 3-17. GST-TIMAP^{WT} reduces cdk2/CyclinA phosphorylation of PP-1cγ. Lanes 1 and 2 display SDS-PAGE gels illustrating reaction contents. Lanes 3-6 exhibit the autoradiograph of the reactions. Lanes 1 and 3 correspond to PP-1cγ plus cdk2/CyclinA, microcystin (MC), and ^{32}P-γ-ATP (lane 5 is the same except the reaction did not contain microcystin). There is a strong band corresponding to phosphorylated PP-1cγ in lane 3, and to a lesser extent in lane 5. Lanes 2 and 4 contain PP-1cγ plus GST-TIMAP (TIMAP^{WT}), microcystin and cdk2/CyclinA with ^{32}P-γ-ATP (lane 6 is the same except the reaction did not contain microcystin). When GST-TIMAP^{WT} is present in the reaction, there is no phosphorylation of PP-1cγ, and the phospho-PP-1c band seen in lane 3 and lane 5 is markedly decreased in lane 4 and in lane 6.

Figure 3-18 depicts the predicted model of TIMAP bound to PP-1c in surface representation. The arrow highlights the distal region of the C-terminal tail where Thr311 (the site of cdk2/CyclinA phosphorylation) would be located on PP-1cγ. The model predicts that the C-terminal tail of PP-1c is surrounded by the ankyrin repeats of TIMAP, and these ankyrin repeats would shield Thr311 from cdk2/CyclinA. The experiments carried out in this section involving cdk2/CyclinA phosphorylation of PP-1c clearly indicated that when GST-TIMAP binds PP-1c, cdk2/CyclinA has a decreased ability to phosphorylate PP-1c. These findings are consistent with the predicted model of TIMAP bound to PP-1c as depicted in figure 3-18.

Figure 3-18. Surface representation of the predicted model of TIMAP bound to PP-1c and the proximity of the cdk2/CyclinA phosphorylation site.
TIMAP (top, shown in cyan) is bound to PP-1c (bottom, depicted in slate) and wraps around the enzyme gripping the C-Terminal tail. TIMAP binding to PP-1c in this manner blocks access to the cdk2/CyclinA phosphorylation site in the C-terminal tail of PP-1c (which is Thr317 in PP-1cβ and Thr311 in PP-1cγ). This mode of association also leaves the active site of PP-1c (denoted by an asterisk) open and accessible to solution. The approximate location of the cdk2/CyclinA phosphorylation site on PP-1c is highlighted by the arrow.

3.8 GST-TIMAP$^{46-453}$ can be phosphorylated by cdk2/CyclinA

While investigating the effect of GST-TIMAP on cdk2/CyclinA phosphorylation of PP-1c, we unexpectedly found that GST-TIMAP$^{46-453}$ can be phosphorylated by cdk2/CyclinA. Interestingly, GST-TIMAP^{WT} is not phosphorylated to a great extent by cdk2/CyclinA, as illustrated in figure 3-19 (panel a). Lane 1 of panel a is an SDS-PAGE gel depicting the cdk2/CyclinA and GST-TIMAP^{WT} reaction contents, and lane 2 is the autoradiograph of the same gel. However, GST-TIMAP$^{46-453}$ and a putative 31 kDa proteolytic fragment of GST-TIMAP$^{46-453}$ are robust substrates for cdk2/CyclinA as presented in figure 3-19 (panel b). Lane 1 of panel b is an SDS-PAGE gel depicting the phosphorylation reaction contents. Lane 2 is an autoradiograph of the same gel. Arrows indicate GST-TIMAP$^{46-453}$ (and proteolytic product), and in the autoradiograph there are bands present indicating phosphorylation.

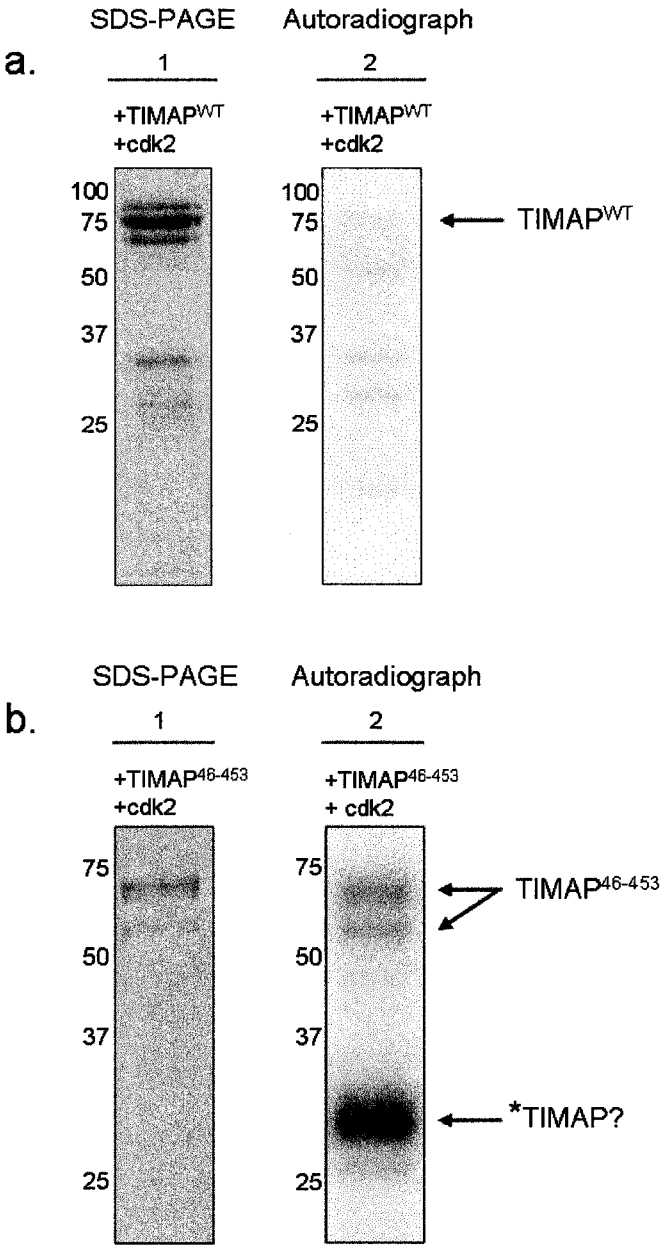

Figure 3-19. GST-TIMAP$^{46-453}$ can be phosphorylated by cdk2/CyclinA.
In both panel a and panel b lane 1 is an SDS-PAGE gel and lane 2 is the corresponding autoradiograph of the gel. Panel a displays the results of phosphorylation of GST-TIMAP^{WT} (TIMAP^{WT}) by cdk2/CyclinA. In the autoradiograph in lane 2 there is not strong evidence of phosphorylation of GST-TIMAP^{WT}. In comparison, panel b depicts the results of phosphorylation of GST-TIMAP$^{46-453}$ with cdk2/CyclinA. In the autoradiograph in lane 2 there are bands which correspond to phosphorylated GST-TIMAP$^{46-453}$ (marked by an arrow, TIMAP$^{46-453}$) and a proteolytic degradation product that is robustly phosphorylated by cdk2/CyclinA (denoted by an asterisk).

Chapter 4: Discussion, Conclusions and Future Directions

4.1 Discussion

4.1.1 Predicted mechanism of interaction between TIMAP and PP-1c

The structural model of TIMAP predicts binding to PP-1c via amino acids ^{63}KVSF^{66}, the RVXF motif required for TIMAP binding to PP-1c (figure 3-1). This was expected from the model as it has been shown that if the ^{63}KVSF^{66} motif is mutated to ^{63}KASA^{66} this abrogates the interaction between PP-1c and TIMAP [61]. It is well documented that the RVXF motif is required by PP-1c regulatory proteins for interaction with the phosphatase (refer to section 1.3.2, p.12). Immediately C-terminal to the ^{63}KVSF^{66} motif marks the beginning of the ankyrin repeats of TIMAP, which are predicted by the model to wrap around the C-terminal tail of PP-1c.

The amino acid sequence of TIMAP predicts 5 ankyrin repeats using a sequence analysis program such as SMART [83,84], however, the predicted model contains 8 ankyrin repeats. An ankyrin repeat is a structural motif in proteins composed of a recurring pattern of α-helix-loop-α-helix-β-hairpin (described in section 1.4.3, p.23). This discrepancy in the number of sequence-predicted versus model-predicted ankyrin repeats may be due to the fact that the model was constructed on the basis of sequence similarity (and using the crystal structure as a template) of MYPT1, which also contains 8 copies of the structural motif.

It is not uncommon for ankyrin repeat containing proteins to have more of these motifs in their crystal structures than predicted by computer programs [85]. Analysis of MYPT1 with the sequence analysis program SMART predicts only 6 ankyrin repeats, and the crystal structure contains 8. The amino acid sequence of TIMAP predicts 5

ankyrin repeats using SMART compared to the 8 predicted by our model. When programs such as SMART predict ankyrin repeats, only the strongest consensus sequence for the structural motif will be designated an ankyrin repeat- therefore, when a crystal structure is solved of a protein there may be additional motifs not predicted by the automated program. These can be considered "non-canonical" ankyrin repeats as they often do not follow the typical "canonical" α-helix-loop-α-helix-β-hairpin structural motif.

The 5 ankryin repeats predicted from the amino acid sequence of TIMAP are numbered 1, 2, 3, 6, and 7 in the model (figure 3-1). These repeats all contain the "canonical" α-helix-loop-α-helix-β-hairpin motif of an ankyrin repeat, and thus repeats 4, 5, and 8, which do not have all of the above elements (4 and 8 lack the β-hairpin loop and 8 lacks the N-terminal α-helix), are not predicted by the amino acid sequence.

4.1.2 Expression and purification of GST-TIMAP

We initially attempted to express hexa-His-tagged bovine TIMAP, which was unsuccessful as it did not produce soluble protein. For expression of TIMAP a Glutathione S-Transferase (GST) affinity tag was chosen since GST tags have a reputation for aiding in solubility of proteins which are insoluble or difficult to express [80].

We opted to pursue studies of TIMAP without removing the GST tag, as it has been shown that GST does not bind to PP-1c, and that GST has no effect on PP-1c catalytic activity [32]. Studies of the closely related MYPT3 were also carried out as a GST-fusion protein [57]. It was confirmed that GST does not interact with PP-1c using

microcystin sepharose (figure 3-6) and that GST has no effect on PP-1c phosphatase activity toward phosphorylase *a* and PNPP substrates. For these reasons it was deemed sufficient to carry out investigations with GST-TIMAP.

However, there was one issue using GST-TIMAP. A drawback to using the GST tag is the ability of the tag to dimerize, i.e. bind to itself [86,87]. This provided some obstacles in terms of strategies used to purify the GST-TIMAP to 100% homogeneity. The GST affinity resin glutathione sepharose 4B was utilized in purification of GST-TIMAP to obtain >90% pure protein preparations. Due to the ability of the GST-tag to dimerize, difficulties were encountered in separating proteolytically degraded GST-TIMAP from the full length of the intended construct being expressed. This effect was particularly evident when gel filtration chromatography had little effect on protein purity. To pursue structural studies of TIMAP in the future, the GST-tag will have to be removed which will inevitably lead to 100% purity in TIMAP preparations.

4.1.3 GST-TIMAP binds PP-1cβ and PP-1cγ attached to microcystin sepharose

GST-TIMAP was found to interact with both PP-1cβ and PP-1cγ immobilized on microcystin sepharose (figure 3-5). The microcystin sepharose affinity chromatography results have a number of implications. When PP-1c is immobilized on this resin, it is trapped via the phosphatase active site. The active site of PP-1c is distant from the RVXF binding groove where regulatory proteins of PP-1c bind to the phosphatase. This implies that when GST-TIMAP bound to PP-1c attached to microcystin sepharose, the interaction was via the RVXF motif of TIMAP (which is amino acids ^{63}KVSF^{66}), as predicted by the model (figure 3-1). These results also indicated that GST-TIMAP binding to PP-1c does not occlude the active site of the phosphatase. In the event that TIMAP binding to PP-1c

did block the active site of the phosphatase, PP-1c would be unable to bind to the microcystin sepharose. The microcystin sepharose data provided initial support for the predicted model which proposes that TIMAP binds via ^{63}KVSF^{66} to PP-1c and wraps around the phosphatase, leaving the active accessible to solvent (figure 3-1).

It has recently been shown that TIMAP associates with PP-1cβ endothelial cells [62], and work by our collaborators in Dr Barbara Ballermann's laboratory (University of Alberta) has demonstrated that endogenous TIMAP co-immunoprecipitates with PP-1cβ in glomerular endothelial cells (Dr Barbara Ballermann, personal communication). This is in line with previous findings that other MYPT family proteins such as MYPT1, MYPT2, and MYPT3 have been found to associate with PP-1β in live cells [12,58,88].

GST-TIMAP was able to interact with both PP-1cβ and PP-1cγ immobilized on microcystin sepharose. Our collaborators in the Ballermann Group have similar findings, that PP-1cα, PP-1cβ and PP-1cγ all co-immunoprecipitate with TIMAP over-expressed in Madin-Darby canine kidney (MDCK) epithelial cells (Dr Barbara Ballermann, personal communication). The PP-1c isoforms are divergent in amino acid sequence in their N- and C-terminal regions. It is thought that the difference in the C-terminal amino acid sequence gives rise to the PP-1c isoform specificity of different regulatory proteins [14,16]. The microcystin sepharose data, combined with the findings of the Ballermann Group suggest that interaction between ^{63}KVSF^{66} of TIMAP and PP-1c overrides any secondary discriminatory interactions that are formed between the C-terminal tail of PP-1c and TIMAP. It is possible that endogenous TIMAP interacts with other isoforms of PP-1c in cell lines other than endothelial cells.

It should be noted that the microcystin sepharose results do not address the binding affinity of TIMAP to the different isoforms of PP-1c. In order to accurately determine the "affinity" or preference of TIMAP for either PP-1c isoform, K_D values would have to be determined.

4.1.4 GST-TIMAP inhibits PP-1c phosphorylase *a* activity

Here GST-TIMAP was determined to be a potent inhibitor of PP-1c activity toward phosphorylase *a* substrate (figure 3-7, 3-8, and table 3-1). The inhibition of both PP-1cβ and PP-1cγ by GST-TIMAP was in the sub-nanomolar range, and this is on par with inhibition by the potent toxin microcystin which inhibits PP-1cβ at an IC_{50} of 5nM and PP-1cγ at an IC_{50} of 0.3nM [38].

There was a striking difference between the shorter form of GST-TIMAP$^{46-292}$ and the longer GST-TIMAP$^{46-453}$ and GST-TIMAP^{WT} forms in terms of ability to inhibit PP-1c toward phosphorylase *a*. GST-TIMAP$^{46-292}$ was ~100-fold less potent inhibiting PP-1c activity compared to GST-TIMAP$^{46-453}$ and GST-TIMAP^{WT}. Two conclusions can be drawn from this data. First, the N-terminal ankyrin repeat region of TIMAP is able to inhibit PP-1c activity toward phosphorylase *a*. Second, an additional site of interaction exists between TIMAP and PP-1c that increases inhibition of PP-1c catalytic activity. The remarkable difference in inhibition between GST-TIMAP$^{46-292}$ and GST-TIMAP$^{46-453}$ indicates that between residues 292 and 453 of TIMAP there are contacts made with PP-1c that augment the inhibition of phosphatase activity.

The inhibition of PP-1c toward *p*-nitrophenol phosphate (PNPP) substrate reinforces both the predicted model of TIMAP bound to PP-1c and also the existence of

another PP-1c regulatory interaction site on TIMAP. GST-TIMAP$^{46-292}$ did not inhibit PP-1c activity toward PNPP substrate (figure 3-14), indicating that the small chemical substrate can enter the active site of the phosphatase. This result was consistent with the concept that the active site of PP-1c is accessible to solvent when TIMAP is bound, as predicted by the model. As mentioned earlier the microcystin sepharose data also provided evidence for an accessible active site, therefore binding of TIMAP and inhibition of phosphatase activity is not due to occlusion of the active site, but possibly by re-modeling of the catalytic centre due to allosteric interactions made by the ankyrin repeats with the enzyme.

The re-modeling of the PP-1c active site is not likely to be very drastic. In the crystal structure of MYPT1 bound to PP-1cβ, the architecture of the PP-1cβ active site is not dramatically changed from the conformation of the phosphatase active site in an unbound PP-1c structure. The position of the β12-β13 loop (a loop known to interact with toxins and inhibitors) of PP-1c is in virtually the same position whether MYPT1 is bound to PP-1c or PP-1c is monomeric. The re-modeling of the PP-1c active site is likely to be very slight, or even possibly due to a change in charge character across the acidic groove, which is thought to facilitate interactions with phosphorylase *a*.

While GST-TIMAP$^{46-292}$ did not inhibit PP-1c toward PNPP substrate, GST-TIMAP$^{46-453}$ and GST-TIMAP^{WT} were found to inhibit phosphatase activity with this substrate (figure 3-9, 3-10 and table 3-2). The abilities of the longer and full length proteins to inhibit PP-1c toward PNPP also supported the existence of an additional PP-1c binding site on TIMAP.

It was significant that the inhibition of PP-1c activity toward PNPP was 160-250-fold less potent than that observed for inhibition of PP-1c activity toward phosphorylase *a* substrate. This reduced inhibition may be further evidence that PNPP can gain access to the active site of PP-1c, providing added support for the model and a predicted solvent accessible active site.

4.1.5 Phospho-mimic mutants of GST-TIMAP$^{46-453}$ inhibit PP-1cβ and PP-1cγ phosphorylase *a* activity with differing potency

The results demonstrating that the phospho-mimic mutants of GST-TIMAP$^{46-453S333D/S337D}$ (S333D/S337D) and GST-TIMAP$^{46-453S333E/S337E}$ (S333E/S337E) bind to PP-1c immobilized on microcystin sepharose were surprising. It had previously been shown that TIMAP$^{S333D/S337D}$ and TIMAP$^{S333E/S337E}$ phospho-mimic mutants exhibited reduced binding to PP-1c in co-immunoprecipitation experiments [61]. These findings suggested that phosphorylation of TIMAP reduces the association between TIMAP and PP-1c. We expected to see a decrease in association between the phospho-mimic mutants of TIMAP and PP-1c. However, the S333D/S337D and S333E/S337E mutants were able to bind to both PP-1cβ and PP-1cγ (figure 3-11). The phospho-mimic mutants do not decrease the binding between TIMAP and PP-1c in our system. This may be due to the higher priority of the RVXF motif interaction of TIMAP-PP-1c over other secondary interaction sites involving the phospho-mimic amino acids. It is also feasible that we cannot replicate the effects seen in live cells as phosphorylation of TIMAP may signal recruitment of another binding partner of TIMAP, decreasing the interaction between TIMAP and PP-1c. Determination of K_D values for binding between PP-1c and TIMAP in the future will be

more conclusive on whether phospho-mimic mutants of TIMAP decrease association between TIMAP and PP-1c.

The phospho-mimic mutants S333D/S337D and S333E/S337E had different effects on the inhibition of PP-1cβ and PP-1cγ. The mutants inhibited PP-1cβ to virtually the same extent as GST-TIMAP$^{46-453}$. However, the S333D/S337D and S333E/S337E mutants were less potent inhibitors of PP-1cγ toward phosphorylase *a*. The findings regarding the decreased inhibition of PP-1cγ by the phospho-mimics further support a PP-1c interaction site on TIMAP in amino acids 292-453. The phospho-mimic amino acids may have a disruptive effect on binding of this potential site to PP-1c, and perhaps loosen the grip that TIMAP has on PP-1c, changing how TIMAP remodels the active site of the phosphatase, resulting in increased phosphatase activity. This effect was not observed toward PP-1cβ. This may be due to differences in the N-terminal region between the phosphatase isoforms, suggesting that the N-terminal region of PP-1c is where the phospho-mimic amino acids interact with the phosphatase.

The S333D/S337D and S333E/S337E mutants were found to be less effective at inhibiting the ability of PP-1c to dephosphorylate PNPP compared to GST-TIMAP$^{46-453}$ (figure 3-14). The fact that the S333D/S337D and S333E/S337E mutants did not potently inhibit PP-1c toward PNPP further supports the existence of a PP-1c interaction site in amino acids 292-453 of TIMAP. The PNPP inhibition data suggests that the active site of PP-1c is accessible to solvent when TIMAP is bound. The data suggest that phosphorylation of TIMAP may not dissociate TIMAP and PP-1c completely, but potentially decrease the amount of TIMAP-PP-1c protein-protein interactions, resulting in a more accessible active site of PP-1c to a small chemical substrate such as PNPP.

4.1.6 TIMAP binding to PP-1c decreases cdk2/CyclinA phosphorylation of PP-1c

All isoforms of PP-1c can be phosphorylated at a threonine residue in the C-terminal tail by cdk2/CyclinA [42,44]. GST-TIMAP was found to reduce this phosphorylation of PP-1c by cdk2/CyclinA (figures 3-15 to 3-17). This result provides support for the model, which predicts that the ankyrin repeats of TIMAP bind and wrap around the C-terminal tail of PP-1c (figures 3-1 and 3-18). In this predicted mode of interaction, the phosphorylation site of PP-1c would be inaccessible to cdk2/CyclinA, resulting in reduced phosphorylation of PP-1c. The ability of GST-TIMAP$^{46-292}$ to reduce cdk2/CyclinA phosphorylation of PP-1c supports the aforementioned predictions.

As described in section 1.3.4 (p.16), when phosphorylated, the PP-1c C-terminal tail folds back into the active site to inhibit phosphatase activity. Since PP-1c auto-dephosphorylates its C-terminal tail, microcystin was included in the cdk2/CyclinA phosphorylation reactions to inhibit PP-1c catalytic activity, allowing for maximal phosphorylation of the phosphatase (compare lanes 3 and 5 in figures 3-15 through 3-17). However when the PP-1c inhibitor was included, GST-TIMAP$^{46-453}$ was phosphorylated by cdk2/CyclinA. The result of this phosphorylation was that GST-TIMAP$^{46-453}$ was less effective preventing phosphorylation of PP-1c (figure 3-16, compare lanes 4 and 6). It is possible that when phosphorylated, GST-TIMAP$^{46-453}$ can no longer associate very tightly to PP-1c. This would explain the decreased ability of GST-TIMAP$^{46-453}$ to prevent phosphorylation of PP-1c.

GST-TIMAP$^{46-292}$ and GST-TIMAP^{WT} were not phosphorylated to the extent of GST-TIMAP$^{46-453}$, leading to the conclusion that GST-TIMAP$^{46-453}$ may be

phosphorylated between Thr292 and Asp453. There are 22 Ser/Thr residues in this stretch between 292 and 453, however there is no consensus cdk2/CyclinA phosphorylation site.

This raises a question as to why the same effect was not observed with GST-TIMAP^{WT}. It is likely that when truncated at amino acid 453, the cdk2/CyclinA phosphorylation site is accessible to solvent and is accessible to the kinase (figure 3-19b). However, in its full length form, TIMAP likely folds in a way that the unidentified site phosphorylated by cdk2/CyclinA between 292 and 453 is masked and no longer accessible to the kinase. A 31 kDa band in the preparation of GST-TIMAP$^{46-453}$ is heavily phosphorylated by cdk2/CyclinA. This is likely a proteolytic degradation fragment of TIMAP, as the same band binds to PP-1c in microcystin sepharose binding experiments (figure 3-5, lane 2 on p.55).

4.2 Summary and Conclusions

In summary, TIMAP has been characterized as a PP-1c regulatory protein that can bind to both PP-1cβ and PP-1cγ and inhibit phosphatase activity toward phosphorylase *a*. Here it has been shown that the ankyrin repeat region of TIMAP is able to inhibit PP-1c toward phosphorylase *a* and may remodel the active site of PP-1c to modulate the specificity of the phosphatase. It has been previously shown that TIMAP targets PP-1c to the LAMR1, and also possibly to moesin, where PP-1c dephosphorylates these substrates [62,63]. The data presented in this thesis add to a picture in which TIMAP is a regulatory protein of PP-1c which binds PP-1c to localize the phosphatase and tailor its activity towards specific substrates.

A three-dimensional structural model of TIMAP bound to PP-1c was generated. This model is supported by biochemical data. Figure 4-1 summarizes the structural model and the findings of this thesis. The inhibition data suggest that the open site of PP-1c is accessible to solvent and small substrates such as PNPP. The inhibition data also suggest a PP-1c interaction domain in residues 292-453, and this interaction may be modulated by the phosphorylation state of TIMAP. The predicted model is also supported by the finding that when TIMAP binds to PP-1c, there is a reduced ability of cdk2/CyclinA to phosphorylate PP-1c. TIMAP may be phosphorylated by cdk2/CyclinA between amino acids 292-453, and this phosphorylation of TIMAP may decrease binding between TIMAP and PP-1c, or may loosen the grip TIMAP has on PP-1c when bound, exposing the cdk2/CyclinA phosphorylation site on PP-1c.

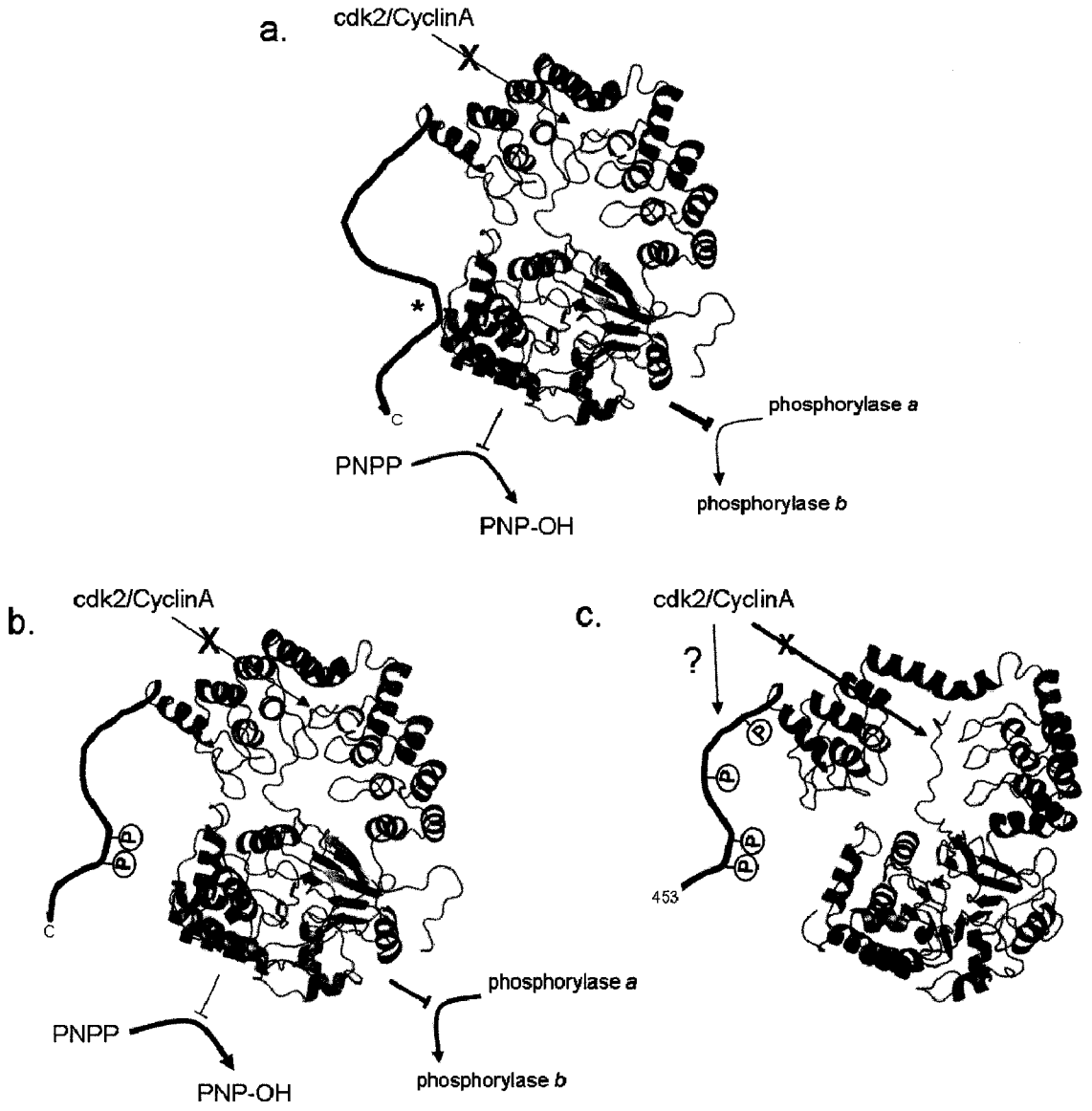
a.
cdk2/CyclinA
X
*
C
PNPP
PNP-OH
phosphorylase a
phosphorylase b
b.
cdk2/CyclinA
X
C
PNPP
PNP-OH
phosphorylase a
phosphorylase b
c.
cdk2/CyclinA
?
X
453

4.3 Future Directions

The work in this thesis adds to the growing body of information about the regulation of PP-1c by TIMAP. There is still much to be learned about TIMAP, its interactions with PP-1c and downstream cellular signaling effects of this interaction. Structural studies will prove to be extremely informative in terms of how TIMAP binds and regulates PP-1c. A crystal structure of TIMAP will provide information as to whether there are 5 ankyrin repeats in TIMAP or 8 as predicted by our model. Furthermore, the PP-1c-TIMAP interaction domain in residues 292-453 could be elucidated.

The structural model predicts a binding interface between TIMAP and LAMR1 on the surface of an α-helix in the ankyrin repeat spanning residues 261-290. Based on the model four residues have been identified as putative interacting residues with LAMR1. Mutagenesis of these residues may be informative in delineating the molecular basis of interaction between TIMAP and the LAMR1. This would allow for creation of a mutant version of TIMAP devoid of binding to LAMR1, which would be useful characterizing signal transduction pathways involving these proteins.

The data presented in this thesis suggest that the ankyrin repeat region of TIMAP binds to PP-1c and grips the C-terminal tail of PP-1c. It would be useful to determine whether a mutant form of TIMAP in which the ankyrin repeats are removed would inhibit PP-1c toward phosphorylase *a*. Using the techniques described in this thesis, it would be possible to map out all the PP-1c binding sites of TIMAP, including the suggested novel interaction site between amino acids 292-453. The data with the S333D/S337D and S333E/S337E mutants, as well as previously published results indicating that phosphorylation of these sites decreases TIMAP-PP-1c interactions [61] suggest that a

stretch of amino acids near these phosphorylation sites is likely the site of interaction (refer to figure 4-1).

GST-TIMAP$^{46-453}$ was phosphorylated by cdk2/CyclinA. Determining whether wild-type TIMAP is phosphorylated in live cells by cdk2/CyclinA would be a major finding. TIMAP contains a nuclear localization signal and TIMAP may shuttle between the nucleus and the plasma membrane. It is possible that TIMAP may regulate PP-1c activity in the nucleus. PP-1c is known to have a role in mRNA splicing, there is evidence that TIMAP can interact with the U5 snRNP-specific protein, a protein involved in this process [89]. It has been suggested that MYPT3 regulates transcription of genes in a manner dependent on its association and regulation of PP-1c activity [59], and perhaps TIMAP functions in the nucleus in a similar capacity. This will provide many alleys of exploration, as a whole nuclear signaling pathway involving PP-1c and TIMAP may be elucidated.

Bibliography

1. Cohen, P. (2002) *Nat Cell Biol* **4**, E127-130
2. Barford, D., Das, A. K., and Egloff, M. P. (1998) *Annu Rev Biophys Biomol Struct* **27**, 133-164
3. Ceulemans, H., and Bollen, M. (2004) *Physiol Rev* **84**, 1-39
4. Cohen, M. S., Zhang, C., Shokat, K. M., and Taunton, J. (2005) *Science* **308**, 1318-1321
5. Honkanen, R. E., and Golden, T. (2002) *Curr Med Chem* **9**, 2055-2075
6. McCluskey, A., Sim, A. T., and Sakoff, J. A. (2002) *J Med Chem* **45**, 1151-1175
7. Liu, J., Farmer, J. D., Jr., Lane, W. S., Friedman, J., Weissman, I., and Schreiber, S. L. (1991) *Cell* **66**, 807-815
8. Cohen, P. T. (2002) *J Cell Sci* **115**, 241-256
9. Bollen, M. (2001) *Trends Biochem Sci* **26**, 426-431
10. Cohen, P. (1989) *Annu Rev Biochem* **58**, 453-508
11. Gallego, M., and Virshup, D. M. (2005) *Curr Opin Cell Biol* **17**, 197-202
12. Moorhead, G., Johnson, D., Morrice, N., and Cohen, P. (1998) *FEBS Lett* **438**, 141-144
13. Andreassen, P. R., Lacroix, F. B., Villa-Moruzzi, E., and Margolis, R. L. (1998) *J Cell Biol* **141**, 1207-1215
14. Terry-Lorenzo, R. T., Carmody, L. C., Voltz, J. W., Connor, J. H., Li, S., Smith, F. D., Milgram, S. L., Colbran, R. J., and Shenolikar, S. (2002) *J Biol Chem* **277**, 27716-27724
15. Gibbons, J. A., Kozubowski, L., Tatchell, K., and Shenolikar, S. (2007) *J. Biol. Chem.* **282**, 21838-21847
16. Terrak, M., Kerff, F., Langsetmo, K., Tao, T., and Dominguez, R. (2004) *Nature* **429**, 780-784
17. Egloff, M. P., Cohen, P. T., Reinemer, P., and Barford, D. (1995) *J Mol Biol* **254**, 942-959
18. Egloff, M. P., Johnson, D. F., Moorhead, G., Cohen, P. T., Cohen, P., and Barford, D. (1997) *Embo J* **16**, 1876-1887
19. Goldberg, J., Huang, H. B., Kwon, Y. G., Greengard, P., Nairn, A. C., and Kuriyan, J. (1995) *Nature* **376**, 745-753
20. Hurley, T. D., Yang, J., Zhang, L., Goodwin, K. D., Zou, Q., Cortese, M., Dunker, A. K., and DePaoli-Roach, A. A. (2007) *J Biol Chem* **282**, 28874-28883
21. Kita, A., Matsunaga, S., Takai, A., Kataiwa, H., Wakimoto, T., Fusetani, N., Isobe, M., and Miki, K. (2002) *Structure* **10**, 715-724
22. Maynes, J. T., Bateman, K. S., Cherney, M. M., Das, A. K., Luu, H. A., Holmes, C. F., and James, M. N. (2001) *J Biol Chem* **276**, 44078-44082
23. Maynes, J. T., Luu, H. A., Cherney, M. M., Andersen, R. J., Williams, D., Holmes, C. F. B., and James, M. N. G. (2006) *J. Mol. Biol.* **356**, 111-120
24. Maynes, J. T., Perreault, K. R., Cherney, M. M., Luu, H. A., James, M. N., and Holmes, C. F. (2004) *J Biol Chem* **279**, 43198-43206
25. Holmes, C. F., Maynes, J. T., Perreault, K. R., Dawson, J. F., and James, M. N. (2002) *Curr Med Chem* **9**, 1981-1989
26. Dawson, J. F., and Holmes, C. F. (1999) *Front Biosci* **4**, D646-658

27. Connor, J. H., Kleeman, T., Barik, S., Honkanen, R. E., and Shenolikar, S. (1999) *J Biol Chem* **274**, 22366-22372
28. Craig, M., Luu, H. A., McCready, T. L., Williams, D., Andersen, R. J., and Holmes, C. F. B. (1996) *Biochem. Cell Biol.* **74**, 569-578
29. Moorhead, G., Mackintosh, R. W., Morrice, N., Gallagher, T., and Mackintosh, C. (1994) *FEBS Lett.* **356**, 46-50
30. Moorhead, G., Mackintosh, C., Morrice, N., and Cohen, P. (1995) *FEBS Lett.* **362**, 101-105
31. Wakula, P., Beullens, M., Ceulemans, H., Stalmans, W., and Bollen, M. (2003) *J Biol Chem* **278**, 18817-18823
32. Johnson, D. F., Moorhead, G., Caudwell, F. B., Cohen, P., Chen, Y. H., Chen, M. X., and Cohen, P. T. W. (1996) *Eur. J. Biochem.* **239**, 317-325
33. Toth, A., Kiss, E., Herberg, F. W., Gergely, P., Hartshorne, D. J., and Erdodi, F. (2000) *Eur J Biochem* **267**, 1687-1697
34. Oliver, C. J., and Shenolikar, S. (1998) *Front Biosci* **3**, D961-972
35. Nakielny, S., Campbell, D. G., and Cohen, P. (1991) *Eur J Biochem* **199**, 713-722
36. Kirchhefer, U., Baba, H. A., Boknik, P., Breeden, K. M., Mavila, N., Bruchert, N., Justus, I., Matus, M., Schmitz, W., Depaoli-Roach, A. A., and Neumann, J. (2005) *Cardiovasc Res* **68**, 98-108
37. Leach, C., Shenolikar, S., and Brautigan, D. L. (2003) *J Biol Chem* **278**, 26015-26020
38. Alessi, D. R., Street, A. J., Cohen, P., and Cohen, P. T. W. (1993) *Eur. J. Biochem.* **213**, 1055-1066
39. Morgan, D. O., Fisher, R. P., Espinoza, F. H., Farrell, A., Nourse, J., Chamberlin, H., and Jin, P. (1998) *Cancer J Sci Am* **4 Suppl 1**, S77-83
40. Harper, J. W., and Adams, P. D. (2001) *Chem. Rev.* **101**, 2511-2526
41. Stevenson-Lindert, L. M., Fowler, P., and Lew, J. (2003) *J. Biol. Chem.* **278**, 50956-50960
42. Dohadwala, M., Silva, E., Hall, F. L., Williams, R. T., Carbonarohall, D. A., Nairn, A. C., Greengard, P., and Berndt, N. (1994) *Proc. Natl. Acad. Sci. U. S. A.* **91**, 6408-6412
43. Kwon, Y. G., Lee, S. Y., Choi, Y. W., Greengard, P., and Nairn, A. C. (1997) *Proc. Natl. Acad. Sci. U. S. A.* **94**, 2168-2173
44. Liu, C. W. Y., Wang, R. H., Dohadwala, M., Schonthal, A. H., Villa-Moruzzi, E., and Berndt, N. (1999) *J. Biol. Chem.* **274**, 29470-29475
45. Berndt, N., Dohadwala, M., and Liu, C. W. (1997) *Curr Biol* **7**, 375-386
46. Somlyo, A. P., and Somlyo, A. V. (2003) *Physiol Rev* **83**, 1325-1358
47. Alessi, D., Macdougall, L. K., Sola, M. M., Ikebe, M., and Cohen, P. (1992) *Eur. J. Biochem.* **210**, 1023-1035
48. Hartshorne, D. J., Ito, M., and Erdodi, F. (2004) *J. Biol. Chem.* **279**, 37211-37214
49. Ito, M., Nakano, T., Erdodi, F., and Hartshorne, D. J. (2004) *Mol. Cell. Biochem.* **259**, 197-209
50. Tanaka, J., Ito, M., Feng, J. H., Ichikawa, K., Hamaguchi, T., Nakamura, M., Hartshorne, D. J., and Nakano, T. (1998) *Biochemistry* **37**, 16697-16703
51. Ichikawa, K., Ito, M., and Hartshorne, D. J. (1996) *J Biol Chem* **271**, 4733-4740
52. Sedgwick, S. G., and Smerdon, S. J. (1999) *Trends Biochem Sci* **24**, 311-316

53. Mosavi, L. K., Cammett, T. J., Desrosiers, D. C., and Peng, Z. Y. (2004) *Protein Sci.* **13**, 1435-1448
54. Li, J. N., Mahajan, A., and Tsai, M. D. (2006) *Biochemistry* **45**, 15168-15178
55. Fujioka, M., Takahashi, N., Odai, H., Araki, S., Ichikawa, K., Feng, J., Nakamura, M., Kaibuchi, K., Hartshorne, D. J., Nakano, T., and Ito, M. (1998) *Genomics* **49**, 59-68
56. Tan, I., Ng, C. H., Lim, L., and Leung, T. (2001) *J Biol Chem* **276**, 21209-21216
57. Skinner, J. A., and Saltiel, A. R. (2001) *Biochem. J.* **356**, 257-267
58. Yong, J., Tan, I., Lim, L., and Leung, T. (2006) *J. Biol. Chem.* **281**, 31202-31211
59. Sueyoshi, T., Moore, R., Sugatani, J., Matsumura, Y., and Negishi, M. (2008) *Mol Pharmacol* **73**, 1113-1121
60. Cao, W., Mattagajasingh, S. N., Xu, H., Kim, K., Fierlbeck, W., Deng, J., Lowenstein, C. J., and Ballermann, B. J. (2002) *Am J Physiol Cell Physiol* **283**, C327-337
61. Li, L., Kozlowski, K., Wegner, B., Rashid, T., Yeung, T., Holmes, C., and Ballermann, B. J. (2007) *J. Biol. Chem.* **282**, 25960-25969
62. Csortos, C., Czikora, I., Bogatcheva, N., Adyshev, D. M., Poirier, C., Olah, G., and Verin, A. D. (2008) *Am J Physiol Lung Cell Mol Physiol*
63. Kim, K., Li, L., Kozlowski, K., Suh, H. S., Cao, W., and Ballermann, B. J. (2005) *Biochem Biophys Res Commun* **338**, 1327-1334
64. Nelson, J., McFerran, N. V., Pivato, G., Chambers, E., Doherty, C., Steele, D., and Timson, D. J. (2008) *Biosci Rep* **28**, 33-48
65. Fulop, T., and Larbi, A. (2002) *Semin Cancer Biol* **12**, 219-229
66. Gauczynski, S., Peyrin, J. M., Haik, S., Leucht, C., Hundt, C., Rieger, R., Krasemann, S., Deslys, J. P., Dormont, D., Lasmezas, C. I., and Weiss, S. (2001) *Embo J* **20**, 5863-5875
67. Mangeat, P., Roy, C., and Martin, M. (1999) *Trends Cell Biol* **9**, 187-192
68. Fukata, Y., Kimura, K., Oshiro, N., Saya, H., Matsuura, Y., and Kaibuchi, K. (1998) *J Cell Biol* **141**, 409-418
69. Doble, B. W., and Woodgett, J. R. (2003) *J Cell Sci* **116**, 1175-1186
70. Laemmli, U. K. (1970) *Nature* **227**, 680-685
71. Zhang, Z., Zhao, S., Zirattu, S. D., Bai, G., and Lee, E. Y. (1994) *Arch Biochem Biophys* **308**, 37-41
72. Guex, N., and Peitsch, M. C. (1997) *Electrophoresis* **18**, 2714-2723
73. Schwede, T., Kopp, J., Guex, N., and Peitsch, M. C. (2003) *Nucleic Acids Res.* **31**, 3381-3385
74. Arnold, K., Bordoli, L., Kopp, J., and Schwede, T. (2006) *Bioinformatics* **22**, 195-201
75. Notredame, C., Higgins, D. G., and Heringa, J. (2000) *J. Mol. Biol.* **302**, 205-217
76. Holmes, C. F. (1991) *Toxicon* **29**, 469-477
77. Lambert, T. W., Boland, M. P., Holmes, C. F. B., Hrudey, S. E. (1994) *Environ. Sci. Technol.* **28**, 753-755
78. An, J., and Carmichael, W. W. (1994) *Toxicon* **32**, 1495-1507
79. Burkhard, P., Stetefeld, J., and Strelkov, S. V. (2001) *Trends Cell Biol.* **11**, 82-88
80. Kim, S. I., Kim, H. Y., Kwak, J. H., Kwon, S. H., and Lee, S. Y. (2000) *Mol. Cells* **10**, 102-107

81. Tran, H. T., Bridges, D., Ulke, A., and Moorhead, G. B. G. (2002) *Biochem. Cell Biol.* **80**, 811-815
82. Hartshorne, D. J., Ito, M., and Erdodi, F. (1998) *J. Muscle Res. Cell Motil.* **19**, 325-341
83. Schultz, J., Milpetz, F., Bork, P., and Ponting, C. P. (1998) *Proc. Natl. Acad. Sci. U. S. A.* **95**, 5857-5864
84. Letunic, I., Copley, R. R., Pils, B., Pinkert, S., Schultz, J., and Bork, P. (2006) *Nucleic Acids Res.* **34**, D257-D260
85. Gaudet, R. (2008) *Mol. Biosyst.* **4**, 372-379
86. Ji, X. H., Zhang, P. H., Armstrong, R. N., and Gilliland, G. L. (1992) *Biochemistry* **31**, 10169-10184
87. Maru, Y., Afar, D. E., Witte, O. N., and Shibuya, M. (1996) *J. Biol. Chem.* **271**, 15353-15357
88. Dent, P., MacDougall, L. K., MacKintosh, C., Campbell, D. G., and Cohen, P. (1992) *Eur J Biochem* **210**, 1037-1044
89. Adyshev, D. M., Kolosova, I. A., and Verin, A. D. (2006) *Mol. Biol. Rep.* **33**, 83-89